

Copyright is owned by the Author of the thesis. Permission is given for a copy to be downloaded by an individual for the purpose of research and private study only. The thesis may not be reproduced elsewhere without the permission of the Author.

**An Investigation of Ru(II) Complexes Containing
Sterically Demanding Imido Ligands**

A thesis presented to Massey University in
partial fulfilment of the requirements for the degree of

MASTER OF SCIENCE

by

Andrew John Steedman

1995

This is dedicated to the Steedman and Turei
ancestries, including present members, and to the dynamic duo, D.M.
and Penfold.

Acknowledgements

I would like to thank sincerely my supervisor, Dr. A.K. Burrell, for his guidance and care free attitude shown through all of it.

I am very grateful for the friendly support of Prof. A.M. Brodie, Assoc.-Prof. E.W. Ainscough, Assoc.-Prof. J.M. Waters and Dr. A.H. Wright during the course of this study.

Also the contribution of the following is gratefully acknowledged; Assoc.-Prof. W.T. Robinson of Canterbury University for X-ray diffraction data collection of two complexes; Mr. J. Hastie for n.m.r. spectra; and Mrs. M. Dick for microanalytical data.

I would also like to thank the other post graduate students of the chemistry department of Massey University, especially Andrew Lowe, Xiaohong Fan, Suba Sivakumaran and Steven Kennedy for their friendship.

Most of all I want to thank Cujo.

Abstract

Monomeric, low oxidation state, ruthenium imido compounds, $(\eta^6\text{-arene})\text{RuN-Ar}'$ (arene = *p*-cymene and C_6Me_6 ; $\text{Ar}' = 2,4,6\text{-tri-}i\text{-tert-butylphenyl}$) have been synthesized from $[(\eta^6\text{-arene})\text{RuCl}_2]_2$ and 4 equiv of LiNHAr' in THF. An X-ray crystal structure of $(\eta^6\text{-}i\text{-p-cymene})\text{Ru=NAr}'$ showed a short Ru-N distance (1.753(3)Å) and a near linear Ru-N-C angle (177.8(4)°) consistent with ruthenium to nitrogen multiple bonding. Reaction of $[(\eta^6\text{-}i\text{-p-cymene})\text{RuCl}_2]_2$ with 4 equiv of LiNHR (R = 2,6-dimethylphenyl or 2,6-diisopropylphenyl) in THF afforded the dimeric ruthenium imido compounds $[(\eta^6\text{-}i\text{-p-cymene})\text{Ru}(\mu\text{-NR})]_2$. An X-ray crystal structure of $[(\eta^6\text{-}i\text{-p-cymene})\text{Ru}(\mu\text{-NAr})]_2$ (Ar = 2,6-diisopropylphenyl) showed an averaged Ru-N distance of 1.974(8)Å and features characteristic of Ru(II) bridging imido complexes. Addition of 2 equiv of LiNHAr to $[(\eta^6\text{-C}_6\text{Me}_6)\text{RuCl}_2]_2$ gave a HCl adduct, $(\eta^6\text{-C}_6\text{Me}_6)\text{RuClNHAr}$, characterisation of the complex was obtained by X-ray diffraction. Reaction of the HCl adduct with phenylisocyanate gave the ureylene metallacycle, $(\eta^6\text{-C}_6\text{Me}_6)\text{RuN}(\text{Ar})\text{C}(\text{O})\text{N}(\text{Ph})$, indicating the presence of an imido intermediate. This complex was shown to have a $\nu(\text{CO})$ band at 1596cm^{-1} and is comparable with other monomeric ureylene complexes. In addition, the complex $[(\eta^6\text{-}i\text{-p-cymene})\text{Ru}(\mu\text{-NAr})]_2$ was made from 2 equiv of the amine, ArNH_2 , and $[(\eta^6\text{-}i\text{-p-cymene})\text{RuCl}_2]_2$ and dehydrochlorinated with $\text{KN}(\text{SiMe}_3)_2$ providing an alternative route. Further, an X-ray crystal structure of the amine complex, $(\eta^6\text{-}i\text{-p-cymene})\text{RuCl}_2(\text{ArNH}_2)$ was obtained. The reaction of $(\text{bpy})_2\text{RuCl}_2$ (bpy = 2,2'-bipyridine) with LiNHAr' in THF afforded the complex, $(\text{bpy})_2\text{Ru=NAr}'$, characterised by nmr and elemental analysis.

List of Figures

Figure 1	General Formulation of Oxo Complexes	page 3
Figure 2a	$[(bpy)_2Ru(O)(py)]^{2+}$	page 4
Figure 2b	$Re(O)(\eta^2-MeC\equiv CMe)_2(I)$	page 4
Figure 3	$Cp^*Re(O)_3$; $(bpy)Mo(Et)_2(O)_2$; $CpW(Ph)(\eta^2-PhC\equiv CPh)(O)$	page 5
Figure 4	General Formulation of Nitrido Complexes	page 5
Figure 5	$[Os(N)(O)_3]^-$	page 5
Figure 6	$Re(N)Cl_2(PPh_3)_2$	page 5
Figure 7	General Formulation of Hydrazido Complexes	page 6
Figure 8	Resonance Forms of the Hydrazido Ligand	page 7
Figure 9	$[M(=NNH_2)(DPPE)_2X]^+$; M=Mo, W	page 7
Figure 10	$[M(=NN=CR_2)(DPPE)_2X]^+$; M=Mo, W	page 8
Figure 11	General Formulation of Carbene/Alkylidene Complexes	page 8
Figure 12	$(CO)_5W=C(OCH_3)(CH_3)$	page 9
Figure 13	β -Lactam Synthesis	page 9
Figure 14	$(tBuCH_2)_3Ta=C^tBu(H)$	page 10
Figure 15	" $Cp_2Ti=CH_2$ "	page 10
Figure 16	General Formulation of Carbyne/Alkylidyne Complexes	page 11
Figure 17	$M(\equiv CR)(CO)_4X$; M=Cr, Mo, W	page 12
Figure 18	$CpTa(\equiv CPh)(PMe_3)_2Cl$	page 12
Figure 19	General Formulation of Terminal Imido Complexes	page 13
Figure 20	$Re(=NAr)(PR_3)_2Cl_3$	page 13
Figure 21	Possible Bond Orders of the MNR Moiety	page 13
Figure 22	$W(=CH^tBu)(=NAr)(OR_f)_2$	page 15
Figure 23a	$(Me_3SiO)_4Mo(NHR)_2$; R=1-adamantyl	page 17
Figure 23b	$(Me_3SiO)_2Mo(=NR)_2$; R=1-adamantyl	page 17
Figure 24	Transition State Involving Bridged Oxo and Imido Ligands	page 22
Figure 25	Crystal Structure of $Cp^*Ir(=NAr)$	page 28

Figure 26	Crystal Structure of $(C_6Me_6)Os(=N^tBu)$	page 29
Figure 27	Crystal Structure of <i>trans</i> - $Ru(=NAr)_2(PMe_3)_2$	page 31
Figure 28	$[Tc_2(NAr)_6]$ and $Tc_2(NAr'')_4(\mu-NAr'')_2$	page 35
Figure 29	$Os(NAr)_3$ and $[Os(N^tBu)_2(\mu-N^tBu)]_2$	page 35
Figure 30	Crystal Structure of $[(cym)Ru(\mu-NAr)]_2$	page 45
Figure 31	Crystal Structure of $(cym)RuCl_2NH_2Ar$	page 48
Figure 32	Crystal Structure of $(cym)Ru=NAr'$	page 52
Figure 33	Crystal Structure of $(C_6Me_6)RuClNHAr$	page 57
Figure 34	$Cp^*Ir(RCCRN^tBuRCCR)$; $R=CO_2Me$	page 59
Figure 35	Sterics Versus Reactivity	page 63

List of Tables

Table 1	Terminal Imido Functional Groups	page 27
Table 2	Selected Bond Lengths and Angles for [(cym)Ru(μ -NAr)] ₂	page 44
Table 3	Selected Bond Lengths and Angles for (cym)RuCl ₂ NH ₂ Ar	page 47
Table 4	Comparative ¹ H Chemical Shift and Coupling Constants for the Aromatic Protons of the <i>p</i> -Cymene Ligand	page 50
Table 5	Comparative ¹ H Chemical Shifts of the Isopropyl and Methyl Groups of the <i>p</i> -Cymene Ligand	page 50
Table 6	Comparative ¹³ C Chemical Shifts of <i>ipso</i> , <i>ortho</i> , <i>meta</i> and <i>para</i> -carbons of the Imido Ligand	page 51
Table 7	Selected Bond Lengths and Angles for (cym)Ru=NAr'	page 51
Table 8	¹³ C Chemical Shifts of <i>ipso</i> , <i>ortho</i> , <i>meta</i> and <i>para</i> -carbons of the Imido Ligand for (C ₆ Me ₆)Ru=NAr'	page 54
Table 9	Selected Bond Lengths and Angles for (C ₆ Me ₆)RuClNHAr	page 56
Table 10	Comparative Ru-N Distances	page 56
Table 11	Comparative Ru-Cl Distances	page 58
Table 12	Comparative ¹ H Chemical Shifts of Septets Due to the Ar Ligand	page 62
Table 13	Comparative ¹ H Chemical Shifts of the <i>tert</i> -butyl Groups	page 67
Table 14	Comparative ¹ H Chemical Shifts of the Ar Ligand, NH ₂ Group and I.R. Peaks of the NH ₂ Group for the Ru and Rh Amine Complexes	page 69

Abbreviations

Ac	-COCH ₃
Ar	2,6-diisopropylphenyl
Ar'	2,4,6-tri- <i>tert</i> -butylphenyl
Ar''	2,6-dimethylphenyl
bpy	2,2'-bipyridine
Bu	butyl
Cp	cyclopentadienyl
Cp*	pentamethylcyclopentadienyl
DMAC	dimethylacetylenedicarboxylate
dme	dimethoxyethane
dmtc	dimethyldithiocarbamate (R ₂ NCS ₂ ⁻)
DPPE	1,2-bis(diphenylphosphino)ethane
Et	ethyl
I.R.	Infra-red
Me	methyl
mnt	maleonitriledithiolate [η^2 -S ₂ C ₂ (CN) ₂] ²⁻
nmr	nuclear magnetic resonance
OTf	Triflate (OSO ₂ CF ₃) ⁻
Ph	phenyl
Pr	propyl
Pr ⁱ	<i>iso</i> -propyl
py	pyridine
R _f	OCMe(CF ₃) ₂
^t Bu	<i>tert</i> -butyl
thf	tetrahydrofuran
tol	tolyl (4-C ₆ H ₄ Me)
tpy	2,2':6',2''-terpyridine
X	anionic ligand

Table of Contents

Chapter One

Introduction	page 2
– Terminal Oxo Complexes	page 3
– Terminal Nitrido Complexes	page 5
– Terminal Hydrazido Complexes	page 6
– Carbene and Alkylidene Complexes	page 8
– Carbyne and Alkylidyne Complexes	page 11
– Terminal Imido Complexes	page 12
– Synthetic Methods for Introducing Terminal Imido Ligands	page 16
– Known Metal Terminal Imido Complexes of Os(II), Ir(III) and Ru	page 26

Chapter Two

Results and Discussion	page 34
– The Role of Sterics	page 34
– Synthesis of Precursors	page 36
– Synthetic Method	page 40
(i) the strategy	page 40
(ii) reactions of [(cym)RuCl ₂] ₂	page 42
(iii) reactions of [(C ₆ Me ₆)RuCl ₂] ₂	page 53
– Reactivity of the imido and amido ligand	page 59
– Possible mechanisms of imido formation from LiNHR	page 64
– Future work	page 66
– Summary	page 69

Chapter Three

Experimental Section	page 72
– General	page 72
– Compounds	page 72
# $[(\eta^6\text{-C}_6\text{Me}_6)\text{RuCl}_2]_2$	page 72
# $(\text{bpy})_2\text{RuCl}_2$	page 73
# $[(\text{cym})\text{Ru}=\text{NAr}']_n$	page 74
# $[(\text{C}_6\text{Me}_6)\text{Ru}=\text{NAr}']_n$	page 75
# $[(\text{cym})\text{Ru}=\text{NAr}]_n$	page 76
# $[(\text{cym})\text{Ru}=\text{NAr}'']_n$	page 77
# $(\text{C}_6\text{Me}_6)\text{RuClNHAr}$	page 78
# $(\text{C}_6\text{Me}_6)\text{RuN}(\text{Ph})\text{C}(\text{O})\text{N}(\text{Ar})$	page 79
# $(\text{bpy})_2\text{Ru}=\text{NAr}'$	page 80
# $(\text{cym})\text{RhCl}_2\text{NH}_2\text{Ar}$	page 81
# $(\text{cym})\text{RuCl}_2\text{NH}_2\text{Ar}$	page 82

Chapter Four

Tables of ^1H and ^{13}C Data	page 84
– ^1H nmr of $(\text{cym})\text{RhCl}_2\text{NH}_2\text{Ar}$	page 84
– ^1H nmr of $[(\text{cym})\text{Ru}=\text{NAr}'']_n$	page 85
– ^{13}C nmr of $[(\text{cym})\text{Ru}=\text{NAr}'']_n$	page 86
– ^1H nmr of $[(\text{cym})\text{Ru}=\text{NAr}]_n$	page 87
– ^{13}C nmr of $[(\text{cym})\text{Ru}=\text{NAr}]_n$	page 88
– ^1H nmr of $(\text{cym})\text{RuCl}_2\text{NH}_2\text{Ar}$	page 89
– ^{13}C nmr of $(\text{cym})\text{RuCl}_2\text{NH}_2\text{Ar}$	page 90
– ^1H nmr of $[(\text{cym})\text{Ru}=\text{NAr}']_n$	page 91

– ^{13}C nmr of $[(\text{cym})\text{Ru}=\text{NAr}']_n$	page 92
– ^1H nmr of $[(\text{C}_6\text{Me}_6)\text{Ru}=\text{NAr}']_n$	page 93
– ^{13}C nmr of $[(\text{C}_6\text{Me}_6)\text{Ru}=\text{NAr}']_n$	page 94
– ^1H nmr of $(\text{C}_6\text{Me}_6)\text{RuClNHAr}$	page 95
– ^{13}C nmr of $(\text{C}_6\text{Me}_6)\text{RuClNHAr}$	page 96
– ^{13}C nmr of $(\text{cym})\text{RhCl}_2\text{NH}_2\text{Ar}$	page 96
– ^1H nmr $(\text{bpy})_2\text{Ru}=\text{NAr}'$	page 97
– ^1H nmr of $(\text{C}_6\text{Me}_6)\text{RuN}(\text{Ph})\text{C}(\text{O})\text{N}(\text{Ar})$	page 98
– ^{13}C nmr of $(\text{C}_6\text{Me}_6)\text{RuN}(\text{Ph})\text{C}(\text{O})\text{N}(\text{Ar})$	page 99
Appendix	
Crystal Structures	page 101
– $[(\text{cym})\text{Ru}=\text{NAr}]_n$	page 102
– $[(\text{cym})\text{Ru}=\text{NAr}']_n$	page 103
– $(\text{C}_6\text{Me}_6)\text{RuClNHAr}$	page 104
– $(\text{cym})\text{RuCl}_2\text{NH}_2\text{Ar}$	page 105
References	page 106

Chapter One

Introduction

In recent years few areas of inorganic chemistry have experienced the exceptional growth associated with transition metal complexes containing metal-ligand multiple bonds. Firing the growth of this field are the important chemical processes associated with multiply bonded ligands. Such species are present on the catalytic surface in a wide variety of crucial industrial processes. They constitute the “business end” of some of the most useful reagents for laboratory scale synthesis. They are involved in a fascinating array of enzymatic transformations. The oxo and nitrido moieties in particular are essential building blocks for a new generation of electronic materials.

The proliferation in the field of imido chemistry has the potential to increase our understanding of the properties pertaining to complexes containing metal-nitrogen ($M=N-R$) multiple bonded ligands. The imido moiety and the complex itself can embody a unique set of properties ranging from remarkable stability to extreme reactivity, which are dependent on the metal, its oxidation state, the ancillary ligands, as well as the nature of R.

The use of highly polar M-N linkages and nucleophilic imido ligands are emerging areas of future utility as sites for C-H bond activation. Also, the design of electrophilic imido ligands will be possible as more is understood about imido chemistry. Such NR transfer reagents are certain to play a role in alkene aziridination systems.

Application of imido compounds as model species in catalytic processes involving nitrogen is flourishing. Among the most important of these is propylene ammoxidation and hydrodenitrogenation (HDN) catalysis. The use of $M(=NR)(=CHR)(OR)_2$ complexes of molybdenum and tungsten in metathesis polymerisations are extremely important. Development of technetium and rhenium compounds in radiopharmaceutical and other biological applications is an important developing area of imido chemistry.

The following discussion includes an overview of complexes containing metal-oxygen (oxo), metal-nitrogen (nitrido, hydrazido, imido) and metal-carbon (alkylidene, alkylidyne) multiple bonds. The many methods for introducing terminal imido ligands are then

covered with illustrative examples. Finally, low oxidation state osmium and iridium terminal imido complexes and the known ruthenium terminal imido compounds are discussed in detail.

Terminal Oxo Complexes:

Metal-oxo (Fig. 1) complexes were the first known compounds containing metal-ligand multiple bonds. As such their chemistry has been most extensively developed.^{1,2} Sodium ferrate, Na_2FeO_4 , was synthesized³ in 1702 and compounds such as OsO_4 , KMnO_4 and K_2CrO_4 were known to chemists in the early nineteenth century. The multiple bonded character of metal-oxo complexes was widely accepted by 1938.



Figure 1

Complexes containing terminal oxo substituents are known for all the transition metals of the vanadium through iron triads. The metals of the titanium triad tend to form bridged rather than terminal oxo structures. However, coordinative saturation of the metal enforces the terminal oxo structure and as a result several terminal oxotitanium complexes have been structurally characterised.²

The vast majority of oxo complexes have d^0 , d^1 or d^2 configurations,⁴ giving support to the oxo ligand being best described as a closed-shell anion, O^{2-} . Productive π -bonding with a metal center therefore requires that the metal d-orbitals be empty, in other words that the metal center be in a high oxidation state with a low d-electron count.⁵ Although in the last few years a handful of d^4 oxo compounds⁶ and d^5 species have been prepared,⁷ the d^4 oxo species are either very reactive or adopt an unusual structure to promote multiple bonding. The d^4 Ru oxo complex, $[(\text{bpy})_2\text{Ru}(\text{O})(\text{py})]^{2+}$ (Fig. 2a) is a very reactive oxidant⁸ and the d^4 oxo complex, $\text{Re}(\text{O})(\eta^2\text{-MeC}\equiv\text{CMe})_2(\text{I})$ (Fig. 2b) adopts an unusual tetrahedral structure.⁹

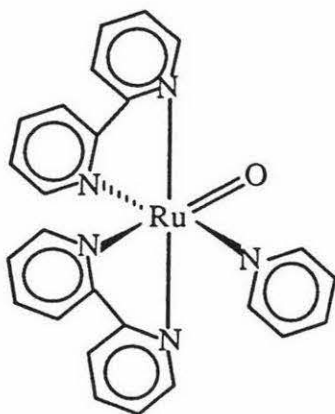


Figure 2a

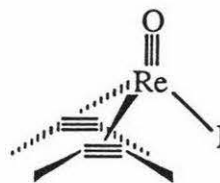


Figure 2b

The use of metal-oxo complexes as oxidants in organic synthesis is one important and long standing application of metal oxo derivatives.¹⁰⁻¹³

Nature also makes use of terminal imido ligands to carry out oxidations. Enzymes of the cytochrome P-450 family contain an oxo-iron porphyrin system and are involved in a wide range of biological oxidation processes.¹⁴ A second family of oxo-metal based enzymes are the molybdenum or tungsten containing “oxo-transferases” which are involved in both oxidative and reductive processes.¹⁵

Metal-oxo species are present on the surface of industrially important heterogeneous catalysts. For example the oxidation of propylene to acrolein¹⁶ and the oxidation of C4's to butadiene¹⁷ involve the use of bismuth molybdate catalysts. Also iron molybdate catalysts are utilised for the oxidation of methanol to formaldehyde.¹⁸ Oxo ligands are also utilised in industrial processes involving homogeneous catalysis. For example, vanadium-oxo complexes catalyse the rearrangement of allylic or propargylic alcohols in the manufacture of terpene alcohols and of vitamin A.¹⁹

Organometallic chemists have begun to appreciate the ability of the oxo ligand to stabilise high oxidation states. This stabilisation has been applied to the synthesis of both σ and π organotransition metal derivatives, for example, of vanadium(V), rhenium(VII), molybdenum(VI) and tungsten(VI). Figures 3 illustrates three such complexes.²⁰

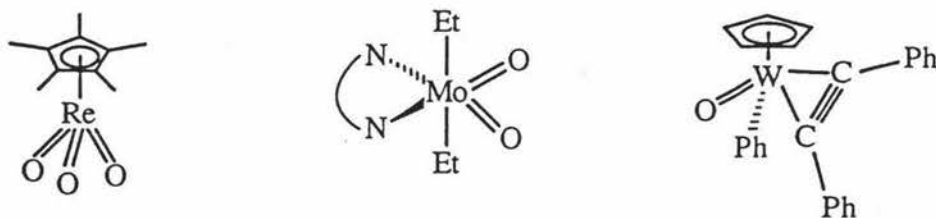


Figure 3

Terminal Nitrido Complexes:

Multiple bonded nitrido complexes (Fig. 4) are now known for all of the metals of vanadium through iron triads. However, the examples of iron, niobium and tantalum are of the bridged variety.



Figure 4

The first nitrido complex to be synthesized was the so-called "potassium osmiumate" (Fig. 5) reported by Fritsche and Struve in 1847.²¹ However, it was not until 1901 that the presence of a nitrido ligand in the complex was recognised.²² The first neutral mononuclear nitrido complex did not appear until Chatt and coworkers report of $\text{Re}(\equiv\text{N})(\text{PPh}_3)_2\text{Cl}_2$ (Fig. 6) in 1963.²³

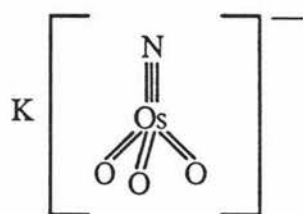


Figure 5

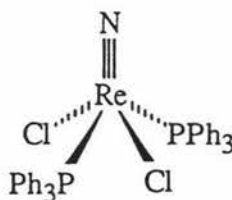


Figure 6

Complexes with terminal nitrido ligands are believed to contain metal-nitrogen triple bonds, or at least to be best described by that resonance structure, on the basis of crystallographic and spectroscopic data.²⁴ The strong preference of nitrido ligands for the

formation of triple bonds is illustrated by the lack of dinitrido compounds, in which the ligands would have to share a metal π -orbital. As with the oxo ligand, the nitrido ligand is best described as a closed-shell anion, N^{3-} . There is as yet no fully characterised transition metal nitrido compound with a greater than d^2 configuration.

The ability of the nitrido ligand to stabilise organotransition metal species was recognised by Chatt, who reported a series of aryl rhenium nitrido complexes, $Re(\equiv N)Ar_2(PR_3)_2$.²⁵

The field of electronic materials is an emerging area of application of nitrido compounds. The ability of niobium(III) nitride to form films that are strong, stable and superconducting²⁶ has been of interest for some time. A recent theoretical study by Hoffman *et al.* pointed out a number of parallels between transition metal nitrides and such organic conductors as polyenes and phosphazenes²⁷ has fueled current interest in the electronic properties of transition metal nitrides.

Terminal Hydrazido Complexes:

Terminal hydrazido complexes (Fig. 7) are now known for the metals of vanadium, niobium, tantalum, titanium, tungsten and rhenium.



Figure 7

A variety of structural types and resonance forms are possible for the hydrazido ligand (Fig 8). The conjugation of a substituent lone pair with a metal-ligand triple bond splits the degeneracy of the p-orbitals of the triple bond. Calculations on hydrazido²⁸ complexes, indicate that the amino lone pair is very involved in the bonding and that there is significant multiple bond character to the N-N bond.

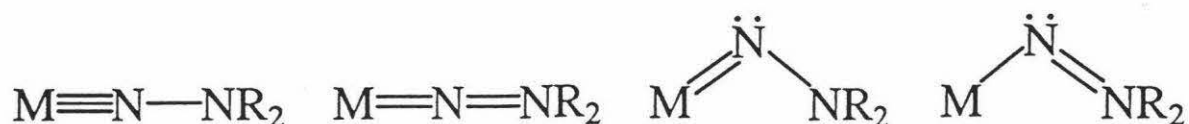


Figure 8

The chemistry of hydrazido complexes in general and their role in nitrogen fixation in particular have been the subject of several reviews.³⁰ Hydrazido ligands are of particular importance because of their suggested intermediacy in the reduction of dinitrogen by metal complexes and metalloenzymes. As such the focus of activity on hydrazido compounds has been the Institute for Nitrogen Fixation at Sussex University. In 1972 this organisation reported the synthesis of $M(=NNH_2)(DPPE)_2X$ ($M=Mo, W$; Fig. 9) hydrazido complexes accomplished by protonation of tungsten or molybdenum dinitrogen complexes.^{31a}

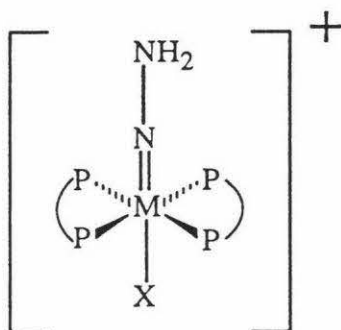


Figure 9

Such complexes, it was shown, undergo a number of C-N bond-forming reactions. A simple example being formation of the diazoalkane complex ($M=Mo, W$; Fig. 10), ultimately allowing the direct conversion of dinitrogen to organonitrogen derivatives.²⁹

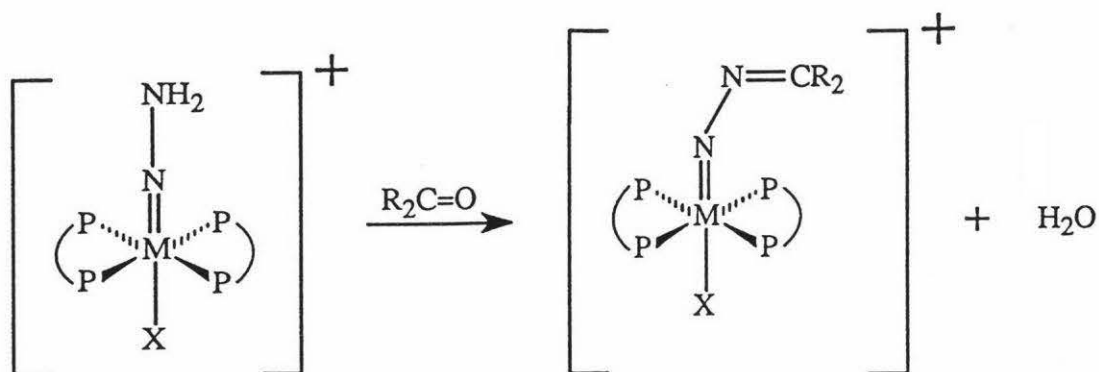


Figure 10

Carbene and Alkylidene Complexes:

Complexes that contain $\text{M}=\text{C}$ double bonds (Fig. 11) can be termed loosely into two divisions; carbene and alkylidene complexes. They were first prepared by Fischer by the interaction of acylate anions with electrophiles.^{31b} These compounds were 18-electron species in low oxidation states and have been called *carbene complexes*. Subsequently, compounds in high oxidation states with 10 to 16 electron counts have been made and these have been termed *alkylidene complexes*.



Figure 11

Alkylidene ligands are best described as CR_2^{2-} only when they lack heteroatom substituents and are bound to high-oxidation state metal centers.^{31c} The CR_2 group is also often treated as a neutral ligand (a carbene) in particular when the carbon bears a substituent with lone pairs such as alkoxy or an amino group (Fischer carbene complexes).^{31d}

Ab initio calculations support earlier results^{31d,e} that the metal-carbon interaction consists of a σ and a π bond. Recent calculations using high levels of theory^{31f} suggests that Schrock alkylidenes form ethylene-like covalent double bonds, but Fischer carbenes bond to a metal center via donor-acceptor interactions.

The first carbene complex reported was by Fischer and Maasboel in 1964 (Fig. 12).³² The carbene moiety in these compounds has a pronounced tendency to behave as a carbon electrophile and it has become evident that such electrophilic properties are shared by other carbene complexes, some of which do not contain a heteroatom substituent.

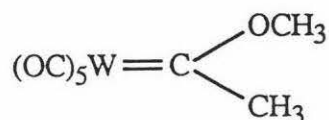


Figure 12

Fischer carbene complexes are of considerable importance as key intermediates in catalysis. Iron methylene species are finding use as stoichiometric cyclopropanation agents³³ and chromium analogues of $(\text{CO})_5\text{W}=\text{CCH}_3(\text{OCH}_3)$ (Fig. 12) are used increasingly in organic chemistry as reagents for two powerful synthetic transformations; the β -lactam synthesis³⁴ (Fig. 13) and the Dötz naphthoquinone synthesis.³⁵

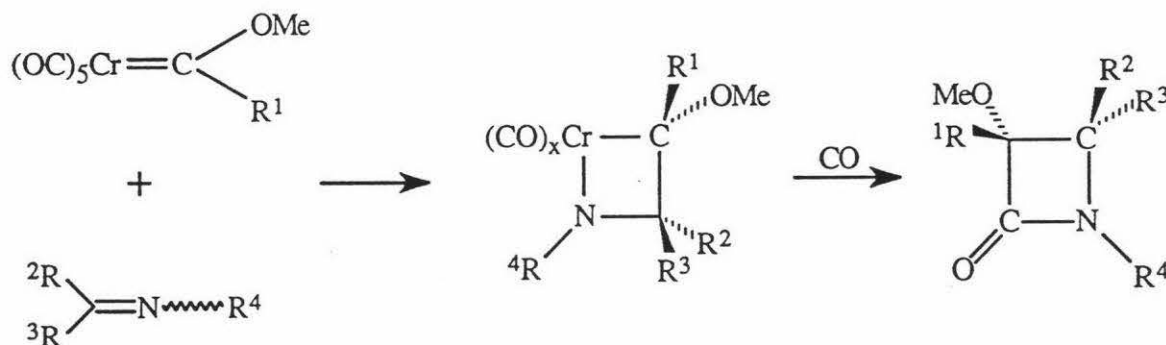


Figure 13

In 1973 the field of transition metal alkylidene chemistry was born. In the course of an attempted synthesis of pentakisneopentyl tantalum(V), Schrock instead isolated the complex $(^t\text{BuCH}_2)_3\text{Ta}=\text{C}^t\text{Bu}(\text{H})$ (Fig. 14), a tantalum neopentylidene derivative.³⁶

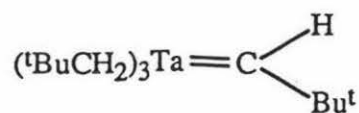


Figure 14

While at the same time Fred Tebbe found that treatment of Cp_2TiCl_2 with trimethylaluminium afforded a “masked” form of the titanium methylene complex, $\text{Cp}_2\text{Ti}=\text{CH}_2$ (Fig. 15).³⁷ Indeed, in its reaction chemistry this adduct behaves as though it were a free methylene complex and it is because of this that “the Tebbe-Grubbs reagent” has assumed considerable importance in synthetic organic chemistry.³⁸

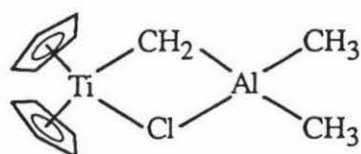
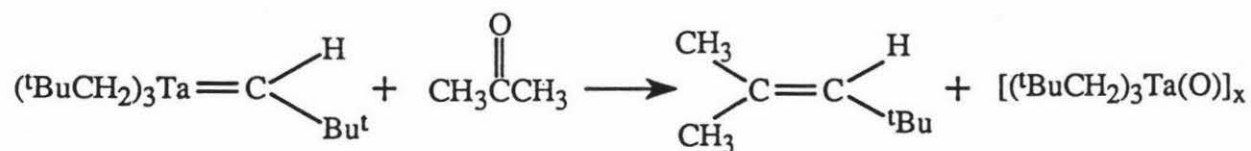


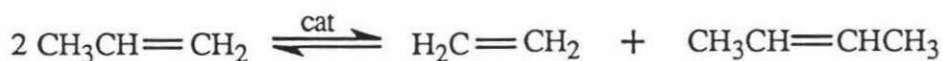
Figure 15

In contrast to the Fischer carbenes, the alkylidene ligands behave chemically as carbon nucleophiles. A feature of alkylidene reactivity is the tendency to undergo “Wittig-like” olefination reaction with organic carbonyl compounds. In a pioneering study,³⁹ Schrock demonstrated that the tantalum neopentylidene complex of figure 14 would promote carbonyl-olefination of aldehydes and ketones in direct analogue to phosphorus ylides (Equ. 1).⁴⁰ Significantly, several types of carbonyl compounds that do not react readily with Wittig reagents would undergo Wittig-like reactions with the tantalum reagent. These include esters, amides and CO_2 .⁵

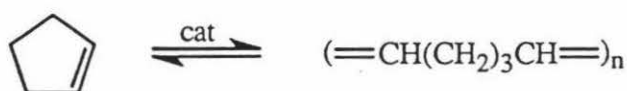


Equation 1

Alkylidene catalysts are proposed to be involved in the olefin metathesis reaction (Equ. 2),⁴¹ and ring-opening polymerisation, utilising a homogeneous catalyst (Equ. 3).⁴² It has been suggested by Green, Rooney and coworkers⁴³ that Ziegler-Natta olefin polymerisation may in some cases proceed via the intermediacy of alkylidene species.



Equation 2



Equation 3

Carbyne and Alkylidyne Complexes:

Although there seems to be a chemical basis for distinguishing between the low-valent carbynes on the one hand and the d^0 alkylidyne on the other, the distinction is less clear cut than in the case of the carbene/alkylidene dichotomy. One complication arises in assigning the oxidation state of these species. Alkylidyne ligands (Fig. 16) have been described as CR^{3-} , CR neutral and CR^+ , so there is often an ambiguity in assigning oxidation states in alkylidyne compounds. The description of the alkylidyne ligand as CR^{3-} , is most accurate in high oxidation state complexes of electropositive metals such as tantalum or tungsten. As CR^{3-} , the alkylidyne ligand is a better π -donor than N^{3-} , NR^{2-} and O^{2-} ; when taken as CR^+ it is a better π -acceptor than CO .⁴⁴



Figure 16

The first carbyne complex reported were the complexes $M(\equiv CR)(CO)_4X$ ($M=Cr, Mo, W$; Fig. 17) in 1973 by Fischer *et al.*⁴⁵ Five years later, Schrock⁴⁶ reported the synthesis of the neutral d^0 alkylidyne complex shown in figure 18.

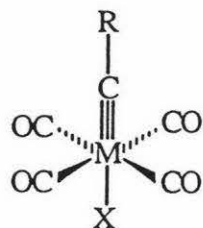


Figure 17

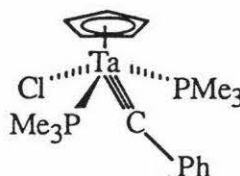
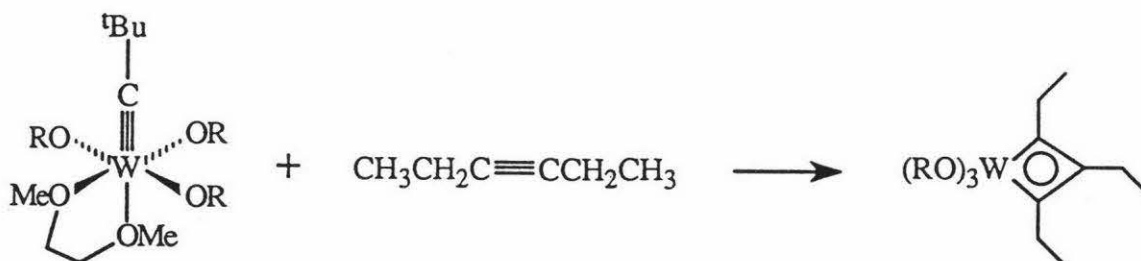


Figure 18

Studies of alkylidyne complexes have afforded the first well-defined catalysts for acetylene metathesis and suggest that known catalysts for this reaction may be converted to alkylidyne species under the right conditions.⁴⁷ Equation 4 shows the reaction of $W(\equiv C^tBu)(dme)(OR)_3$ with 3-hexyne to give a tungstenacyclobutadiene complex, $W(C_3Et_3)(OR)_3$, which can act as a catalyst for the metathesis of disubstituted acetylenes.



Equation 4

Terminal Imido Complexes:

Terminal imido complexes (Fig. 19) are currently known for all the metals of vanadium through iron triads plus iridium.



Figure 19

In 1956 the first organoimido transition metal complex, *t*-butylimidotrioxo osmium(VIII), was reported by Clifford and Kobayashi.⁴⁸ By 1962 an extensive series of arylimido rhenium complexes (Fig. 20) was known.⁴⁹ A review surveying organoimido chemistry through to 1994 has been published.⁵⁰

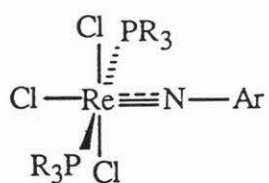


Figure 20

The imido ligand can be considered to bond to a transition metal with one σ and either one or two π interactions. Simple valence bond descriptions suggest that the metal-nitrogen bond order can be inferred from the position of the substituent, at least to a first approximation. A linear M-N-R unit implies that there is a metal-nitrogen triple bond (A; Fig. 21), while substantial bending of the M-N-R linkage (B; Fig. 21) indicates the presence of a lone pair on the nitrogen and is usually taken as evidence for a reduced bond order.⁵¹ However, a linear M-N-R unit with a bond order between 2 and 3 (C; Fig. 21) cannot be ruled out and as such reference to the bond order based on the M-N-R angle must be viewed with caution.

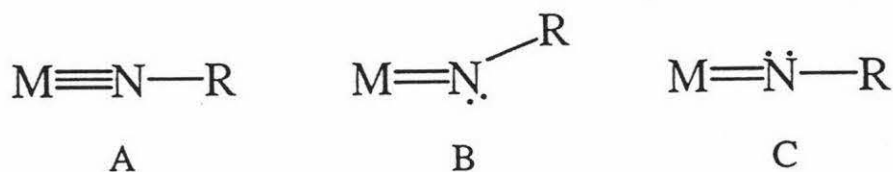
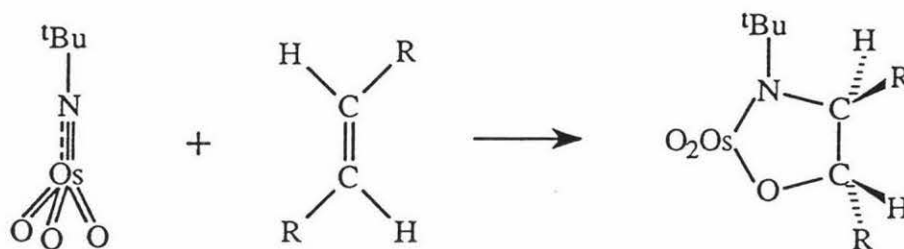


Figure 21

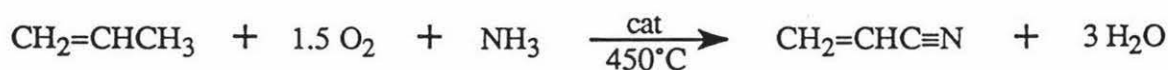
Most structurally characterised M-N-R moieties are near linear suggesting A and C of figure 21. In C, the M=N double bond is maintained if symmetry restrictions (or perhaps a severe energetic mismatch with available metal orbitals) do not allow lone-pair donation. However, in most systems, lone-pair $p(\pi) \rightarrow M(d)$ donation is very effective leading to the linear structure depicted in A with a M-N bond order approaching 3.

The *t*-butylimidotrioxoosmium(VIII) complex and its analogues effect the cis vicinal oxyamination (Equ. 5) of a variety of alkenes in either a stoichiometric or catalytic manner.⁵² Subsequently the synthesis of di, tri and even tetra-imido analogues of osmium tetroxide have been reported that promote the corresponding vicinal diamination reaction.⁵³

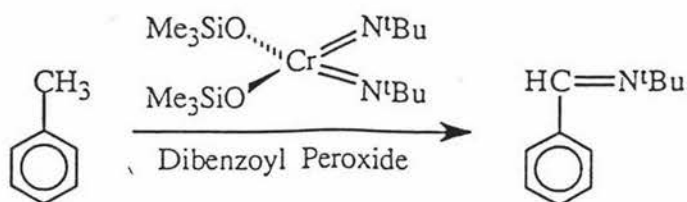


Equation 5

Imido species have been postulated as intermediates in catalytic processes. Surface molybdenum imido species have been suggested in the industrial “ammoxidation” of propylene to acrylonitrile (Equ. 6).⁵⁴ It has been shown that the diimido-chromium(VI) complex in equation 7 reacts with toluene in the presence of a stoichiometric radical source to afford the imine in up to 50% yield.^{54c} This is important since observations on model systems indicate that if imido sites exist, their proposed reaction with alkyl or benzyl radicals are chemically reasonable.



Equation 6

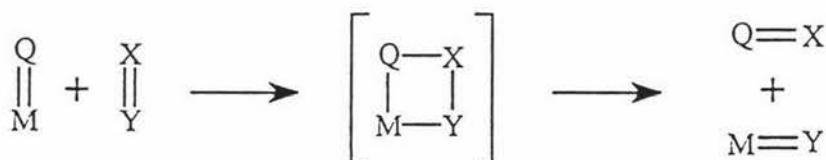


Equation 7

Weiss and coworkers⁵⁴ have utilised imido complexes to catalyse the exchange of imide groups in carbodiimides (Equ. 8). This “aza analogue” of olefin metathesis appears to proceed by a four-center mechanism as shown in equation 9.



Equation 8



Equation 9

Organoimido ligands have come into their own as ancillary ligands in organometallic chemistry and homogeneous catalysis. Of particular interest is Schrock's use of the arylimido ligand in figure 22. The tungsten complex in figure 22 ($\text{R}_f = \text{OCMe}(\text{CF}_3)_2$) is a highly active, neutral olefin metathesis catalyst.^{54c}

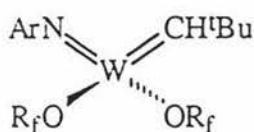


Figure 22

Synthetic methods for introducing terminal imido ligands

There are numerous methods for the synthesis of terminal imido complexes.

The most common are listed below.

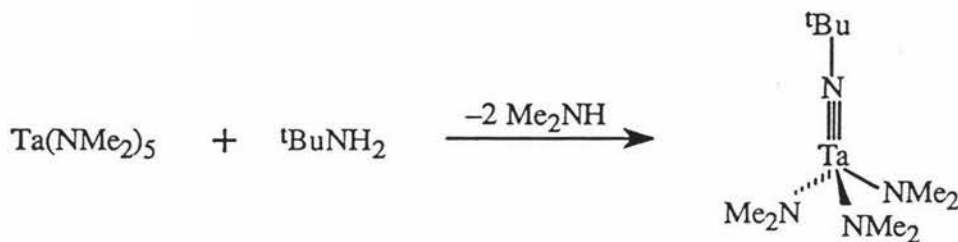
- 1) N-H bond cleavage in amines/amides
- 2) N-Si bond cleavage in silylamines/silylamides
- 3) from isocyanates, phosphinimines, sulfinylamines, carbodiimides, organoimines and related reagents that contain element=N double bonds
- 4) with organic azides, N_3R
- 5) from transition metal-imido species
- 6) methods of limited synthetic use;
 - (i) with azo compounds, $RN=NR$
 - (ii) reaction involving nitriles
 - (iii) electrophilic attack on a nitrido ligand
 - (iv) from a metallaaziridine precursor
 - (v) from cleavage of hydrazines and
 - (vi) from aryl nitroso compounds.

Methods 1 and 2 involve cleavage of a nitrogen α -substituent single bond, 3 and 5 are imido metathesis via net [2+2] reaction with no change in metal oxidation state, 4 and 6(i) involve reagents that can transfer NR with oxidation of the metal center. Each of the above methods is discussed briefly below.

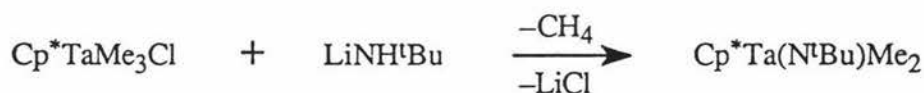
1) N-H bond cleavage in amines/amides:

These can be considered amine or amido deprotonation reactions with a chloride, amide, oxide or alkyl ligand serving as the proton acceptor, or as a formal α -H “abstraction” or “elimination”.

Typical strongly basic leaving groups have been σ alkyl substituents or dialkylamido ligands as shown in equations 10-12.⁵⁷



Equation 10



Equation 11



Equation 12

Steric congestion is frequently a critical factor in promoting formation of ligand-metal multiple bonds. For example the complex $\text{Mo}(\text{NHR})_2(\text{OSiMe}_3)_4$ ($\text{R}=1$ -adamantyl, Fig. 23a) is robust and has been characterised structurally.⁵⁸ Efforts to prepare the complex with $\text{R}=t$ -butyl have instead afforded $\text{Mo}(=\text{NR})_2(\text{OSiMe}_3)_2$ (Fig. 23b).

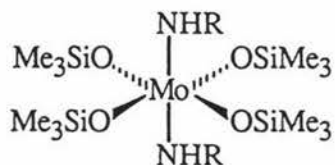


Figure 23a

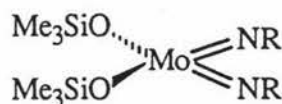
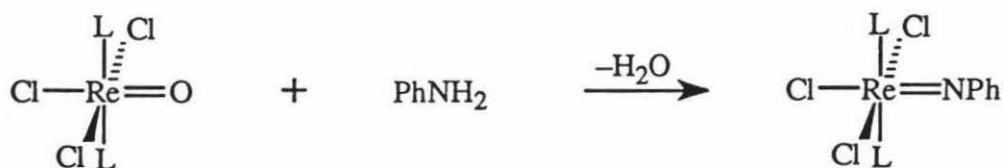


Figure 23b

Synthesis involving the interconversion of a terminal oxo ligand to the imido ligand with loss of H₂O is illustrated in equations 13 (L=PEt₂Ph)⁴⁹ and 14.⁵⁹

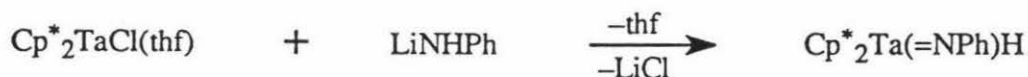


Equation 13



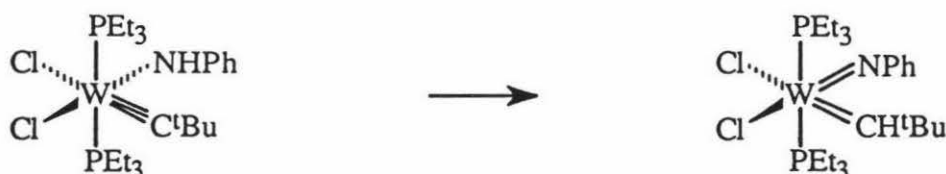
Equation 14

The d² complex Cp*₂TaCl(thf) has proven to be a useful precursor for d⁰ imido complexes by replacement of chloride by [NHR]⁻, followed by α-H elimination from d² “Cp*₂TaNHR” to form the complexes Cp*₂Ta(=NR)H (Equ. 15).⁶⁰



Equation 15

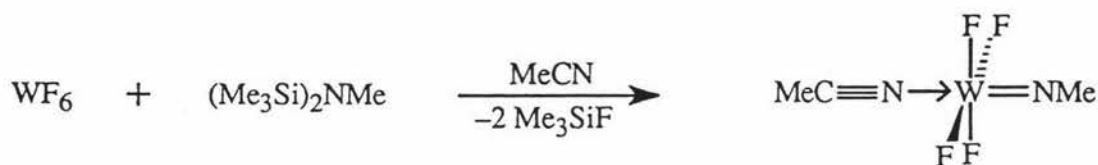
A special case among α-H transfer reactions is that in which the proton (or hydrogen) acceptor is itself another multiply bonded ligand. For example the tungsten alkylidyne complex (Equ. 16) can be converted to the imido/alkylidene complex.⁶¹



Equation 16

2) N-Si bond cleavage in silylamines/silylamides:

The strong bonds that form between silicon and oxygen or halides makes these ligands the most common acceptor in a SiR_3 group transfer that effects cleavage of a N-Si bond. The typical side-products from such reactions are volatile species such as Me_3SiCl or $\text{Me}_3\text{SiOSiMe}_3$, which can simply be distilled away with the solvent. The silicon based approach has been particularly productive for synthesis of imido compounds. An early example was Winfields synthesis of a tungsten methylimido species shown in equation 17.⁶² The reaction of $\text{Me}_3\text{SiNH}^t\text{Bu}$ with NH_4VO_3 affords $\text{V}(=\text{N}^t\text{Bu})(\text{OSiMe}_3)_3$ ⁶³ and reaction of $(\text{Me}_3\text{Si})_2\text{NMe}$ with CpNbCl_4 forms the imido complex $\text{CpNb}(=\text{NMe})\text{Cl}_2$.⁶⁴ A further example with $\text{Me}_3\text{SiNH}^t\text{Bu}$ is shown in equation 18.⁵⁸



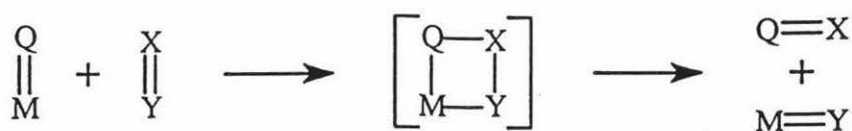
Equation 17



Equation 18

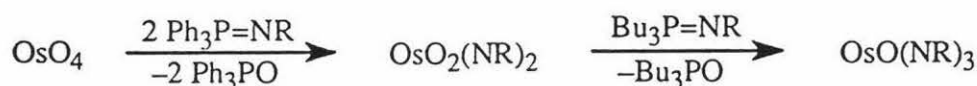
3) from reagents that contain element=N double bonds:

These reactions involve the direct replacement of an existing multiply bonded ligand by another upon treatment with an unsaturated reagent, as shown in equation 19. Isocyanates ($\text{RN}=\text{C}=\text{O}$), phosphinimines ($\text{R}_3\text{P}=\text{NR}$), sulfinylamino ($\text{RN}=\text{S}=\text{O}$), carbodiimides ($\text{RN}=\text{C}=\text{NR}$), organoimines ($\text{RN}=\text{CHR}$) and related reagents that contain element=N double bonds have all been observed to react with metal-ligand double bonds (especially $\text{M}=\text{O}$) in metathesis reactions.



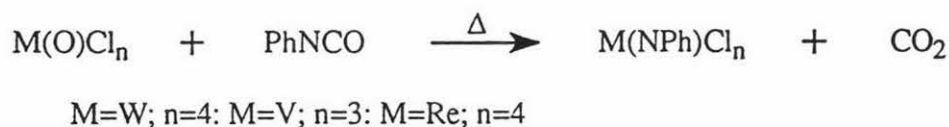
Equation 19

A most intriguing application of this method was in the synthesis of di- and tri-imido analogues of osmium tetroxide by Sharpless and coworkers.⁵³ Triphenylphosphinimines were sufficiently reactive to introduce two imido substituents but the third imido requires the more reactive tributylphosphinimine (Equ. 20).



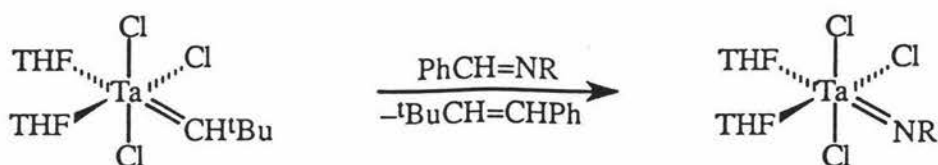
Equation 20

The isocyanate route was first used by Soviet workers to convert $\text{L}_2\text{Cl}_3\text{Re}=\text{O}$ to $\text{L}_2\text{Cl}_3\text{Re}=\text{NPh}$ ($\text{L}=\text{PPhEt}$).⁶⁵ Subsequently this has developed into an important synthetic method, since the products (Equ. 21) are themselves versatile starting materials for a wide range of other imido species.⁶⁶



Equation 21

The conversion of alkylidene complexes into their imido analogues has been exploited by Schrock and coworkers. As shown in equation 22, treatment of group five neopentylidene complexes ($\text{M}=\text{Nb}, \text{Ta}; \text{X}=\text{Cl}, \text{Br}$) with benzylidene alkylamine, $\text{PhCH}=\text{NR}$, affords the corresponding organoimido complexes, with concomitant loss of the olefin.⁶⁷



Equation 22

4) with organic azides, N_3R :

The decomposition of azides with formation of dinitrogen is a broadly useful synthetic route to imido complexes.⁶⁸ The extrusion of N_2 as a side-product results in easy product isolation as well as providing a large driving force for such reactions. Equations 23 and 24 show reactions of azides with R being Me_3Si and *p*-tolyl respectively. This method requires the oxidation state of the metal to be increased by 2 units.



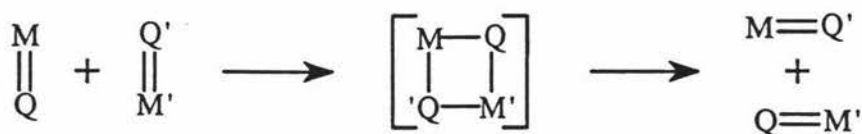
Equation 23



Equation 24

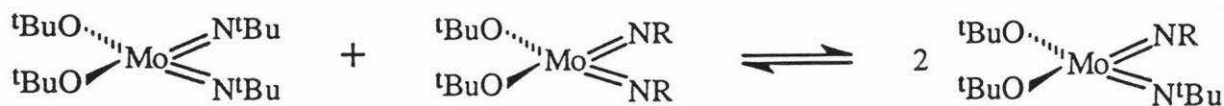
5) from transition metal-imido species:

It has recently been discovered that transition metal imides can undergo facile, bimolecular exchange with other multiply bonded ligands.⁵⁰ The reaction can be considered to proceed in a "Wittig-like" manner as given in equation 25 (c.f. Equ. 19).

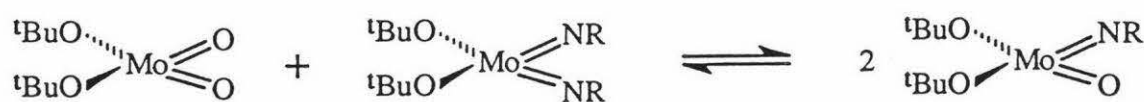


Equation 25

Imido ligand exchange proceeds at room temperature for the four-coordinate species $\text{Mo}(\text{N}^t\text{Bu})_2(\text{O}^t\text{Bu})_2$ and $\text{Mo}(\text{NR})_2(\text{O}^t\text{Bu})_2$ (Equ. 26) and even more rapidly for the oxo-imido ligand exchange shown in equation 27.^{64c} The latter reaction is believed to involve an ordered transition state, involving bridged oxo and imido ligands (Fig. 24) and in general keeping with the four-center mechanism (Equ. 25).^{64c}



Equation 26



Equation 27

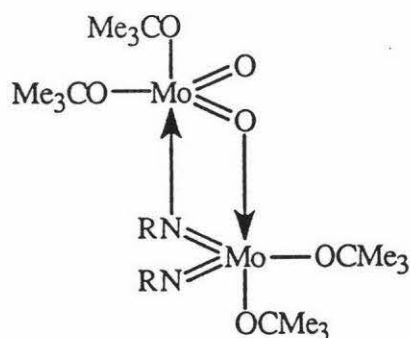


Figure 24

Finally the exchange of alkylidene for imido ligands has been observed according to the reaction shown in equation 28.^{64c}

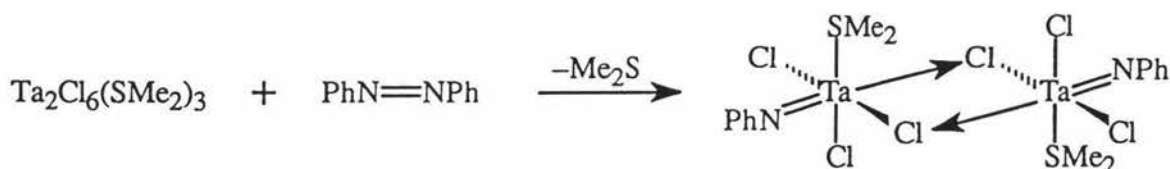


Equation 28

6) methods with limited synthetic use:

(i) with azo compounds, RN=NR:

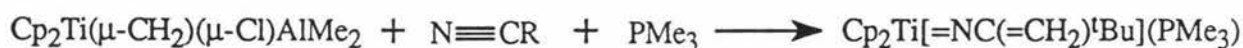
Azoalkanes can be cleaved by low-valent metals to give organoimido complexes. For example, equation 29 proceeds for both niobium and tantalum to give chloride-bridged imido dimers as structurally characterised products.⁶⁹ However, the reaction is limited to the use of azobenzene in the vast majority of cases.⁷⁰



Equation 29

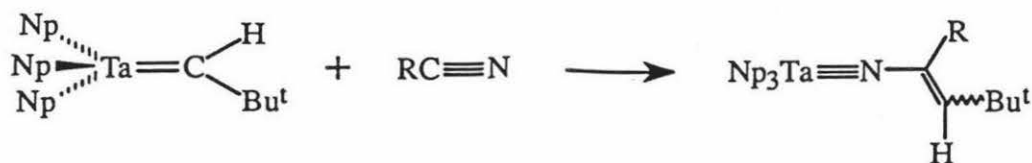
(ii) reaction involving nitriles:

Titanocene metallacyclobutanes react with nitriles in the presence of a lewis base such as trimethylphosphine to afford vinylimido complexes of titanocene. The reaction of $\text{Cp}_2\text{Ti}(\mu\text{-CH}_2)(\mu\text{-Cl})\text{AlMe}_2$, $\text{N}\equiv\text{CR}$ ($\text{R}=\text{tBu}$, 1-ad) and excess PMe_3 , in the presence of DMAP (to scavenge AlMe_2Cl) afford the vinylimido complexes shown in equation 30.⁷² These compounds also arise from the reaction of titanacyclobutane $\text{Cp}_2\text{Ti}[\text{CH}_2\text{CH}(\text{tBu})\text{CH}_2]$ with $\text{N}\equiv\text{CR}$ and excess PMe_3 .⁷²



Equation 30

Tantalum alkylidene complexes have been shown to react with nitriles with formation of an imido ligand ($\text{R}=\text{Me}$, Ph ; Equ. 31).⁷¹ This is however, a rare example, with no subsequent reports of other alkylidene complexes reacting in this way.



Equation 31

(iii) electrophilic attack on a nitrido ligand:

The complexes $(\text{dmtc})_3\text{Mo}\equiv\text{N}$, where dmtc is dimethyldithiocarbamate, apparently contain an unusually electron-rich nitrido ligand that can be alkylated even with methyl iodide to afford a cationic methylimido compound, $[(\text{dmtc})_3\text{Mo}=\text{NMe}]^+$. A number of other alkylating and acylating agents react similarly, including PhCOCl , $[\text{R}_3\text{O}]\text{BF}_4$, $[\text{Ph}_3\text{C}]\text{BF}_4$ and even 2,4-dinitrophenyl chloride.⁷³

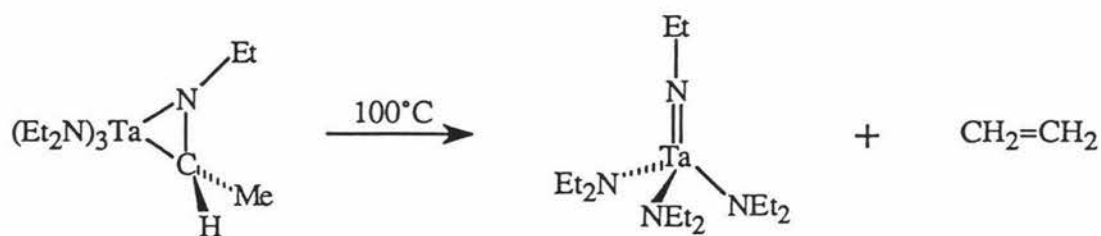
One notable example is the alkylation of the nitrido ligand in $[n\text{-Bu}_4\text{N}][\text{Ru}(\equiv\text{N})(\text{CH}_2\text{SiMe}_3)_4]$. Treatment of the complex with Me_3SiOTf (Et_2O , -30°C) affords oily, orange crystals of $\text{Ru}(\text{=NSiMe}_3)(\text{CH}_2\text{SiMe}_3)_4$ in 92% yield (Equ 32). This was the first characterised ruthenium-imido complex.⁷⁴



Equation 32

(iv) from a metallaaziridine precursor:

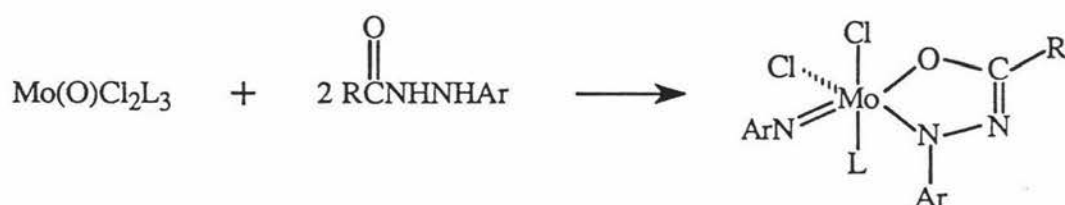
Takahashi *et al.* have reported that treatment of TaCl_5 with lithium diethylamide at low temperature produces an η^2 -Schiff's base derivative ethyliminoethyl-(C,N)tris(diethylamido)tantalum.⁷⁵ On heating to 100°C , this complex undergoes clean first order loss of ethylene to afford the ethylimido compound (Equ. 33). Although this synthetic route is rare, a recent example resulting in the formation of a metallocycle imido ligand was reported in 1992.⁷⁶



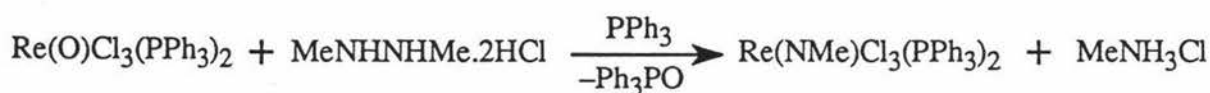
Equation 33

(v) from cleavage of hydrazines:

A series of organoimido complexes have been prepared by the cleavage of unsymmetrical acyl hydrazines according to equation 34 (R=alkyl, aryl; L=PMePh₂, PEt₂Ph).⁷⁷ The cleavage of symmetrical hydrazines has been used to synthesize alkylimido rhenium complexes.⁷⁸ Although the mechanism of the reaction is unknown, the reaction is suggested to follow equation 35. This method is rare with the molybdenum and rhenium examples constituting its use to date.



Equation 34

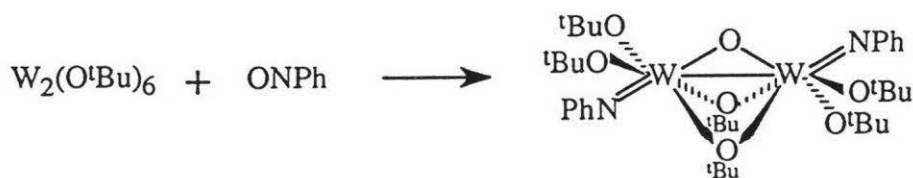


Equation 35

(vi) from aryl nitroso compounds:

In a paper by Cotton *et al.* was the first reaction of a nitroso compound, nitrosobenzene (C₆H₅NO) with W₂(OCMe₃)₆ (Equ. 36). This gave a product in which a remarkable double oxidative addition has occurred leading to the formation of W=N double

bonds with concomitant loss of the $W \equiv W$ bond.⁷⁹ The arylnitroso-ligand, ONtol, of $Re(ONtol)Cl_3(OPPh_3)$ can easily be deoxygenated by transferring the oxygen to a reducing agent such as tertiary phosphine, PPh_3 (Equ. 37) or cyclohexyl isocyanide. The reaction with triphenylphosphine requires acetonitrile as solvent.⁸⁰



Equation 36



Equation 37

Known metal terminal imido complexes of Os(II), Ir(III) and Ruthenium

This section summaries the known imido-metal functional groups of ruthenium and emphasises complexes of d^6 $Os=NR$ and d^6 $Ir=NR$. Presented in table 1 are the known terminal imido complexes of the transition metals. For descriptions of each functional group listed in table 1, refer to the excellent review "Organoimido Complexes of the Transition Metals" by David E. Wigley.⁵⁰

d^0 Ti=NR	d^{0-2} V=NR d^0 V(=NR) ₂	d^{0-2} Cr=NR d^{0-2} Cr(=NR) ₂ d^0 Cr(=NR) ₄	d^2 Mn=NR d^2 Mn(=NR) ₂ $d^{0,1}$ Mn(=NR) ₃	d^3 Fe=NR	
d^0 Zr=NR	$d^{0,2}$ Nb=NR d^0 Nb(=NR) ₂ d^0 Nb(=NR) ₃ d^0 Nb(=NR) ₄	d^{0-4} Mo=NR d^{0-2} Mo(=NR) ₂ d^0 Mo(=NR) ₃ d^0 Mo(=NR) ₄	$d^{2,3}$ Tc=NR $d^{0,1}$ Tc(=NR) ₂ d^{0-2} Tc(=NR) ₃	d^{2-4} Ru=NR $d^{2,4}$ Ru(=NR) ₂	
d^0 Hf=NR	$d^{0,2}$ Ta=NR d^0 Ta(=NR) ₂ d^0 Ta(=NR) ₃	d^{0-4} W=NR $d^{0,2}$ W(=NR) ₂ d^0 W(=NR) ₃ d^0 W(=NR) ₄	$d^{0-4,6}$ Re=NR $d^{0-2,4}$ Re(=NR) ₂ d^{0-2} Re(=NR) ₃ d^0 Re(=NR) ₄	$d^{0,2-4,6}$ Os=NR $d^{0,2,4}$ Os(=NR) ₂ d^{0-2} Os(=NR) ₃ d^0 Os(=NR) ₄	d^6 Ir=NR

Table 1: Terminal imido functional groups

-Low valent iridium and osmium

In 1989 Bergman *et al.* reported the first examples of an iridium imido complex. Reacting dimeric $[\text{Cp}^*\text{IrCl}_2]_2$ with 4 equiv of LiNH^tBu affords yellow crystals of monomeric $\text{Cp}^*\text{Ir}=\text{N}^t\text{Bu}$ in high yield, along with the by-product $\text{H}_2\text{N}^t\text{Bu}$.⁸¹ The complexes $\text{Cp}^*\text{Ir}=\text{NR}$ [$\text{R}=\text{SiMe}_2^t\text{Bu}$, 2,6-dimethylphenyl (Ar'') and 2,6-diisopropylphenyl(Ar)] are all similarly prepared. Although $\text{Cp}^*\text{Ir}=\text{NAr}''$ and $\text{Cp}^*\text{Ir}=\text{NAr}$ have been prepared by reacting $\text{Cp}^*\text{IrCl}_2\text{Ar}''\text{NH}_2$ and $\text{Cp}^*\text{IrCl}_2\text{ArNH}_2$ with $\text{K}[\text{N}(\text{SiMe}_3)_2]$ or from imido exchange between $\text{Cp}^*\text{Ir}=\text{N}^t\text{Bu}$ and free H_2NR ($\text{R}=\text{Ar}''$ or Ar), which also forms $\text{H}_2\text{N}^t\text{Bu}$.^{81a} Despite the formal oxidation state and the low coordination number of the Ir(III) compounds, they were found to be monomeric by X-ray diffraction studies. Shown in figure 25 is the crystal structure of $\text{Cp}^*\text{Ir}=\text{NAr}$, which has a Ir-N-C angle of $174.0(6)^\circ$.

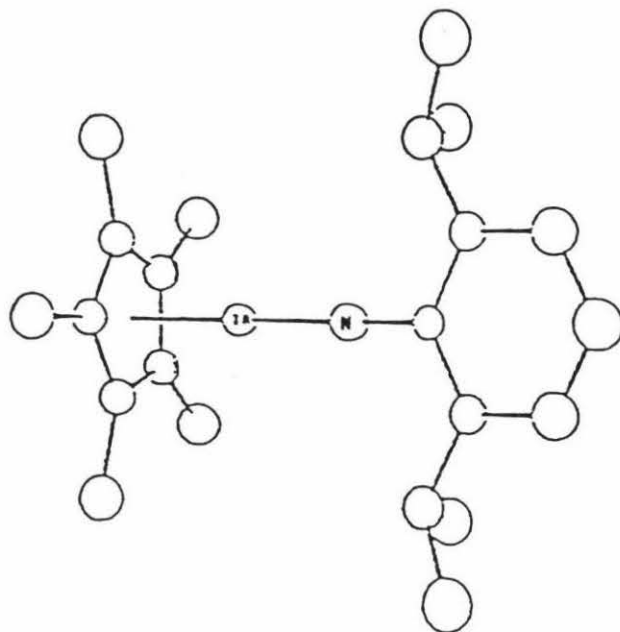


Figure 25

While many osmium imido complexes are known, very few examples of low valent osmium imides have been characterised. One exception is the d^6 complexes reported by Bergman in 1991.^{82a} These osmium complexes resulted from an extension of the $Cp^*Ir=NR$ chemistry, to the group 8 metals.

The known d^6 compounds are all formed from the reactions of $LiNHR$, where R is tBu , Ar or Ar'' with the halide precursors $[(\eta^6\text{-arene})OsCl_2]_2$ ($\eta^6\text{-arene} = C_6Me_6$ or cym) or with imido exchange from the N^tBu to the NAr'' imido ligand. Thus, $[(\eta^6\text{-arene})OsCl_2]_2$ reacts with 2 equiv of $LiNH^tBu$ per osmium to form the d^6 compounds $(\eta^6\text{-arene})Os=N^tBu$, which can then react with NH_2Ar'' to form $(\eta^6\text{-arene})Os=NAr''$ and NH_2^tBu .⁸² The complex $(\eta^6\text{-}C_6Me_6)Os=N^tBu$ was shown to be monomeric by a crystal structure determination (Fig. 26).^{82b} The complexes $(cym)Os=N^tBu$ and $(cym)Os=NR$ ($R = Ar$ or Ar'') are inferred to be monomeric on the basis of spectroscopic data.

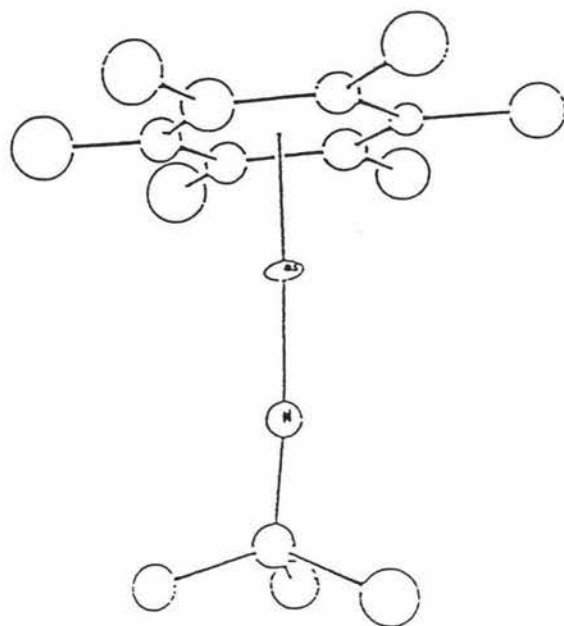


Figure 26

-Ruthenium

The chemistry of ruthenium imides has developed slowly compared to that of osmium, with only a handful of compounds known. A number of bridging imido ligands have been identified in clusters. But it was not until 1992 that the first X-ray structure of a terminal mononuclear imido complex of ruthenium was reported.

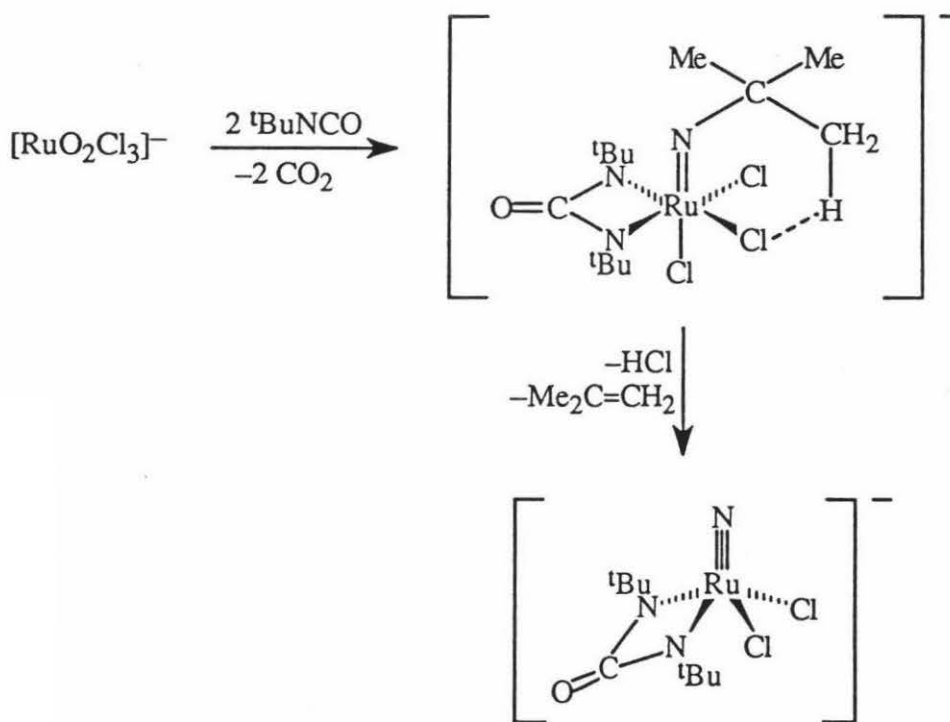
The first characterised ruthenium-imido complex was reported by Shapley and coworkers⁷⁴ in 1988. Alkylation of the nitrido ligand in $[n\text{-Bu}_4\text{N}][\text{Ru}(\equiv\text{N})(\text{CH}_2\text{SiMe}_3)_4]$ with Me_3SiOTf affords oily, orange crystals of $\text{Ru}(=\text{NSiMe}_3)(\text{CH}_2\text{SiMe}_3)_4$ in 92% yield. This complex is difficult to characterise due to its extreme air and moisture sensitivity. Both ruthenium nitrido anions $[\text{Ru}(\equiv\text{N})(\text{CH}_2\text{SiMe}_3)_4]^-$ and $[\text{Ru}(\equiv\text{N})\text{Me}_4]^-$ can be methylated using MeI , $[\text{Me}_3\text{O}][\text{BF}_4]$ or MeOTf , but the resulting products are thermally unstable.

Wilkinson and coworkers⁸³ described the reaction of $\text{Ru}_2(\mu\text{-O})_2(\text{CH}_2\text{SiMe}_3)_6$ with PhNCO to generate brown, microcrystalline $\text{Ru}_2(=\text{NPh})_2(\text{CH}_2\text{SiMe}_3)_6$ in moderate yield. While its structure is not known, a strong I.R. band at 1132cm^{-1} is assigned as a terminal imido $\nu(\text{Ru}=\text{N})$ band, however, a structure containing asymmetrically bridged $\mu\text{-NPh}$ groups cannot be ruled out in view of the problems with such I.R. assignments.⁸⁴ A similar reaction

of $\text{Ru}_2(\mu\text{-O})_2(\text{CH}_2\text{SiMe}_3)_6$ with $\text{Me}_3\text{P}=\text{NSiMe}_3$ affords orange crystals of $\text{Ru}_2(=\text{NSiMe}_3)_2(\text{CH}_2\text{SiMe}_3)_6$ in low yield.⁸³

Terminal imido complexes of Ru(IV) are proposed on the basis of only indirect evidence. Thus, electrochemical experiments in which the oxidation of ammonia to nitrate is observed lead to the proposal that unstable $[\text{Ru}(\text{NH}_3)(\text{tpy})(\text{bpy})]^{3+}$ undergoes disproportionation to form the imido complexes $[\text{Ru}(=\text{NH})(\text{tpy})(\text{bpy})]^{2+}$ and $[\text{Ru}(\text{NH}_3)(\text{tpy})(\text{bpy})]^{2+}$.⁸⁵

Although not directly observed, there is compelling evidence for the participation of d^2 $\text{Ru}(=\text{NR})_2$ complexes in a number of reactions. For example, the reaction of $[\text{PPh}_4][\text{RuO}_2\text{Cl}_3]$ with excess ${}^t\text{BuNCO}$ leads to the isolation of the nitrido salt $[\text{PPh}_4][\text{N}=\text{Ru}(\text{N}{}^t\text{BuC}(\text{O})\text{N}{}^t\text{Bu})\text{Cl}_2]$ (Equ. 38).⁸⁶ This complex is proposed to arise via the intermediacy of an imido complex such as $[\text{Ru}(=\text{N}{}^t\text{Bu})_2\text{Cl}_3]^-$, which cycloadds another isocyanate to form the N,N'-ureato ligand (Equ. 38).



Equation 38

The only example of the d^4 $\text{Ru}(=\text{NR})_2$ moiety was reported in 1992 by Wilkinson and coworkers.⁸⁷ The reaction of *trans*- $\text{RuCl}_2(\text{PMe}_3)_4$ with an excess of LiNHAr in THF, afforded an orange solution containing an amido species. Upon O_2 oxidation, a blue-green solution forms that affords blue crystals of diamagnetic *trans*- $\text{Ru}(=\text{NAr})_2(\text{PMe}_3)_2$ in 16% yield. The structure of this complex reveals a square-planar derivative in which the molecule lies on a center of symmetry with *trans* imido groups (Fig. 27).

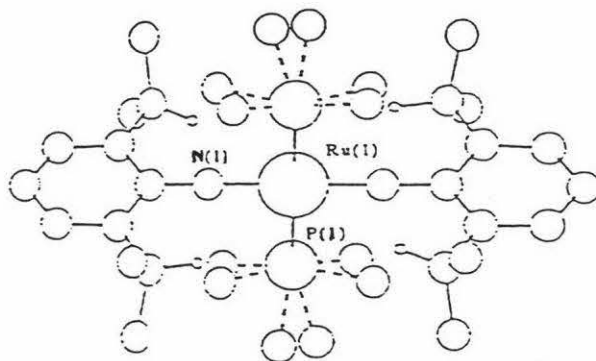


Figure 27

In summary, only a handful of ruthenium terminal imido complexes are known, with only one fully characterised. In contrast numerous terminal imido complexes of osmium from d^0 to d^6 have been reported. Also fully characterised terminal imido complexes are known for d^6 Os and d^6 Ir. It is therefore reasonable that similar complexes should exist for ruthenium and rhodium. It appears that terminal imido complexes of rhodium are extremely reactive and as such no rhodium compounds have been reported.⁵⁰ With a number of ruthenium terminal imido complexes known,⁵⁰ it would seem reasonable that a terminal d^6 ruthenium imido complex should be stable. Thus, Schrock *et al.* attempted the synthesis of " $(\text{C}_6\text{H}_6)\text{Ru}=\text{NAr}$ " using the sterically demanding 2,6-diisopropylphenylimido (Ar) ligand. However, reaction of $[(\text{C}_6\text{H}_6)\text{RuCl}_2]_2$ with 4 equiv of LiNHAr in ether lead to the bridging imido complex, $[(\text{C}_6\text{H}_6)\text{Ru}(\mu\text{-NAr})]_2$, shown by X-ray diffraction.⁸⁸

This thesis presents the use of the sterically demanding imido ligands, 2,6-diisopropylphenyl (Ar) and 2,4,6-tri-*tert*-butylphenyl (Ar'), to synthesize the first d^6 ruthenium

terminal imido complexes. The results obtained with the Ar' imido ligand has resulted in the recent publication of a paper.⁸⁹

Chapter Two

Results and Discussion

The imido ligand has received considerable attention in recent years, primarily because of its ability to stabilise high oxidation states by multiple electron donation.⁵ Relatively few studies have focused on terminal imido complexes of the later transition elements.^{50,81,82,90} particularly those of low valent ruthenium.^{50,88} Recent studies by Schrock⁸⁸ and Michelman⁹¹ on Ru(II) imido complexes have afforded dimeric complexes containing bridging imido ligands.

By use of an imido ligand with greater steric demand than the 2,6-diisopropylphenylimido ligand previously used, the synthesis of a monomeric complex containing a terminal imido ligand may be feasible.

The following discussion covers the strategy behind the synthetic method used to synthesize the imido complexes, including remarks on the precursors and the necessary use of sterics. Details of the crystal structures of $[(\text{cym})\text{Ru}=\text{NAr}']_n$, $[(\text{cym})\text{Ru}=\text{NAr}]_n$, $(\text{C}_6\text{Me}_6)\text{RuClNHAr}$ and $(\text{cym})\text{RuCl}_2\text{NH}_2\text{Ar}$, where Ar is 2,6-diisopropylphenyl and Ar' is 2,4,6-tri-*t*-butylphenyl, are given and the surprising lack of reactivity towards alkynes is noted. Finally a few words on future directions ends this section.

The Role of Sterics

The use of sterically demanding ligands has been investigated for technetium, rhenium and osmium. The effect of increasing the size of the imido ligand is most strikingly illustrated in the case for technetium. Tetrahydrofuran solutions of $[\text{Tc}(\text{NAr})_3\text{I}]$ react quickly at room temperature with sodium metal to form $[\text{Tc}_2(\text{NAr})_6]$ in high yield.⁹² An X-ray structure analysis of a single crystal of $[\text{Tc}_2(\text{NAr})_6]$ reveals an unprecedented "ethanelike" structure (Fig. 28a). Recently the analogous reaction of $[\text{Tc}(\text{NAr}')_3\text{I}]$, where Ar' is 2,6-dimethylphenyl, with Na metal gave the edge-bridged tetrahedral dimer, $\text{Tc}_2(\text{NAr}')_4(\mu\text{-NAr}')_2$ (Fig 28b).⁹³ Moving from the imido ligand Ar' to the larger Ar ligand has effected a change in geometry from a complex with 4 terminal and 2 bridging imido ligands, to a complex containing 6 terminal imido ligands.

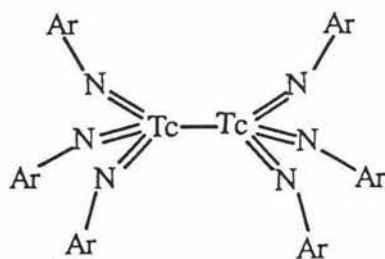


Figure 28a

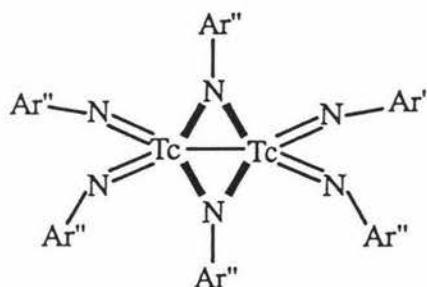


Figure 28b

A similar situation is suggested in the case of rhenium.⁹² The reduction of $[\text{Re}_2(\text{N}^t\text{Bu})_3(\text{OSiMe}_3)]$ with sodium amalgam⁹⁴ affords the edge-bridged tetrahedral dimer, $[\text{Re}_2(\text{N}^t\text{Bu})_4(\mu\text{-N}^t\text{Bu})_2]$. Preliminary work indicates that reduction of $[\text{Re}(\text{NAr})_3\text{I}]$ with sodium affords “ethanelike” $[\text{Re}_2(\text{NAr})_6]$ in good yield.⁹⁵ All previous examples of structurally characterised M_2E_6 complexes (where E stands for dianionic ligands such as N^tBu , S, Se which form multiple bonds to the metal center⁴) are edge-bridged tetrahedral dimers with sterically less demanding ligands such as S, Se and N^tBu . This preference has also been extensively demonstrated for M_2X_6 complexes, where X is a monoanionic ligand. They adopt a dimeric structure of edge-bridged tetrahedra for non-bulky X ligands and an “ethanelike” structure for bulky X ligands.⁶ A further example occurs with osmium. Reaction of OsO_4 with 3 equiv of ArNCO afforded the trigonal planar $\text{Os}(\text{NAr})_3$ in 50% yield (Fig 29a).⁹⁶ However reaction of $\text{Os}(\text{N}^t\text{Bu})_4$ with tertiary phosphines (PPh_3 , PMePh_2) in THF gives the phosphine imides $\text{R}_3\text{P}=\text{N}^t\text{Bu}$ and the Os(VI) dimer $[\text{Os}(\text{N}^t\text{Bu})_2(\mu\text{-N}^t\text{Bu})]_2$ (Fig 29b).⁹⁷

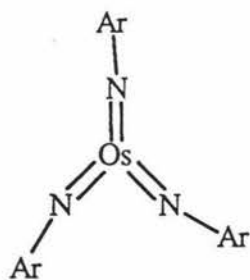


Figure 29a

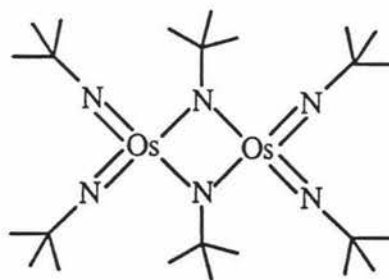


Figure 29b

These examples suggest that steric factors can control the conversion from the dimer to monomer structure. It only seems reasonable that Schrock's⁸⁸ Ru(II) dimer, $[(C_6H_6)Ru(\mu-NAr)]_2$ can be converted to the monomeric form by increasing the steric congestion about the metal center. This can be easily achieved by increasing the size of the imido ligand and/or the arene ring substituents.

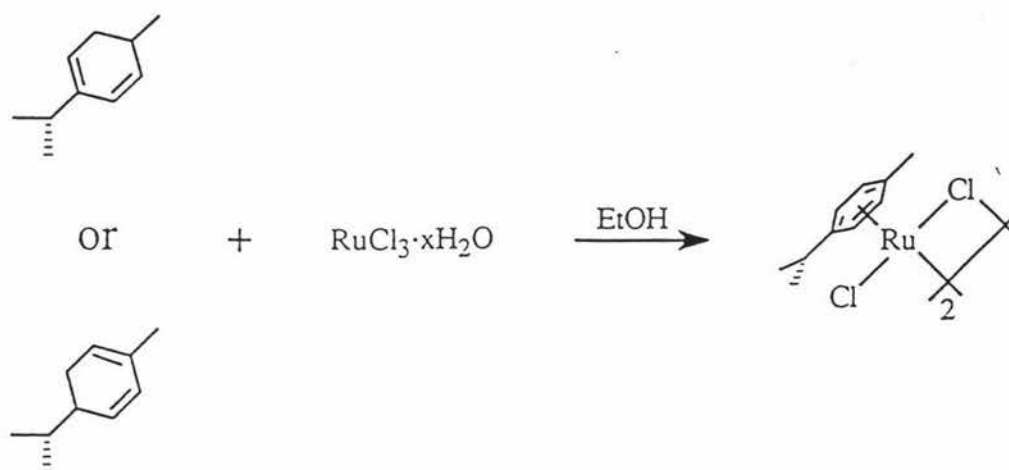
It is clear from the examples above that the sterically demanding imido ligand, Ar, has been large enough to effect the conversion of bridging to terminal imido ligands. However just as an insurance policy, the use of the even more sterically demanding ligand, Ar' (2,4,6-tri-*t*-butylphenyl), will be utilised as well as Ar'' (2,6-diisopropylphenyl) and Ar''' (2,6-dimethylphenyl).

Synthesis of Precursors

The following includes a brief discussion on the synthesis of the precursors. These include the ruthenium and rhodium chlorodimers, and the 2,4,6-tri-*t*-butylphenylimido ligand. More detail on the synthetic methods of the precursors can be found from the references cited.

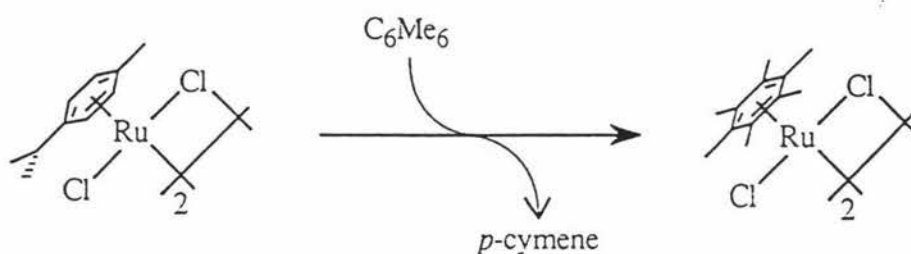
(i) the chlorodimers:

The method used to synthesis the chlorodimer, $[(cym)RuCl_2]_2$ has been developed not only for *p*-cymene⁹⁸, but also benzene⁹⁹ and substituted benzene derivatives, such as xylene, mesitylene^{99b} and 1,3,5-triphenylbenzene.¹⁰⁰ The method involves the dehydrogenation of cyclohexadiene derivatives by ethanolic solutions of $RuCl_3 \cdot xH_2O$ (Equ. 39; for *p*-cymene).¹⁰¹



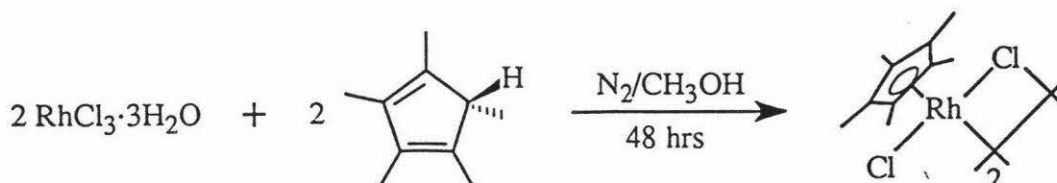
equation 39

The hexamethyl derivative, $[(\text{C}_6\text{Me}_6)\text{RuCl}_2]_2$, is obtained via arene ligand exchange. It is readily obtained by displacement of the labile *p*-cymene ligand, by fusing the *p*-cymene chlorodimer with hexamethylbenzene (Equ 40).^{98,102} This method involves the use of Filter Aid and a sublimation step. To avoid this sublimation the use of Soxhlet extraction was employed (see experimental section for details).



Equation 40

The chlorodimer, $[\text{Cp}^*\text{RhCl}_2]_2$, is a precursor to a wide range of $(\eta^5\text{-pentamethylcyclopentadienyl})\text{rhodium}$ complexes. They have previously been prepared by the reaction of hexamethylbicyclo[2.2.0]hexa-2,5-diene (hexamethyl Dewar benzene) with the metal trichloride.¹⁰³ However the procedure used here utilises the more readily available pentamethylcyclopentadiene.¹⁰⁴ Rhodium trichloride trihydrate and pentamethylcyclopentadiene are refluxed in methanol, under N_2 , for 48 hours (Equ. 41) giving a 85% yield.



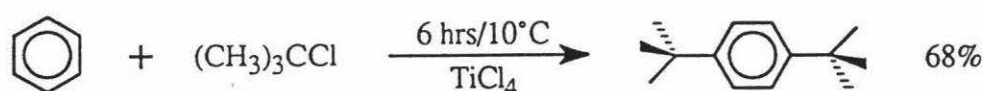
Equation 41

(ii) Ligands:

2,6-dimethylphenyl aniline (Ar'') and 2,6-diisopropylphenyl aniline (Ar) were purchased from aldrich. 2,4,6-tri-*t*-butylphenyl aniline (Ar') was prepared using a modification of previously reported procedures.^{105,106}

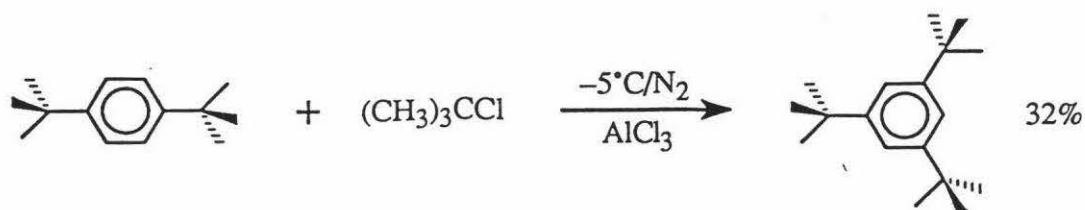
The Ar' imido ligand precursor was synthesized from benzene through two Friedal-Crafts alkylation steps to the 1,3,5-tri-*t*-butylbenzene compound. Then a nitration and reduction afforded the 2,4,6-tri-*t*-butylaniline compound, which was reacted with *n*-BuLi in benzene to afford the lithiated form.

The first step involved the use of TiCl₄ as the catalyst for the alkylation of benzene (Equ. 42). While TiCl₄ is not as active catalytically as AlCl₃, certain advantages over the latter are its solubility in organic solvents and the absence of much polyalkylation, all disubstituted products being para only.¹⁰⁵



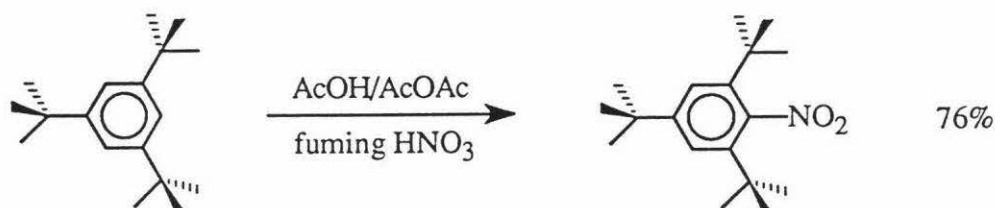
Equation 42

The second alkylation step involved the use of AlCl₃ and (CH₃)₃CCl at -5°C (Equ. 43).¹⁰⁶



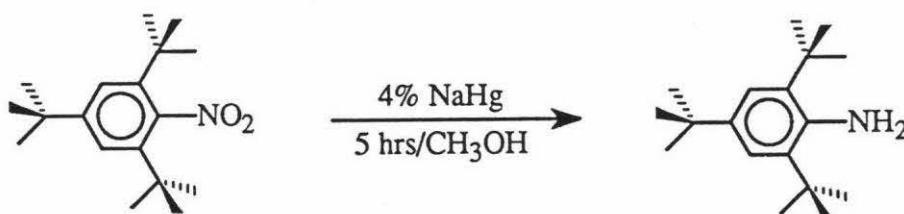
Equation 43

1,3,5-tri-*t*-butylbenzene was then carefully nitrated with fuming nitric acid in an acetic acid/acetic anhydride solution (Equ. 44).¹⁰⁶



Equation 44

Reduction of the nitro compound proved to be a struggle. Unsuccessful attempts were made to reduce 2,4,6-tri-*t*-butylnitrobenzene by reduction with stannous chloride, with zinc/conc. HCl at reflux for 3 hours and 24 hours, and with hydrogenation using Pd/C overnight. Finally, sodium amalgam was found capable of bringing about this reduction (Equ. 45).¹⁰⁶ The literature yield of 64% was never achieved, with the yield of the reduction of 24%, and this was only achieved after standing the solution for several months.



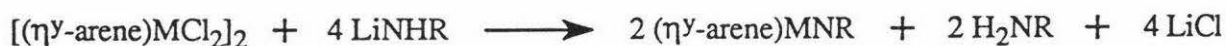
Equation 45

Synthetic Method

The following explores the strategy behind the simple one-step metathesis reaction employed to generate imido complexes and the products afforded from it. Also used is an alternative synthetic method, previously used by Bergman *et al.*^{81a} in the case of Ir(III) terminal imido complexes. Two possible mechanisms have been proposed for the synthesis of imido complexes using LiNHR reagents. Reference to these mechanisms is discussed, including the isolation of an HCl adduct common to both mechanistic pathways. Finally, the replacement of the η^6 -arene ligand with 2,2'-bipyridine is investigated with an encouraging result.

(i) the strategy:

The general strategy, shown in equation 46, has been successfully employed for iridium, osmium and Schrock's⁸⁸ Ru(II) bridging imido dimer.



$y=6$; $\text{M}=\text{Os}$; arene=cym; $\text{R}=\text{tBu}$, Ar'' , Ar

$y=6$; $\text{M}=\text{Os}$; arene= C_6Me_6 ; $\text{R}=\text{tBu}$

$y=6$; $\text{M}=\text{Ru}$; arene=benzene; $\text{R}=\text{Ar}''$, Ar

$y=5$; $\text{M}=\text{Ir}$; arene= Cp^* ; $\text{R}=\text{tBu}$, SiMe_2tBu , Ar'' , Ar

Equation 46

In 1989 a paper by Bergman *et al.*^{81b} reported a simple conversion of $[\text{Cp}^*\text{IrCl}_2]_2$ to the imido complexes Cp^*IrNR ($\text{R}=\text{tBu}$, SiMe_2tBu , Ar'' and Ar). Reaction of $[\text{Cp}^*\text{IrCl}_2]_2$ with 4 equiv of LiNHR in THF gives the compounds in high yield. Since $[(\eta^6\text{-C}_6\text{R}_6)\text{MCl}_2]_2$ ($\text{M}=\text{Os}$, Ru) complexes are isoelectronic with $[(\eta^5\text{-C}_5\text{Me}_5)\text{MCl}_2]_2$ ($\text{M}=\text{Rh}$, Ir) complexes they might react to give complexes analogous to the Cp^*IrNR compounds. In support of this, treatment of $[(\text{cym})\text{OsCl}_2]_2$ or $[(\text{C}_6\text{Me}_6)\text{OsCl}_2]_2$ with 4 equiv of LiNH^tBu in THF provides the terminal imido complexes $(\text{cym})\text{OsN}^t\text{Bu}$ and $(\text{C}_6\text{Me}_6)\text{OsN}^t\text{Bu}$ in 85-95%

yield.^{82a} In a later paper^{82b} the complexes (cym)OsNAr'' and (cym)OsNAr were prepared in an analogous manner.

With all these examples, it seems reasonable that the ruthenium analogue could also be synthesized in the same manner. That is, the reaction of $[(\eta^6\text{-arene})\text{RuCl}_2]_2$, where $\eta^6\text{-arene}$ is *p*-cymene or C_6Me_6 , with 4 equiv of LiNHR ($\text{R}=\text{Ar}, \text{Ar}', \text{Ar}''$) should afford the appropriate imido complexes, $(\eta^6\text{-arene})\text{RuNR}$. In fact Schrock et al.⁸⁸ synthesized the bridging imido complexes, $[(\eta^6\text{-C}_6\text{H}_6)\text{Ru}(\mu\text{-NAr}'')]_2$ and $[(\eta^6\text{-C}_6\text{H}_6)\text{Ru}(\mu\text{-NAr})]_2$ by reaction of 4 equiv of the appropriate LiNHR with $[(\eta^6\text{-C}_6\text{H}_6)\text{RuCl}_2]_2$ in ether.

A necessary advantage of this synthetic route is the ability to alter the functionalities at both the $\eta^6\text{-arene}$ and imido, R, group. The hypothesis that increased steric congestion about the metal center forces monomer formation in favour of dimerisation could only be explored with the ability to functionalise the precursors.

Scheme I shows the synthetic method used, the products were characterised by nmr and elemental analysis. However, these techniques were inconclusive as to the formulation of these complexes. That is, which complexes are dimers with bridging imido ligands and which are monomers containing a terminal imido ligand. The only conclusive method for determining the nature of these complexes is a single crystal X-ray determination. Mass spectrometry techniques in New Zealand proved inadequate for these very sensitive compounds.



$\eta^6\text{-arene}=\text{cym}; \text{R}=\text{Ar}'', \text{Ar}, \text{Ar}'$

$\eta^6\text{-arene}=\text{C}_6\text{Me}_6; \text{R}=\text{Ar}'$

Scheme I

The strategy was unsuccessful for the synthesis of $(\text{C}_6\text{Me}_6)\text{RuNAr}''$ and $(\text{C}_6\text{Me}_6)\text{RuNAr}$, producing intractable mixtures. One problem with the isolation of these complexes is their high solubility. They are soluble in aromatic solvents, THF, hexane and

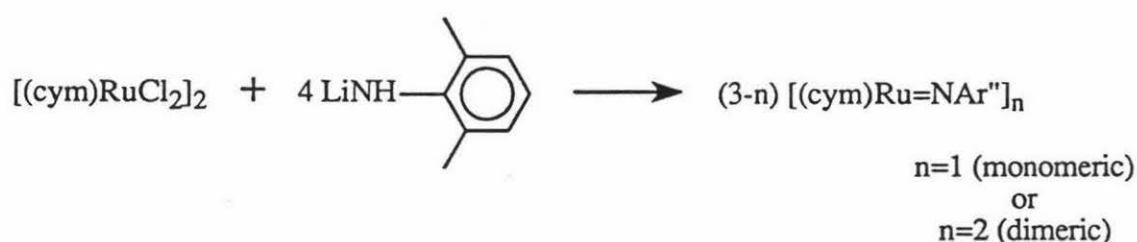
heptane, however their solubility in hexamethyldisiloxane is only slight. Unlike the iridium analogues,^{81a} the ruthenium imido compounds are highly sensitive to air and moisture. All nmr samples had to be run in teflon sealed nmr tubes to avoid degradation while waiting for analysis. Such sensitivity makes obtaining acceptable elemental analysis results difficult, however acceptable results were obtained for the complexes.

(ii) Reactions of [(cym)RuCl₂]₂:

The following describes the reactions of [(cym)RuCl₂]₂ with LiNHR, where R is Ar'', Ar and Ar'. The discussion will focus on the spectroscopic characteristics of the complexes and for two such complexes crystallographic details are given. Also the reaction of the free amine, ArNH₂, with [(cym)RuCl₂]₂ is mentioned as an alternative synthetic method.

- with LiNHR'':

Reaction of [(cym)RuCl₂]₂ with 4 equiv of LiNHR'' in THF resulted in the isolation of a brown solid in 38% yield (Scheme II; see page 77 for experimental details). Due to the products high solubility, cooling to -35°C in toluene was needed to remove the product from solution.



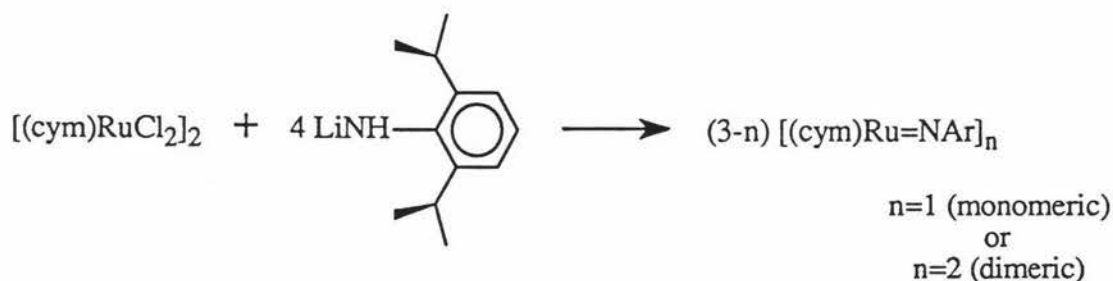
Scheme II

An important feature of the ¹H nmr (see page 85 and 86 for details of the ¹H and ¹³C nmr) is the absence of a singlet corresponding to a N-H substituent. This indicates the

presence of an imido complex as opposed to an amido complex (i.e. -NHR). The seven peaks of a septet can be clearly seen at 2.20ppm with a coupling constant of 6.9Hz. This is assigned to the secondary carbon of the isopropyl group of the *p*-cymene and is consistent to that of the (cym)OsNAr'' complex^{82b}, which reports the septet at 2.14ppm with J=6.9Hz. The ¹³C nmr shows the *ipso*-carbon of the Ar'' ligand, as expected, lies far downfield at 169.7ppm with the *ortho*-, *meta*- and *para*-carbons further upfield at 127.7, 126.0 and 121.6ppm respectively. This again is consistent with the osmium analogue,^{82b} (cym)OsNAr'', with the *ipso*-, *ortho*-, *meta*- and *para*-carbons at 167.6, 127.5, 127.3 and 121.8ppm respectively. Numerous attempts were made to obtain crystals suitable for X-ray diffraction study, however, none were suitable.

- with LiNHAr:

Reaction of [(cym)RuCl₂]₂ with 4 equiv of LiNHAr in THF resulted in the isolation of a dark green solid in 37% yield (Scheme III; see page 76 for experimental details). Cooling to -35°C was not required to isolate the product as in the Ar'' complex, instead evaporation of a benzene solution was sufficient to isolate the complex.



Scheme III

Again the ¹H nmr indicated the absence of a NH group, dismissing the possibility of the isolation of an amido complex (see page 87 and 88 for details of the ¹H and ¹³C nmr). Unlike the septet due to the isopropyl group of the *p*-cymene ligand, the expected septet due to the isopropyl groups of the Ar ligand is a single broad peak at 3.61ppm. This broadening of the septet was also observed in the complex, (cym)Os=NAr,^{82b} where a broad

signal at 3.59ppm was assigned to the secondary carbon of the isopropyl groups of the Ar ligand. The ^{13}C nmr spectrum is very similar to that of $[(\text{cym})\text{Ru}=\text{NAr}]_n$.

Suitable crystals of $[(\text{cym})\text{Ru}=\text{NAr}]_n$ ($n=1$ or 2) were obtained by evaporation of a benzene/hexamethyl-disiloxane solution. The refined structure depicted in figure 30,¹⁰⁷ confirms that $[(\text{cym})\text{Ru}=\text{NAr}]_n$ exists as the dimeric bridged imido complex, $[(\text{cym})\text{Ru}(\mu\text{-NAr})]_2$.

Ru(1)–N(1)	1.959(8)	Ru(1)–N(1)–Ru(2)	88.5(3)
Ru(1)–N(2)	1.977(7)	Ru(1)–N(2)–Ru(2)	88.2(3)
Ru(2)–N(1)	1.985(8)	N(1)–Ru(1)–N(2)	78.5(3)
Ru(2)–N(2)	1.976(8)	N(1)–Ru(2)–N(2)	77.9(3)
Ru(1)–Ru(2)	2.7515(12)	Ru(1)–Ru(2)–N(1)	45.4(2)
		Ru(1)–Ru(2)–N(2)	45.9(2)
		Ru(2)–Ru(1)–N(1)	46.1(2)
		Ru(2)–Ru(1)–N(2)	45.9(2)

Table 2; Selected bond lengths(Å) and bond angles(°)

The structure of $[(\text{cym})\text{Ru}(\mu\text{-NAr})]_2$ is very similar to that of the previously reported complex $[(\text{C}_6\text{H}_6)\text{Ru}(\mu\text{-NAr})]_2$ ⁸⁸ in that there is a distinct deformation of the Ru-N plane. The nitrogen atoms are bent some 1.188(8)Å above an ideal 'flat' Ru-N plane. Also the Ru-Ru distance, 2.7515(12)Å, is short and falls within the range of known Ru-Ru bonds. This is more likely due to the geometry imposed by the bridging imido ligands than the presence of a Ru-Ru bond. A fact that is supported by the appearance of only one signal for the isopropyl groups on the $\mu\text{-NAr}$ ligands indicating rapid inversion in solution. The aryl planes are oriented approximately perpendicular to their respective Ru_2N planes. It should be noted that the analogous osmium complex, $(\text{cym})\text{Os}=\text{NAr}$, is reported to be monomeric on the basis of spectroscopic data.⁸²

Clearly, the steric pressure around the metal center must be increased even more to isolate the terminal ruthenium imido complex.

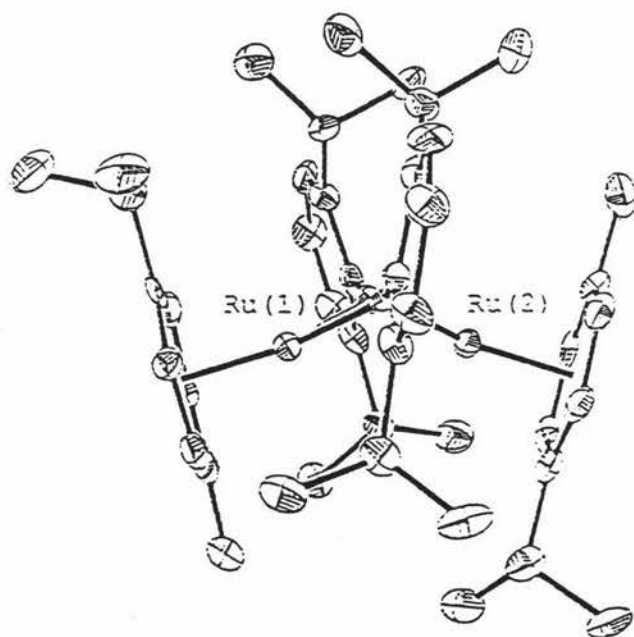
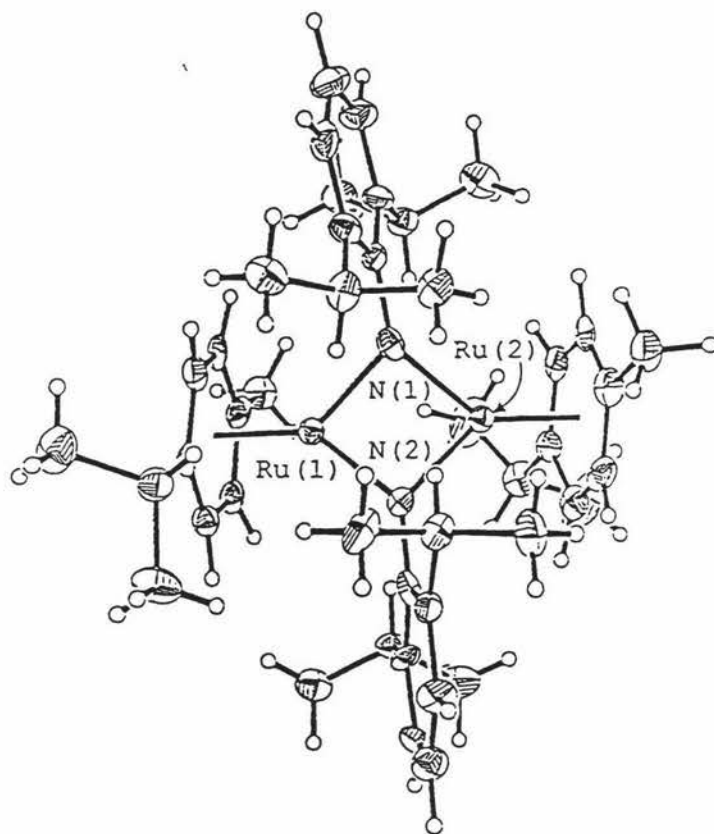
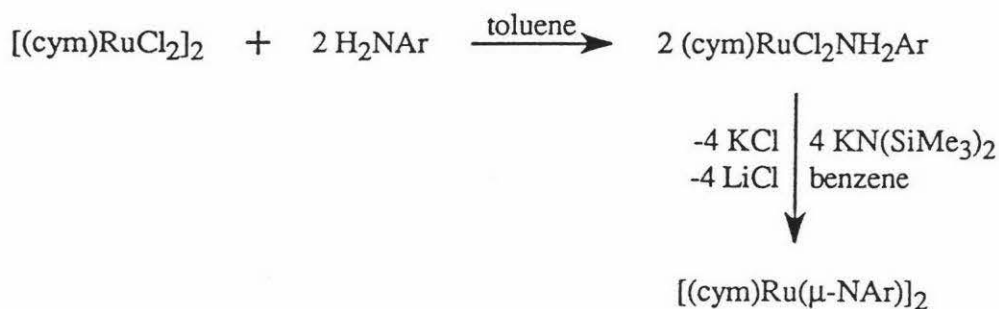


Figure 30

– with ArNH₂:

In an attempt to find a higher yielding route to [(cym)Ru(μ-NAr)]₂ a further method of synthesis was employed with reaction of [(cym)RuCl₂]₂ with 2 equiv of ArNH₂, followed by a dehydrochlorination step with KN(SiMe₃)₂ (Scheme IV; see page 76 and 82 for experimental details). This procedure was used successfully with iridium for the amines, ^tBuNH₂ and ArNH₂.^{81a}



Scheme IV

The solution of (cym)RuCl₂NH₂Ar was removed of toluene *in vacuo*, resulting in the isolation of a yellow solid in 76% yield. The dehydrochlorination step afforded a green-black solid that was extracted with toluene to provide the bridging imido complex in 68% yield. The overall yield for the two steps is 51%, an improvement of 15% over the method of scheme III. In a dissertation by Michelman⁹¹ the reaction of [(cym)RuCl₂]₂ with 2 equiv of ^tBuNH₂ in dichloromethane was shown to afford the amine complex, (cym)RuCl₂NH₂^tBu. Attempts to dehydrohalogenate the complex with KN(SiMe₃)₂, MeLi or DNB were unsuccessful.⁹¹ As shown in scheme IV, the dehydrohalogenation of the Ar analogue with KN(SiMe₃)₂ afforded the imido complex in 68% yield.

Due to the complexes greater solubility in chloroform, compared with benzene, the ¹H and ¹³C nmr spectra were run with deuterated chloroform as the solvent (see page 89 and 90 for details of the ¹H and ¹³C nmr).

The ^1H nmr spectrum of $(\text{cym})\text{RuCl}_2\text{NH}_2\text{Ar}$ is similar to that of the bridging imido complex, $[(\text{cym})\text{Ru}(\mu\text{-NAr})]_2$. The presence of a broad singlet at 4.76ppm, assigned to a NH_2 group, confirms the compound to be an amine complex. The signal due to the secondary carbon of the isopropyl groups are clearly seen to be septets at 3.44ppm ($J=6.7\text{Hz}$) found for the Ar ligand and 2.91ppm ($J=7.0\text{Hz}$) found for the *p*-cymene ligand. The ^{13}C nmr spectrum is very similar to that of $[(\text{cym})\text{Ru}(\mu\text{-NAr})]_2$, however, the secondary aromatic carbons of the *p*-cymene ring (expected to be around 77 to 79ppm) are hidden by the solvent, deuterated chloroform, which appears at 77.0ppm. Two peaks can be clearly seen in the I.R. at 3300 and 3252cm^{-1} associated to the NH_2 .

Crystals of $(\text{cym})\text{RuCl}_2\text{NH}_2\text{Ar}$ suitable for X-ray analysis were obtained by evaporation of a toluene solution. The refined structure (2 independent molecules were in the asymmetric unit) is depicted in figure 31.¹⁰⁷

Ru(1)–N(1)	2.188(12)	Ru(1)–N(1)–C(111)	122.9(9)
Ru(1)–Cl(11)	2.408(5)	N(1)–Ru(1)–Cl(11)	80.3(4)
Ru(1)–Cl(12)	2.425(5)	N(1)–Ru(1)–Cl(12)	80.6(4)
N(1)–C(111)	1.44(2)	Cl(11)–Ru(1)–Cl(12)	88.9(2)

Table 3; Selected bond lengths(Å) and bond angles(°).

The average N–Ru–Cl angles of $80.3(4)^\circ$ and $80.6(4)^\circ$ are comparable to the N–Ru–Cl angle of $(\text{C}_6\text{Me}_6)\text{RuClNHAr}$ at $84.4(6)^\circ$ (see page 56) and the average Ru–N–C angle of $122.9(9)^\circ$ is nine degrees lower than in the HCl adduct at $132(2)^\circ$ (see page 56). The Ru(II) amine complexes $[(\text{Cp})\text{Ru}(\text{NH}_3)(\text{PPh}_3)_2]^+$ and $(\text{cym})\text{RuCl}_2\text{NH}_2\text{tol}$ have Ru–N distances of $2.172(3)\text{Å}$ ⁷⁰ and $2.118(2)\text{Å}$ ¹⁰⁸ which compare well with the Ru–N distance of $2.188(12)\text{Å}$ obtained for the $(\text{cym})\text{RuCl}_2\text{NH}_2\text{Ar}$ complex. Also the average Ru–N distance is greater than

that of the HCl adduct at 1.94(2)Å (see page 56) and the dimer [(cym)Ru(μ -NAr)]₂ at 1.974(8)Å. The average Ru–Cl distances of 2.408(5)Å and 2.425(5)Å compare well with the complexes (Cp*)RuCl(PPh₃)₂, (Cp)RuCl(PMe₃)₂ and (cym)RuCl₂NH₂tol with Ru–Cl distances of 2.453(2)Å¹⁰⁹, 2.44Å¹⁰⁹ and 2.41(1)Å¹⁰⁸ respectively, and are slightly greater than the Ru–Cl distance of (C₆Me₆)RuClNHAr at 2.378(6)Å (see page 56).

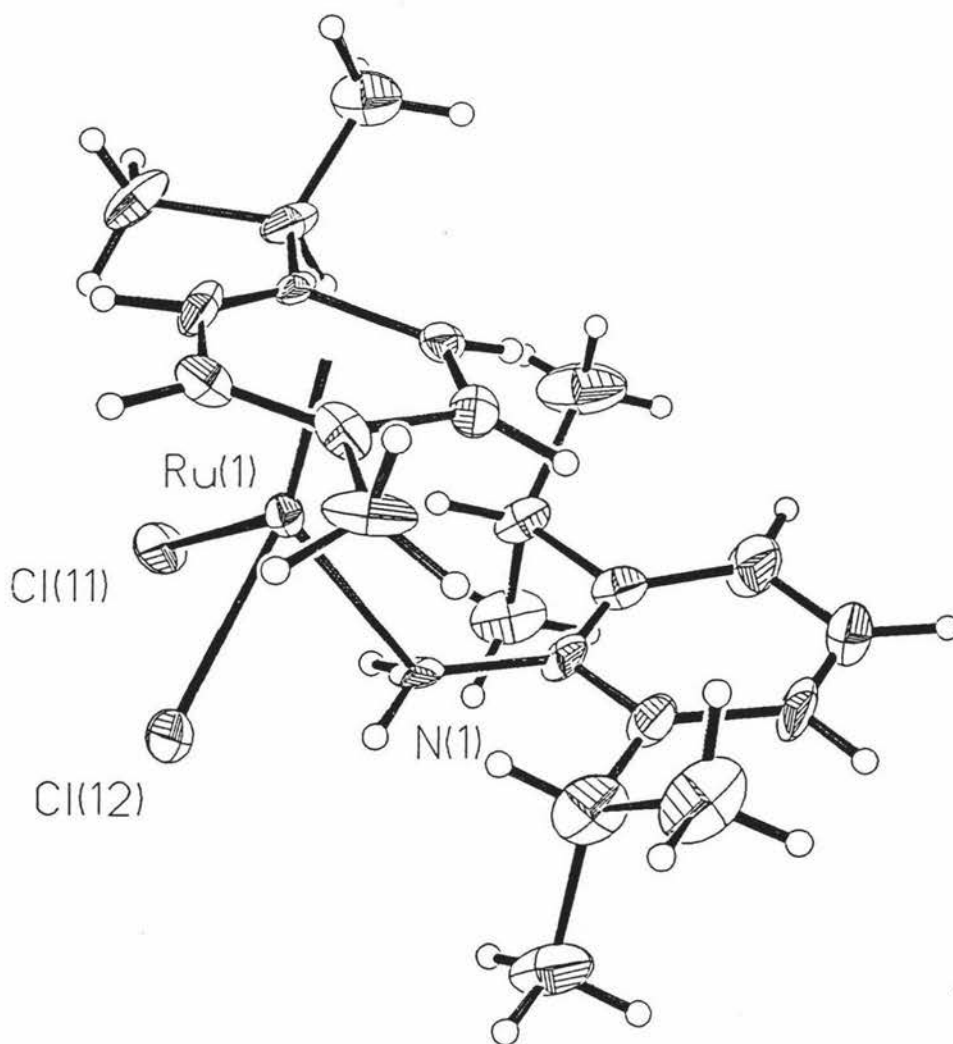
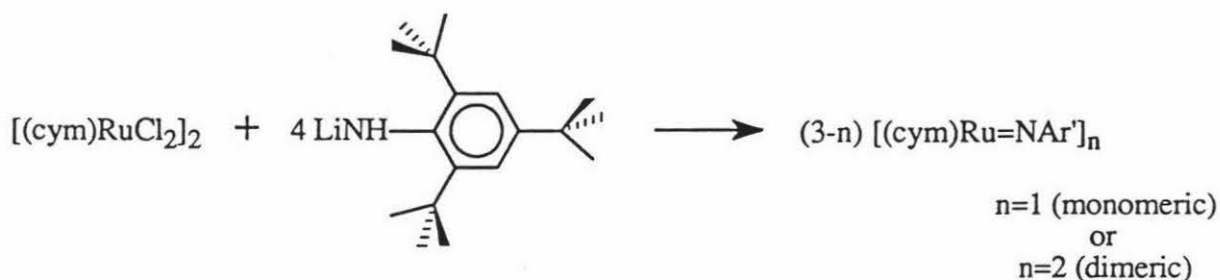


Figure 31

- with LiNHAr':

Reaction of $[(\text{cym})\text{RuCl}_2]_2$ with 4 equiv of LiNHAr' in THF resulted in the isolation of a green solid in 47% yield (Scheme V; see page 74 for experimental details). As in the Ar case, evaporation of a benzene solution was required to isolate the product.



Scheme V

The ^1H nmr indicates the product to contain the NR moiety, as opposed to NHR or NH_2R , by the absence of a NH signal (see page 91 and 92 for details of the ^1H and ^{13}C nmr). Table 4 shows the ^1H nmr chemical shifts of the *p*-cymene aromatic protons for each of the imido complexes. Notice the movement to greater downfield positions as the imido ligand size increases from Ar'' to Ar'. A similar trend is seen with the *p*-cymene aliphatic protons (table 5).

<i>p</i> -cymene Aromatic Protons (^1H)		
	Chemical Shift (ppm)	Coupling Constant (Hz)
[(cym)Ru(μ -NAr'')] ₂	4.37	6.0
	4.26	5.9
[(cym)Ru(μ -NAr)] ₂	4.74	5.9
	4.55	5.9
[(cym)Ru=NAr'] _n	5.11	6.2
	5.03	6.2

Table 4

^1H Methyl Signals (ppm)			
	^1H <i>p</i> -cymene Septet (ppm)	Doublet	Singlet
[(cym)Ru(μ -NAr'')] ₂	2.20	0.97	1.73
[(cym)Ru(μ -NAr)] ₂	2.52	1.03	1.76
[(cym)Ru=NAr'] _n	2.65	1.19	2.01

Table 5

Again, the ^{13}C spectrum is similar to that of the Ar'' and Ar complexes. One noteworthy point is the large difference of chemical shift at the *para*-carbon between [(cym)Ru=NAr']_n (n=1 or 2) and the bridging imido complexes, shown in table 6.

^{13}C Chemical shifts of the imido ligand aromatic carbons (ppm)				
	<i>ipso</i>	<i>ortho</i>	<i>meta</i>	<i>para</i>
$[(\text{cym})\text{Ru}(\mu\text{-NAr}')_2]$	169.7	127.7	127.6	121.6
$[(\text{cym})\text{Ru}(\mu\text{-NAr})_2]$	167.7	128.7	123.3	122.9
$[(\text{cym})\text{Ru}=\text{NAr}']_n$	157.9	148.1	121.7	145.6

Table 6

The physical and spectroscopic data for $[(\text{cym})\text{Ru}=\text{NAr}']_n$ are very similar to that of $[(\text{cym})\text{Ru}(\mu\text{-NAr})_2]$ and so the only conclusive method for determining the structure was a single crystal X-ray analysis. Suitable crystals were obtained from the evaporation of a benzene/hexamethyldisiloxane solution. The molecular geometry (2 independent molecules were in the asymmetric unit), depicted in figure 32¹⁰⁷ clearly show a monomeric complex containing a terminal imido ligand.

Ru(1)–N(1)	1.751(11)	Ru(1)–N(1)–C(121)	178.5(12)
Ru(2)–N(2)	1.756(12)	Ru(2)–N(2)–C(221)	177.0(10)
N(1)–C(121)	1.39(2)		
N(2)–C(221)	1.39(2)		

Table 7; Selected bond lengths(Å) and bond angles(°)

The averaged Ru-N-C angle is approximately linear at 177.8(4)°. The averaged Ru-N distance is consistent with multiple-bond character expected of a terminal imido ligand^{5,50} and compares well with the only other structurally characterised terminal imido complex of ruthenium, $\text{Ru}(\text{NAr})_2(\text{PMe}_3)_2$ at 1.785(6)Å.⁸⁷ The Ru-N distance is also similar to

that observed in the related osmium complex $(C_6Me_6)Os=N^tBu$ at $1.737(3)\text{\AA}$ ⁸² and the iridium imido complex, $Cp^*Ir=N^tBu$ at $1.712(7)\text{\AA}$.⁸¹ Surprisingly the aryl groups are in an eclipsed formation.

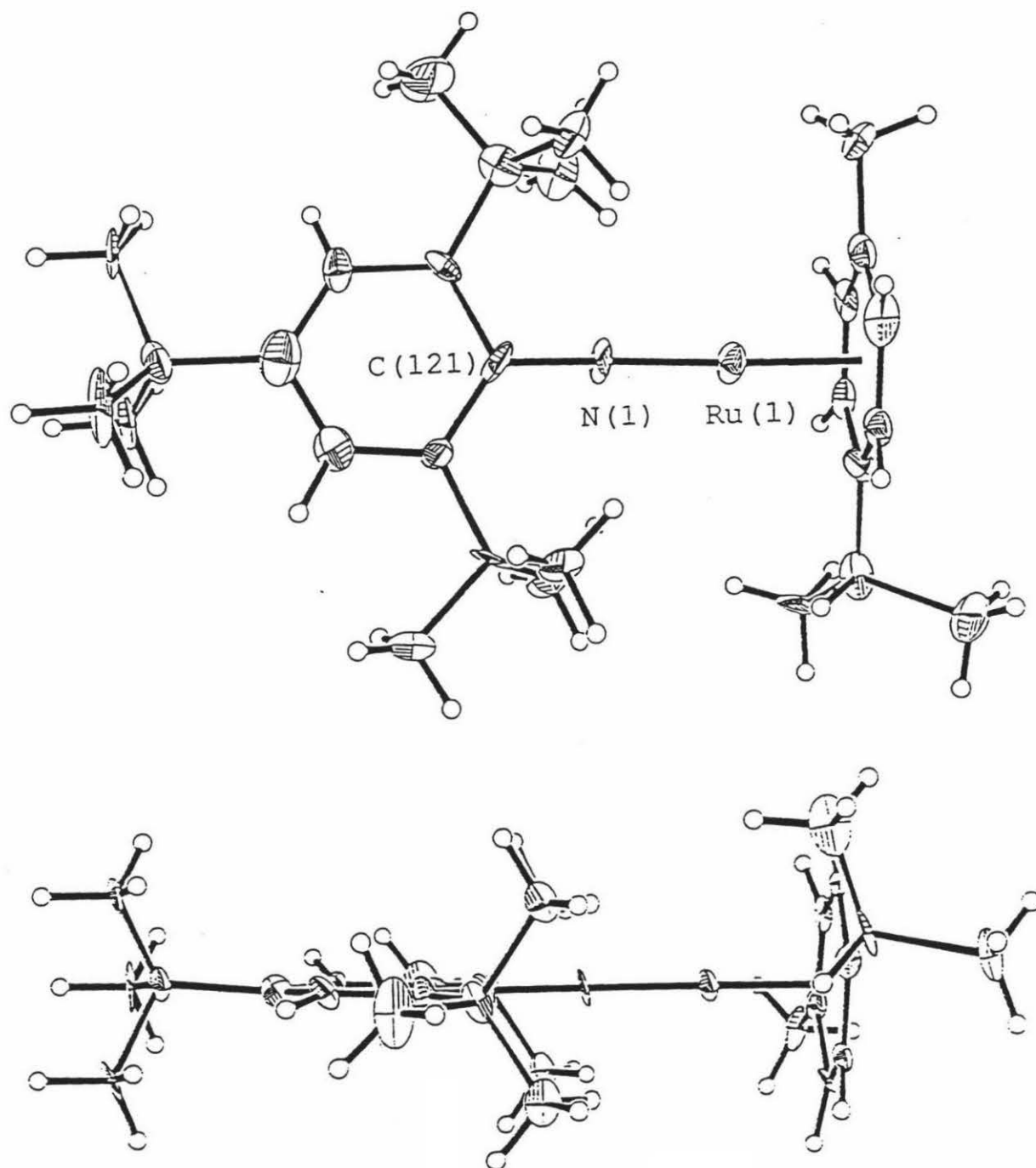


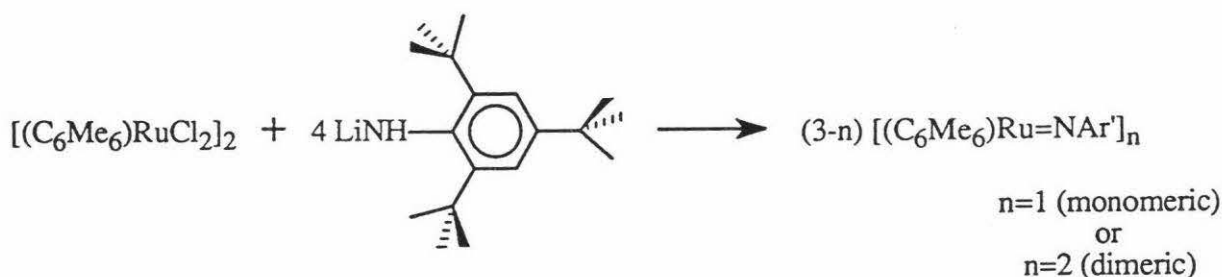
Figure 32

(iii) Reactions of $[(C_6Me_6)RuCl_2]_2$:

The following describes the reaction of $[(C_6Me_6)RuCl_2]_2$ with 4 equiv of $LiNHAr'$ and 2 equiv of $LiNHAr$. The discussion will focus on the spectroscopic characteristics of the complexes isolated and for one such complex crystallographic details are given.

- with 4 $LiNHAr'$:

Reaction of $[(C_6Me_6)RuCl_2]_2$ with 4 equiv of $LiNHAr'$ in THF resulted in the isolation of a green solid in 40% yield (Scheme VI; see page 75 for experimental details). Evaporation of a benzene solution was sufficient to isolate the product.



Scheme VI

In the 1H nmr the methyl signals of the C_6Me_6 ring appear at 2.11 ppm (see page 93 and 94 for details of the 1H and ^{13}C nmr). In comparison, the complex $(C_6Me_6)Os=N^tBu$,^{82b} is observed to show this peak further downfield at 2.37 ppm. The ^{13}C nmr spectrum is similar to that of $(cym)Ru=NAr'$, however, the *ipso*-carbon signal is at a higher upfield position at 146.9 ppm. The comparison of this peak to that found in the $[(cym)Ru(\mu-NAr'')]_2$, $[(cym)Ru(\mu-NAr')]_2$ and $(cym)Ru=NAr'$ complexes (see table 8) illustrates the movement to a position further upfield.

^{13}C Chemical shifts of the imido ligand aromatic carbons (ppm)				
	<i>ipso</i>	<i>ortho</i>	<i>meta</i>	<i>para</i>
$[(\text{cym})\text{Ru}(\mu\text{-NAr}')_2]$	169.7	127.7	127.6	121.6
$[(\text{cym})\text{Ru}(\mu\text{-NAr})_2]$	167.7	128.7	123.3	122.9
$(\text{cym})\text{Ru}=\text{NAr}'$	157.9	148.1	121.7	145.6
$(\text{C}_6\text{Me}_6)\text{Ru}=\text{NAr}'$	146.9	128.7	121.6	128.4

Table 8

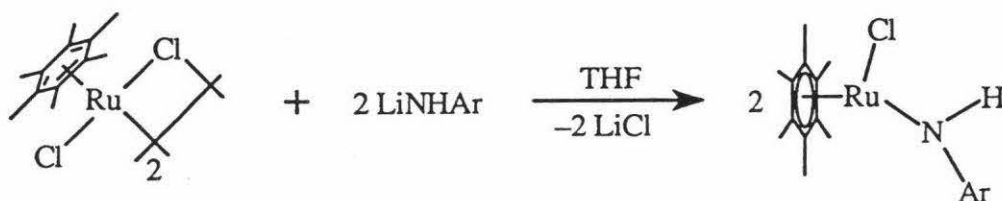
The aromatic carbons of the C_6Me_6 ring are positioned at 89.2ppm, slightly further downfield than found in $(\text{C}_6\text{Me}_6)\text{Os}=\text{N}^t\text{Bu}$ at 82.8ppm.^{82b} The opposite situation occurs with the methyl signals of the C_6Me_6 ring. The complex $(\text{C}_6\text{Me}_6)\text{Os}=\text{N}^t\text{Bu}$ shows a peak at 19.7ppm,^{82b} while for $[(\text{C}_6\text{Me}_6)\text{Ru}=\text{NAr}']_n$, this peak moves upfield by 1.5ppm to 18.2ppm.

Numerous attempts were made to obtain crystals, however, only very thin plate-like crystals unsuitable for X-ray diffraction were grown. However, given the greater steric pressure about the ruthenium atom in the complex, $[(\text{C}_6\text{Me}_6)\text{Ru}=\text{NAr}']_n$, compared with the known terminal imido complex, $(\text{cym})\text{Ru}=\text{NAr}'$, it would seem reasonable to expect the complex to contain a terminal imido ligand and thus be best formulated as $(\text{C}_6\text{Me}_6)\text{Ru}=\text{NAr}'$.

– with 2 LiNHAr:

The reaction of $[(\text{C}_6\text{Me}_6)\text{RuCl}_2]_2$ with 4 equiv of LiNHAr affords an intractable mixture. However, on occasion a small amount of red solid could be obtained. The proton nmr of this solid, although very complex, had a signal around 10 ppm. This led to the theory that the red product may be from the result of incomplete reaction, the peak at 10 ppm in the ^1H

nmr indicating the presence of a $-NHR$ ligand. Assuming this to be the case, then this red product, $(C_6Me_6)RuClNHAr$ could be obtained by reaction with 2 equiv of $LiNHR$ instead of 4. Thus, the reaction of $[(C_6Me_6)RuCl_2]_2$ with 2 equiv of $LiNHR$ in THF produced a gradual colour change from a black solution to red overnight (see page 78 for experimental details). After workup the red solid was isolated in 65% yield and was found to be the HCl adduct of $(C_6Me_6)Ru=NAr$, with the NH resonance at 10.18 ppm seen in the 1H nmr (Equ 47; see page 95 and 96 for details of the 1H and ^{13}C nmr). Attempts at the synthesis of $(cym)RuClNHAr$ in the same way afforded a small amount of the imido complex, $[(cym)Ru(\mu-NAr)]_2$, but no HCl adduct.



Equation 47

The dehydrochlorination of the amine complex in scheme IV (see page 46) to the imido complex could in theory be applied to the HCl adduct. However, attempts at dehydrochlorination of the HCl adduct with $KN(SiMe_3)_2$ produced an intractable mixture. It is interesting, that the imido complex $(C_6Me_6)Ru=NAr$ is unable to be synthesized from 4 equiv of $LiNHR$, but the HCl adduct can be with 2 equiv of $LiNHR$. While the complex $(cym)Ru=NAr$ can be synthesized from $LiNHR$, but the HCl adduct cannot. An explanation of this maybe in the relative stabilities of the bridging imido complex, $[(cym)Ru(\mu-NAr)]_2$, and the terminal imido complex, $(C_6Me_6)Ru=NAr$. The bridging imido complex is relatively stable and is formed readily from 4 equiv of $LiNHR$, while the terminal imido complex is unstable and is not formed from $LiNHR$. Instead the more stable HCl adduct is formed.

The complex $(C_6Me_6)RuClNHAr$, was very air sensitive and even in the dry box would turn brown over a period of days, presumably due to slow decomposition. Due to extreme sensitivity only a poorly formed crystal could be used for a X-ray diffraction study.

Ru(1)–N(1)	1.94(2)	Ru(1)–N(1)–C(41)	132(2)
Ru(1)–Cl(1)	2.378(6)	N(1)–Ru(1)–Cl(1)	84.4(6)
N(1)–C(41)	1.43(2)		

Table 9; Selected bond lengths(Å) and bond angles(°).

Again, suitable crystals of $(C_6Me_6)RuClNHAr$ were obtained by evaporation of a benzene/hexamethyldisiloxane solution. The crystal structure of $(C_6Me_6)RuClNHAr$ is shown in figure 33.¹⁰⁷ The Ru–N distance of 1.94(2)Å is similar to the Ru–N distance of the dimer, $[(cym)Ru(\mu-NAr)]_2$ at 1.974(8)Å and Schrock's dimer, $[(C_6H_6)Ru(\mu-NAr)]_2$ at 1.96(1)Å.⁸⁸ The Ru–N distance is significantly shorter than that found in the bridging amido complex, $[(Cp^*)Ru(\mu-NHPh)]_2$ at 2.109(8)Å¹¹⁰ and significantly longer than the Ru–N distance found in the complex $[Ru\{NH(C_6H_{11})\}\{OCe_2C(O)O\}_2][NPr_4]$ at 1.818(6)Å (table 10).¹¹¹

	Ru–N Distances (Å)	Reference
$(C_6Me_6)RuClNHAr$	1.94(2)	
$[(cym)Ru(\mu-NAr)]_2$	1.974(8)	89
$[(C_6H_6)Ru(\mu-NAr)]_2$	1.96(1)	88
$[(Cp^*)Ru(\mu-NHPh)]_2$	2.109(8)	110
$[Ru\{NH(C_6H_{11})\}\{OCe_2C(O)O\}_2]^-$	1.818(6)	111

Table 10

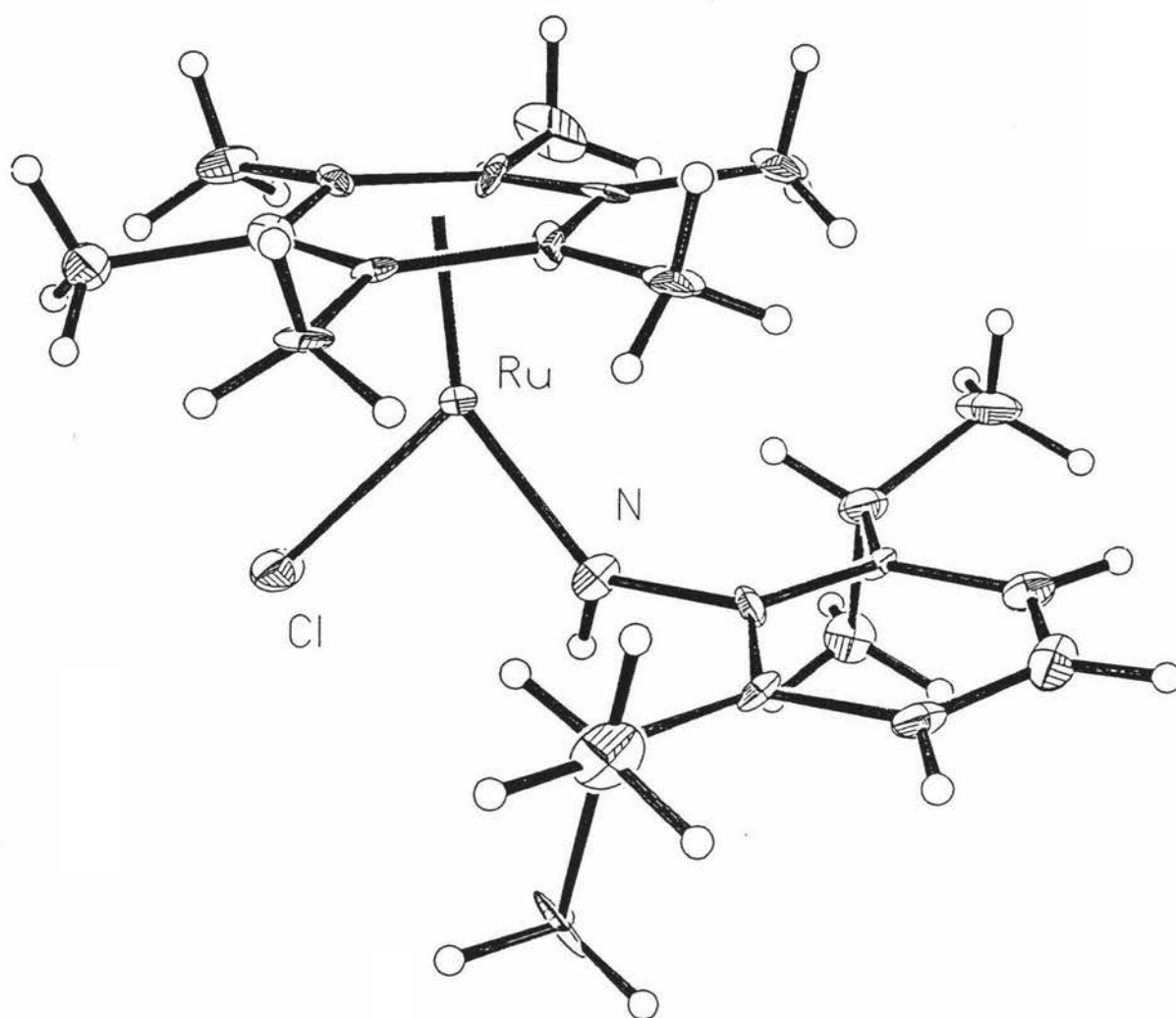


Figure 33

The Ru-Cl distance of 2.378(6)Å is in the range found for other structurally characterised Ru(II) complexes, with the complexes Cp^{*}RuCl(PPrⁱ₃), Cp^{*}RuCl(PPh₃)₂ and CpRuCl(PMe₃)₂ having Ru-Cl distances of 2.365(2)Å, 2.453(2)Å and 2.44Å respectively (table 11).¹⁰⁹ Also the Ru-N-C angle of 132(2)° is consistent with that found in the amido complex [Ru{NH(C₆H₁₁)}{OCEt₂C(O)O}₂][NPr₄] at 132.3(4)°.¹¹¹

	Ru–Cl Distances (Å)	Reference
(C ₆ Me ₆)RuClINHAr	2.378(6)	
Cp*RuCl(PPr ⁱ ₃)	2.365(2)	109
Cp*RuCl(PPh ₃) ₂	2.453(2)	109
CpRuCl(PMe ₃) ₂	2.44	109

Table 11

– Summary:

The synthetic strategy developed from Bergman *et al.*^{81,82} proved to be successful in generating Ru(II) imido complexes in moderate yields. Also, by use of an alternative synthetic method the bridging imido complex, [(cym)Ru(μ-NAr)]₂, was synthesized in an improved yield. The spectroscopic characteristics of the imido complexes proved to be similar and as a result obtaining crystal structures was vital to distinguish between the bridging and terminal imido complexes. The crystal structures showed a bridging imido complex, [(cym)Ru(μ-NAr)]₂, and a terminal imido complex, (cym)Ru=NAr' and hence illustrated the need for the very sterically demanding imido ligand, Ar', to necessitate formation of the terminal imido complex. An investigation into the effects changing the arene ligand has on imido formation was also carried out and resulted in the formation of the terminal imido complex, (C₆Me₆)Ru=NAr', and the HCl adduct of (C₆Me₆)Ru=NAr.

Reactivity of the Imido and Amido Ligand

The following presents firstly the results of reacting acetylenes with the terminal imido complex, $(\text{cym})\text{Ru}=\text{NAr}'$, and secondly, the reaction of phenylisocyanate with the amido complex, $(\text{C}_6\text{Me}_6)\text{RuClNHAr}$, and the implications thus resulting.

- reaction of $(\text{cym})\text{Ru}=\text{NAr}'$ with acetylenes:

Reaction of acetylenes with complexes containing metal-ligand multiple bonds are most common for oxo¹¹², alkylidene¹¹³ and alkylidyne¹¹⁴ complexes. Although the terminal imido ligand is less susceptible to reaction with acetylenes, a handful of high valent compounds have been shown to be reactive towards acetylenes. Terminal imido complexes of osmium,¹¹⁵ molybdenum,¹¹⁶ rhenium¹¹⁷ and zirconium¹¹⁸ react with acetylenes with displacement of one ligand for the alkyne. Also, the tantalum complex, $\text{Ta}(\text{NAr})\text{Cl}_3(\text{py})_2$ reacts with a variety of acetylenes in the presence of NaHg .¹¹⁹ Attempts at reacting $\text{Cp}^*\text{Ir}=\text{N}^t\text{Bu}$ with 1-phenylpropyne or 2-butyne even at 85°C were unsuccessful.^{81b} However, the reaction of the acetylene, dimethylacetylenedicarboxylate (DMAC), has been known to occur with coordinate in a η^2 fashion to imido complexes, for example, in the complex, $(\text{dmtc})_2\text{Mo}(\text{Ntol})(\text{DMAC})$.¹²⁰ However, the reaction of $\text{Cp}^*\text{Ir}=\text{N}^t\text{Bu}$ towards DMAC at room temperature afforded a complexed pyrrole to which the Cp^*Ir fragment is bound in a η^4 fashion (Fig. 34).⁹⁰

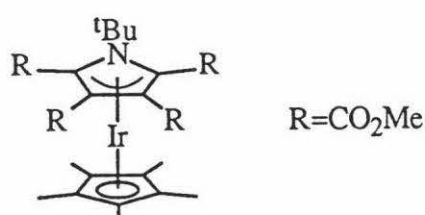


Figure 34

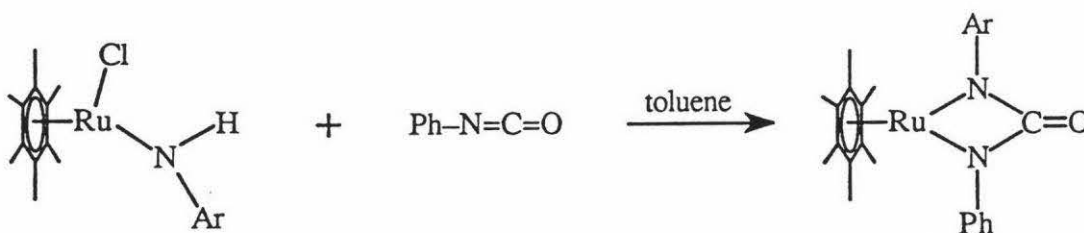
The success of the reaction of $\text{Cp}^*\text{Ir}=\text{N}^t\text{Bu}$ with DMAC and the unusual product isolated prompted the similar reaction with $(\text{cym})\text{Ru}=\text{NAr}'$ to be investigated. Reaction of 2 equiv of DMAC to a solution of $(\text{cym})\text{Ru}=\text{NAr}'$ in toluene produced a colour change from dark green to yellow. Work up of the yellow solution afforded a yellow solid in high yield.

However, the proton nmr was complex, although the methyl signals of the acetyl groups could be seen as could the isopropyl/methyl signals of the η^6 -arene ring. Attempts at recrystallising the solid were unsuccessful and purification has proven difficult.

The reaction of diphenylacetylene, phenylacetylene and 2-butyne with $(\text{cym})\text{Ru}=\text{NAr}'$ even at 60°C were unsuccessful, affording back the starting material. Initially this was a surprise (as row 2 transition metals are considered to be more reactive than the row 3 transition metals), however on investigation of the crystal structure of $(\text{cym})\text{Ru}=\text{NAr}'$, the proposal that increasing the size of the imido group to Ar' , to necessitate the formation of the monomer, decrease reactivity by physically shielding the site of reactivity, i.e. the ruthenium-nitrogen bond. As such the acetylenes could not gain close proximity to the Ru-N bond for formation of a transition state species necessary for complete reaction.

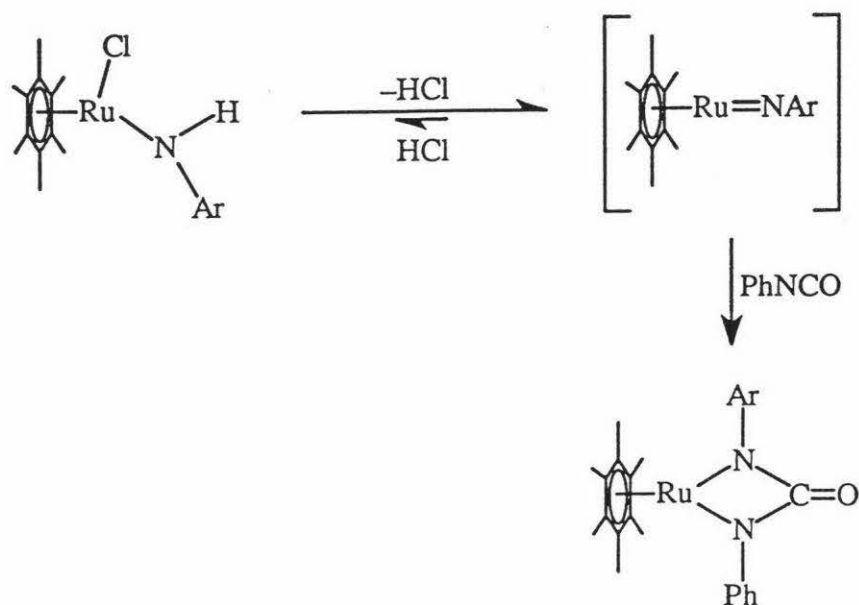
– reaction of PhNCO :

The reaction of isocyanates towards terminal imido complexes is common⁵⁰ and in particular the reaction of PhNCO towards $(\text{cym})\text{Os}=\text{N}^t\text{Bu}$, to provide an ureylene metallacycle, has been reported.⁸² However, the reaction of $(\text{C}_6\text{Me}_6)\text{RuClNHAr}$ in benzene with 1 equiv of PhNCO , producing a colour change from red to yellow almost immediately, was unexpected (Equ. 48; see page 79 for experimental details).



Equation 48

A plausible explanation of this reaction is the possible equilibrium between the HCl adduct and the terminal imido species (Scheme VII) in solution. The addition of PhNCO drives the equilibrium to the right by reaction with the imido to form the ureylene complex.



Scheme VII

This provides evidence for the presence of a multiple bond in the imido complex, $[(C_6Me_6)Ru=NAr]_n$, in fact the HCl adduct is effectively the trapped form of the reactive $(C_6Me_6)Ru=NAr$ terminal imido complex. As has been seen with the lack of reactivity of the terminal imido complex, $(cym)Ru=NAr'$, towards acetylenes. A balance must be reached whereby the steric congestion about the ruthenium is enough to enforce monomeric formation but not enough to hinder the reactivity of the terminal imido complex by shielding the reactive center, i.e. the multiple bond.

Figure 35 illustrates the problem, and maybe possible answers. The terminal imido complex, $(cym)Ru=NAr'$ is stable but unreactive, while $(C_6Me_6)Ru=NAr$ is reactive but unstable. By using an appropriate combination of **A** and **B**, it is hoped a terminal imido complex can be synthesized that allows room for substrates to gain access to the multiple bond and hence react. But retain enough steric congestion about the ruthenium atom to inhibit the formation of a bridging imido complex.

The 1H nmr of the ureylene complex shows a multiplet at 7.30ppm due to the phenyl protons (see page 98 and 99 for details of the 1H and ^{13}C nmr). The doublet and triplet of the Ar ring can be clearly seen at 7.07ppm ($J=8.1Hz$) and 7.18ppm ($J=7.7Hz$) respectively. The expected septet due to the secondary carbon of the isopropyl group of the Ar ligand is a

single broad peak at 3.13ppm (table 12). The signals due to the phenyl ring and CO can clearly be seen at 123.9 to 140.2 and 170.4ppm respectively. The ureylene complex, (cym)Os[(N^tBu)₂CO],^{82b} exhibits the CO signal at 174.4ppm.

The formulation of the ureylene metallacycle in equation 48 is based on elemental analysis, proton and carbon-13 nmr and a sharp band at 1596cm⁻¹ in the I.R. Carbonyl adsorptions for other monomeric ureylene complexes range from 1608 to 1698cm⁻¹.¹²¹ The ruthenium complex, (cym)Ru(PMe₃)[(Ntol)₂CO] shows this band at 1608cm⁻¹.⁹¹

¹ H Chemical Shifts of the Ar Imido Ligand Septets and Coupling Constants			
	Chemical Shift (ppm)	Multi	Coupling Constant (Hz)
(C ₆ Me ₆)RuN(Ph)C(O)N(Ar)	3.13	br s	
[(cym)Ru(μ-NAr)] ₂	3.61	br s	
(cym)RuCl ₂ NH ₂ Ar	3.44	sept	6.7
(C ₆ Me ₆)RuClNHAr	3.63	sept	6.6

Table 12

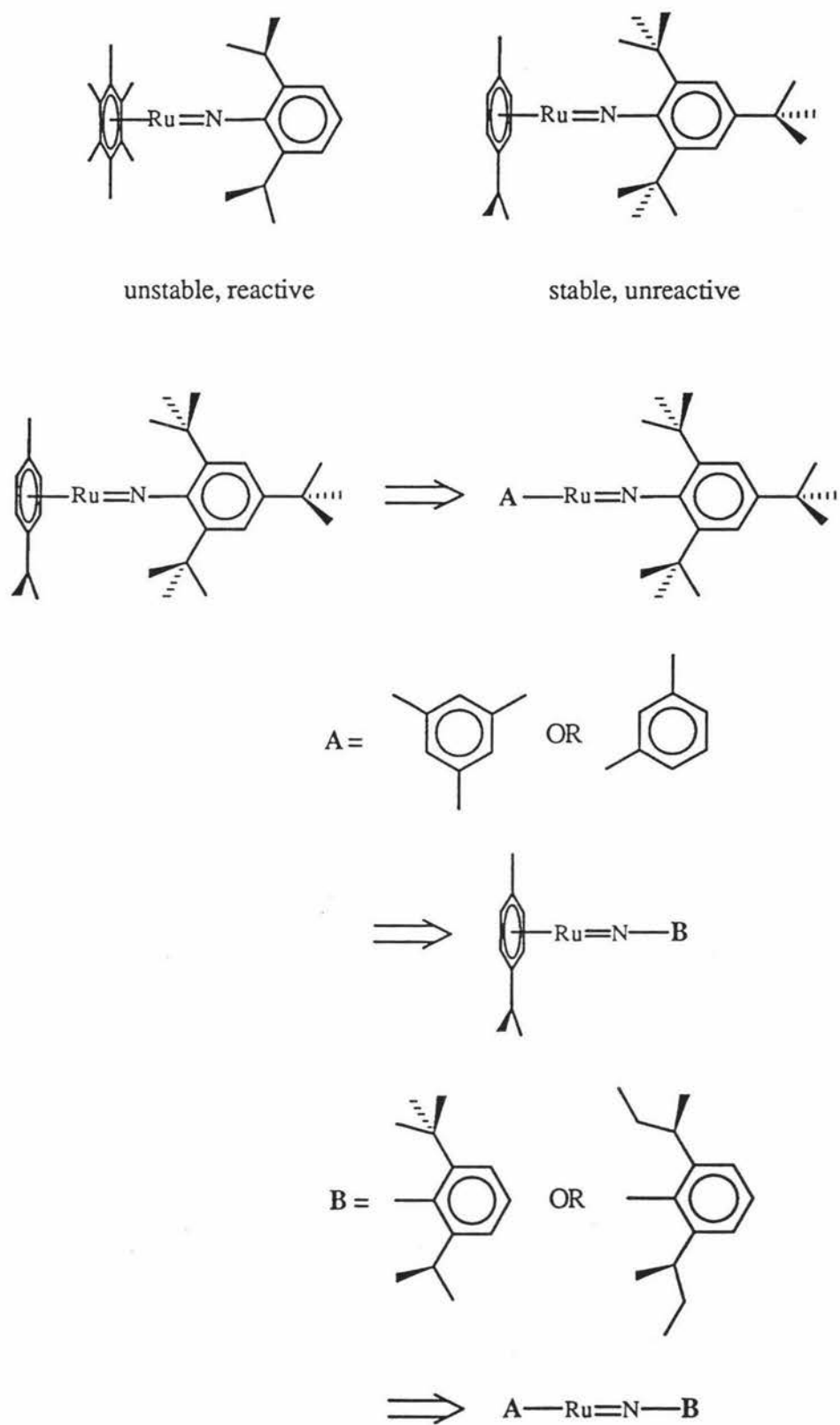


Figure 35

The failure to form the imido complex, $[(C_6Me_6)Ru=NAr]_n$, lead to the discovery that the HCl adduct, $(C_6Me_6)RuClNHAr$, can be synthesized. Its reaction with phenylisocyanate provided evidence for the existence of the terminal imido complex, $(C_6Me_6)Ru=NAr$. The fact that this complex is very reactive and hence unstable provides impetus for the synthesis of a terminal imido complex with similar reactivity but increased stability.

Possible mechanisms of imido formation from LiNHR

Two plausible routes to the formation of imido complexes from the reaction of 4 equiv of LiNHR have been proposed. The first is shown in scheme VIII. This involves the formation of the HCl adduct from the first 2 equiv of LiNHR, followed by attack of the second 2 equiv of LiNHR to form a bisamide complex. This can then lose 2 NH_2R by α -elimination to form the imido complex. Alternately, once the HCl adduct is formed, it can then be dehydrochlorinated by the second 2 equiv of LiNHR (acting as a base), again affording the imido complex (Scheme IX). Both Bergman *et al.*,^{81a} with regards to $Cp^*Ir=NR$ synthesis, and Schrock *et al.*⁸⁸ in the synthesis of the ruthenium dimer $[(C_6H_6)Ru(\mu-NR)]_2$ ($R=Ar'$, Ar) pointed out the validity of both schemes, however no preferences were made.

Support for the dehydrohalogenation step occurs in the reaction of $\text{Cp}^*_2\text{Zr}(\text{SH})(\text{I})$ with $\text{KN}(\text{SiMe}_3)_2$ to give $\text{Cp}^*_2\text{Zr}=\text{S}$, which can be trapped by dative ligands.¹²⁴ Also consistent with scheme IX is the synthesis and dehydrochlorination of the amine coordinated compounds $\text{Cp}^*\text{IrCl}_2\text{NH}_2\text{R}$ to the imido complexes^{81a} and the successful dehydrochlorination of $(\text{cym})\text{RuCl}_2\text{NH}_2\text{Ar}$ to $[(\text{cym})\text{Ru}(\mu\text{-NAr})]_2$ as described earlier (see page 46).

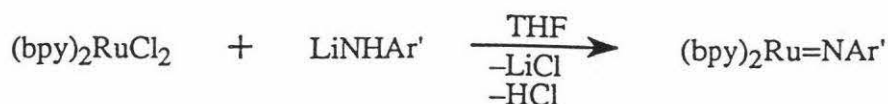
The chelating bisamide complex $\text{Cp}^*\text{Rh}[o\text{-C}_6\text{H}_4(\text{NH})_2]$ has been prepared by the deprotonation of *o*-phenylenediamine in the presence of $[\text{Cp}^*\text{RhCl}_2]_2$ ¹²⁵ and the proposed α -elimination is a common route to metal-ligand multiple bonds.⁵

For sterically demanding R groups, such as Ar', the bisamide complex of scheme IV may not form due to steric congestion about the metal center. The question is at what point, as the size of the R group increases, would the bisamide complex become unfavoured, if at all? It may be possible that dimer imido formation occurs via scheme VIII and monomer imido formation via scheme IX, based on steric grounds.

Future Work

Following the same strategy used to synthesize the η^6 -arene imido complexes, the synthesis of imido complexes of the formulation $(\text{bpy})_2\text{RuNR}$, where R is Ar or Ar' were investigated. Imido complexes containing the 2,2'-bipyridine ligand are known. In a paper by Nielson,¹²⁶ 2,2'-bipyridyl derivatives of Mo(V), Nb(V) and Ta(V) *t*-butylimido complexes were reported and Maatta¹²⁷ synthesized $\text{Mo}(\text{Ntol})\text{Cl}_3(\text{bpy})_2$ from $\text{Mo}(\text{Ntol})\text{Cl}_4(\text{thf})$ and bpy. However complexes of the formulation $(\text{bpy})_2\text{MNR}$ are unheard of.

Reaction of $(\text{bpy})_2\text{RuCl}_2$ with 2 equiv of LiNHAr' in THF afforded the complex $(\text{bpy})_2\text{Ru}=\text{NAr}'$ (Equ. 49) in 47% yield (see page 80 for experimental details). Removal of a benzene solution to minimal volume and addition of hexamethyldisiloxane induced precipitation of the brown-black product. Reaction with LiNHAr afforded a solid of similar appearance, however elemental analysis results were inconsistent with the expected formulation.



Equation 49

In the ^1H nmr, resonances associated with the aromatic protons of the bipyridine ligand appear between 7.50ppm and 8.64ppm and were assigned as such by their integration (see page 97 for details of the ^1H nmr). Notice that in the terminal imido complexes, $(\text{cym})\text{Ru=NAr}'$ and $(\text{C}_6\text{Me}_6)\text{Ru=NAr}'$, the *tert*-butyl groups at the *ortho* position appeared at a higher downfield position than those in the *para* position (table 13; $\text{Ar}'\text{NO}_2$ is 2,4,6-tri-*t*-butylnitrobenzene and $\text{Ar}'\text{NH}_2$ is 2,4,6-tri-*t*-butylaniline).

	^1H <i>tert</i> -butyl Chemical Shifts (ppm)	
	at <i>ortho</i> -carbon	at <i>para</i> -carbon
$(\text{cym})\text{Ru=NAr}'$	1.87	1.26
$(\text{C}_6\text{Me}_6)\text{Ru=NAr}'$	1.81	1.27
$(\text{bpy})_2\text{Ru=NAr}'$	1.31	1.48
$\text{Ar}'\text{NO}_2$	1.26	1.65
$\text{Ar}'\text{NH}_2$	1.49	1.34

Table 13

The investigation of complexes of the formulation $(\text{L})_n\text{RuNR}$, where L is a polydentate ligand, is a future area of work. Complexes of this formulation are known for molybdenum (L=dmtc, R=tolyl, n=2),¹²⁰ chromium (L=mnt, R=*t*Bu, n=2),¹²⁸ niobium

(L=dmtc, n=3)¹²⁹ and tantalum (L=dmtc, n=3).¹²⁹ Such complexes are not known for the later transition metals, nor for low oxidation state metals. So the preliminary synthesis of (bpy)₂Ru=NAr' provides encouragement to explore the possibility of using other polydentate ligands and transition metals.

The formation of a rhodium amine complex resulted from the initial attempt to synthesize a terminal rhodium imido complex. Reaction of [Cp*^{*}RhCl₂]₂ with 4 equiv of LiNHR (R=Ar, Ar'') yielded a black solid. Although the nmr of this solid was difficult to interpret, it was not representative of the expected imido complex. The first step of scheme IV (see page 46) proceeded in high yield for rhodium (see page 81 for experimental details). However, the dehydrochlorination of the amine complex, Cp*^{*}RhCl₂ArNH₂ afforded a black solid. It is assumed this product or mixture of products is the same as that obtained from reaction of LiNHR with [Cp*^{*}RhCl₂]₂.

In the ¹H nmr of Cp*^{*}RhCl₂NH₂Ar a septet at 3.13ppm can be clearly seen, with a coupling constant of 6.2Hz, and is assigned to the secondary carbon of the isopropyl group (see page 84 and 96 for details of the ¹H and ¹³C nmr). The NH₂ protons are found as a broad singlet at 4.48ppm. The ¹³C nmr is very similar to that of the ruthenium amine complex. The appearance of the aromatic carbons and methyl carbons of the C₅Me₅ ring appear at 93.9 and 9.4ppm respectively. As in the case for ruthenium, two peaks are seen in the I.R. associated with the NH₂ group, these are at 3303 and 3251cm⁻¹ (table 14).

^1H Chemical Shifts of the Ar Ligand (ppm) and I.R. Bands of the NH_2 Group (cm^{-1})					
	aromatic protons (doublets and triplets)	septet proton	methyl protons	NH_2 protons	NH_2 group
$(\text{cym})\text{RuCl}_2\text{NH}_2\text{Ar}$	7.37 and 7.27	3.44	1.32	4.76	3300 and 3252
$\text{Cp}^*\text{RhCl}_2\text{NH}_2\text{Ar}$	7.12 and 6.99	3.13	1.29	4.48	3303 and 3251

Table 14

Summary

The bridging imido complexes $[(\text{cym})\text{Ru}(\mu\text{-NAr}')_2]$ and $[(\text{cym})\text{Ru}(\mu\text{-NAr})_2]$ were fully characterised with a crystal structure of $[(\text{cym})\text{Ru}(\mu\text{-NAr}')_2]$ confirming its dimeric nature and similarities with $[(\text{C}_6\text{H}_6)\text{Ru}(\mu\text{-NAr})_2]$ ⁸⁸ noted. The terminal imido complexes $(\text{C}_6\text{Me}_6)\text{Ru}=\text{NAr}'$ and $(\text{cym})\text{Ru}=\text{NAr}'$ were fully characterised with the monomeric nature of $(\text{cym})\text{Ru}=\text{NAr}'$ confirmed conclusively by crystal structure. The greater steric pressure around the ruthenium atom of $(\text{C}_6\text{Me}_6)\text{Ru}=\text{NAr}'$ compared with $(\text{cym})\text{Ru}=\text{NAr}'$ suggests confidently that the $(\text{C}_6\text{Me}_6)\text{Ru}=\text{NAr}'$ complex is likewise monomeric.

However, the dimeric nature of $[(\text{cym})\text{Ru}(\mu\text{-NAr})_2]$ raises the question, why is the analogous osmium complex,⁸² $(\text{cym})\text{Os}=\text{NAr}$ monomeric? We intend to extend the range of structurally characterised $[(\eta^6\text{-arene})\text{Ru}=\text{NR}]_n$ ($n=1$ or 2) complexes in an attempt to

determine the exact constraints necessary to prevent the formation of bridged imido dimers and to explain the apparent discrepancies between osmium and ruthenium chemistry.

The isolation and characterisation of the amido complex, $(C_6Me_6)RuClNHR$, represents the first of its kind and lends force to the formation of such species in the mechanistic route (using $LiNHR$) leading to imido complexes. Further investigation into a wide range of $(\eta^6\text{-arene})RuClNHR$ complexes is necessary to determine the exact role these complexes could play in the synthetic mechanism of imido complex formation.

It is clear from table 1 (see page 27) that reports of group 9 transition metal terminal imido complexes are scarce. There are no known terminal imido complexes of cobalt or rhodium, and only a handful of iridium terminal imido compounds are known. Initial work into the synthesis of terminal imido complexes of rhodium has started with this thesis.

Chapter Three

Experimental Section

General

Unless otherwise noted all reactions and manipulations were performed in dry glassware under an argon atmosphere in a drybox.

Nuclear magnetic resonance spectroscopy was performed at 6.34 Tesla on a JEOL GX270W Spectrometer operating in the fourier transform mode at 270 MHz for ^1H and ^{13}C nuclei. ^1H nmr spectra were referenced to chloroform at 7.24 ppm or benzene at 7.15 ppm and ^{13}C nmr were referenced to chloroform at 77.0 ppm or benzene at 128 ppm. Elemental analysis was carried out using standard techniques at the microanalytical laboratory of the University of Otago, Dunedin. Infra-red spectra were recorded on a BIO-RAD FTS-40 Spectrophotometer as a thin film of nujol mull between KBr discs.

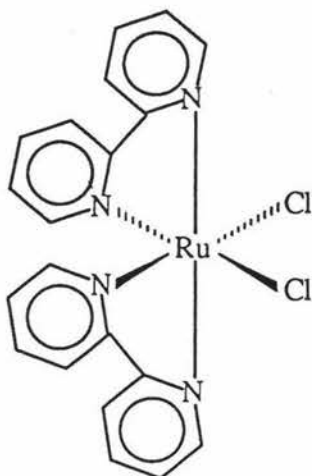
Benzene, toluene and THF was distilled from sodium/benzophenone. Pentane, hexane and hexamethyldisiloxane was distilled from sodium and deuterated benzene from sodium/benzophenone. Unless otherwise noted, all other reagents were used as received from commercial suppliers.

Lithium amides were prepared from the anilines by treatment with *n*-butyllithium in benzene. $\text{Ru}(\text{bpy})_2\text{Cl}_2 \cdot 2\text{H}_2\text{O}$ (bpy=2,2'-bipyridine),¹¹³ $[\text{Cp}^*\text{RhCl}_2]_2$ (Cp^* =pentamethylcyclopentadiene),¹⁰⁴ $[(\eta^6\text{-cym})\text{RuCl}_2]_2$ (cym=*p*-cymene),^{101,114} and 2,4,6-tri-*t*-butylaniline^{105,106} were prepared from literature methods.

Compounds

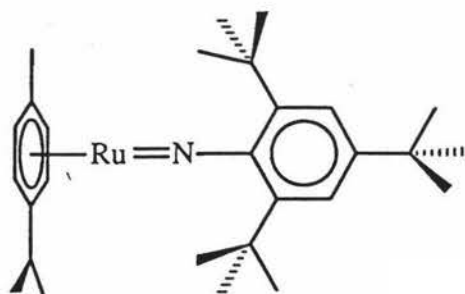


This was prepared by a modification of the literature method: the melt was suspended in diethyl ether and the material removed of hexamethylbenzene by soxhlet extraction using hexane, followed by soxhlet extraction using dichloromethane to obtain the desired product, rather than using Filter Aid and sublimation.¹³⁰



$\text{Ru}(\text{bpy})_2\text{Cl}_2$:

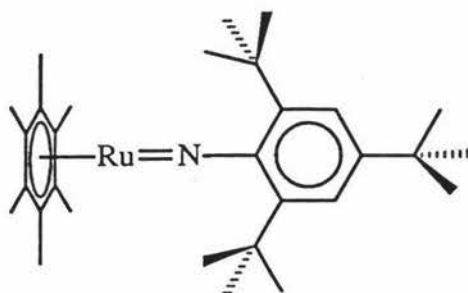
To a suspension of $\text{Ru}(\text{bpy})_2\text{Cl}_2 \cdot 2\text{H}_2\text{O}$ (910mg, 1.749mmoles) in THF (20mL) was added excess TMSCl (5mL). This mixture was stirred at room temperature overnight after which it was a pink colour. The THF was removed *in vacuo* giving 802mg of a pink product in 95% yield. Infra-red spectroscopy confirmed the absence of water.



$(\eta^6\text{-cym})\text{Ru}=\text{NAr}'$:

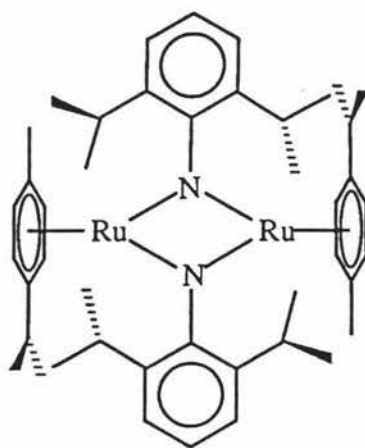
To a suspension of $[(\eta^6\text{-cym})\text{RuCl}_2]_2$ (100mg, 0.163mmoles) in THF (10mL) was added a solution of LiNHAr' (179mg, 0.669mmoles) in THF (5mL). This mixture was stirred at room temperature for 12 hours after which it was a deep-green colour. The THF was removed *in vacuo* and the green solid was extracted with benzene and filtered through Celite. Evaporation of the benzene gave 76mg of a green product in 47% yield.

Anal. Calcd.; C, 67.98; H, 8.76; N, 2.83; Found; C, 66.23; H, 8.61; N, 2.70.



To a suspension of $[(\eta^6\text{-C}_6\text{Me}_6)\text{RuCl}_2]_2$ (100mg, 0.150mmoles) in THF (10mL) was added a solution of LiNHAr' (165mg, 0.617mmoles) in THF (5mL). This mixture was stirred at room temperature for 12 hours after which it was a deep-green colour. The THF was removed *in vacuo* and the black-green solid was extracted with benzene and filtered through Celite. Evaporation of the benzene gave 63mg of a deep green product in 40% yield.

Anal. Calcd.; C, 68.93; H, 9.06; N, 2.68; Found; C, 68.48; H, 9.79; N, 3.39.

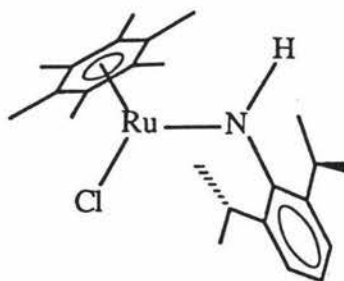


$[(\eta^6\text{-cym})\text{Ru}(\mu\text{-NAr})]_2$:

(a) To a suspension of $[(\eta^6\text{-cym})\text{RuCl}_2]_2$ (100mg, 0.163mmoles) in THF (10mL) was added a solution of LiNHAr (122mg, 0.666mmoles) in THF (5mL). This mixture was stirred at room temperature for 12 hours after which it was a deep-green colour. The THF was removed *in vacuo* and the green-black solid was extracted with benzene and filtered through Celite. Evaporation of the benzene gave 50mg of a green-black product in 37% yield.

Anal. Calcd.; C, 64.36; H, 7.61; N, 3.41; Found; C, 64.53; H, 7.82; N, 3.54.

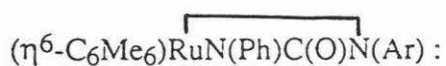
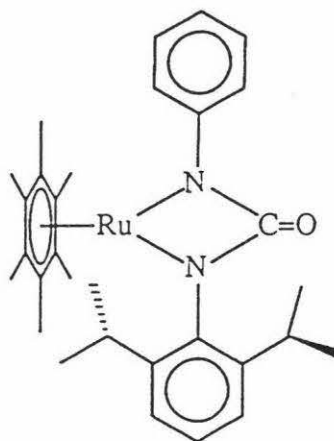
(b) To a suspension of $(\eta^6\text{-cym})\text{RuCl}_2\text{ArNH}_2$ (100mg, 0.207mmoles) in benzene (10mL) was added a solution of potassium bis(trimethylsilyl) amide (83mg, 0.416mmoles) in benzene (5mL). This mixture was stirred at room temperature for 12 hours after which it was a deep-green colour. The benzene was removed *in vacuo* and the green-black solid was extracted with toluene and filtered through Celite. Evaporation of the toluene gave 58mg of a green-black product in 68% yield.



$(\eta^6\text{-C}_6\text{Me}_6)\text{RuClINHAr}$:

To a suspension of $[(\eta^6\text{-C}_6\text{Me}_6)\text{RuCl}_2]_2$ (100mg, 0.150mmoles) in THF (10mL) was added a solution of LiNHAr (57mg, 0.309mmoles) in THF (5mL). This mixture was stirred at room temperature for 12 hours after which it was a dark red colour. The THF was removed *in vacuo* and the dark red solid was extracted with toluene and filtered through Celite. Removal of the toluene to a minimal volume and cooling to -35°C gave 93mg of a red product in 65% yield.

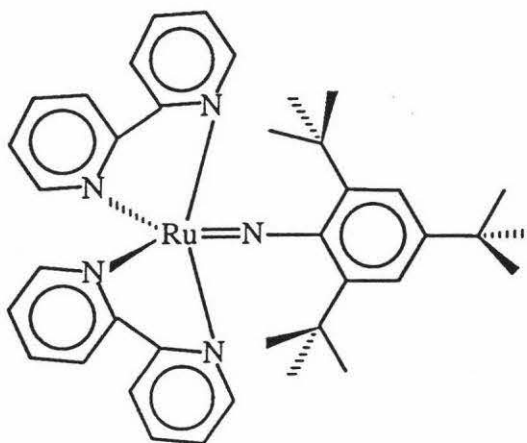
Anal. Calcd.; C, 60.67; H, 7.64; N, 2.95; Found; C, 60.07; H, 7.81; N, 3.06.



To a solution of $(\eta^6\text{-C}_6\text{Me}_6)\text{RuClNHAr}$ (100mg, 0.210mmoles) in benzene (10mL) was added a solution of phenylisocyanate (26mg, 0.218mmoles) in benzene (5mL). This mixture was stirred at room temperature for 12 hours after which it was a yellow colour. The benzene was removed *in vacuo* and the yellow solid was extracted with toluene and filtered through Celite. Reduction in volume of the toluene gave 67mg of a yellow product in 57% yield.

I.R.(KBr); 2965(m), 2925(m), 2292(m), 1777(s), 1718(s), 1596(s), 1500(s), 1443(s), 1385(m), 932(w), 768(m). cm^{-1} .

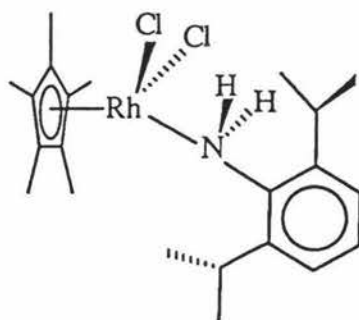
Anal. Calcd.; C, 66.75; H, 7.23; N, 5.02; Found; C, 66.14; H, 7.42; N, 5.13.



$(bpy)_2Ru=NAr'$:

To a solution of $(bpy)_2RuCl_2$ (86mg, 0.178mmoles) in THF (20mL) was added a solution of $LiNHAr'$ (98mg, 0.367mmoles) in THF (5mL). This mixture was stirred at room temperature for 12 hours after which it was a black colour. The THF was removed *in vacuo* and the black solid was extracted with benzene and filtered through Celite. Removal of the benzene to a minimal volume and addition of hexamethyldisiloxane induced precipitation of 55mg of a brown-black product in 47% yield.

Anal. Calcd.; C, 67.83; H, 6.74; N, 10.41; Found; C, 67.99; H, 6.88; N, 9.22.

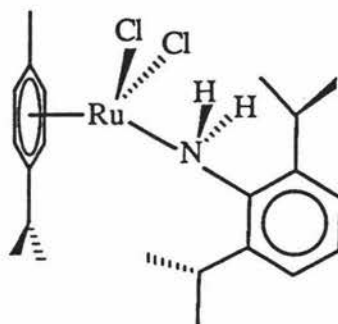


$\text{Cp}^*\text{RhCl}_2\text{ArNH}_2$:

To a suspension of $[\text{Cp}^*\text{RhCl}_2]_2$ (200mg, 0.3244mmoles) in toluene (10mL) was added a solution of NH_2Ar (115mg, 0.650mmoles) in toluene (5mL). This mixture was stirred at room temperature for 12 hours. The toluene was removed *in vacuo* leaving 271mg of a yellow product in 86% yield.

I.R.(KBr); 3303(w), 3251(w), 1601(w), 1585(w), 1575(w), 1161(w), 1081(w), 1013(m), 812(m), 767(w), 722(w). cm^{-1} .

Anal. Calcd.; C, 54.54; H, 7.07; N, 2.89; Found; C, 53.99; H, 7.11; N, 2.98.



$(\eta^6\text{-cym})\text{RuCl}_2\text{ArNH}_2$:

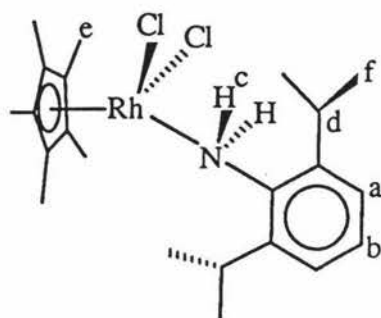
To a suspension of $[(\eta^6\text{-cym})\text{RuCl}_2]_2$ (250mg, 0.204mmoles) in toluene (10mL) was added a solution of NH_2Ar (73mg, 0.412mmoles) in toluene (5mL). This mixture was stirred at room temperature for 12 hours. The toluene was removed *in vacuo* and leaving 150mg of a yellow product in 76% yield.

I.R.(KBr); 3300(w), 3252(w), 1605(w), 1580(w), 1169(w), 1029(m), 877(w), 800(m), 760(w), 719(w). cm^{-1} .

Anal. Calcd.; C, 54.65; H, 6.88; N, 2.90; Found; C, 54.38; H, 6.61; N, 2.97.

Chapter Four

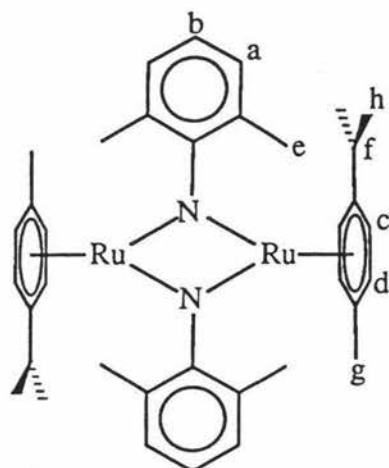
Tables of ^1H and ^{13}C nmr Data



^1H NMR Data for $\text{Cp}^*\text{RhCl}_2\text{ArNH}_2$

$\delta(\text{ppm})^*$	multi	J (Hz)	integral	hydrogen	assignment
7.12	d	7.6	2	a	$(\text{Me}_2\text{CH})_2\text{C}_6\text{H}_3$
6.99	t	7.3	1	b	$(\text{Me}_2\text{CH})_2\text{C}_6\text{H}_3$
4.48	br s	-	2	c	NH_2
3.13	sept	6.2	2	d	$(\text{Me}_2\text{CH})_2\text{C}_6\text{H}_3$
1.63	s	-	15	e	C_5Me_5
1.29	d	6.8	12	f	$(\text{Me}_2\text{CH})_2\text{C}_6\text{H}_3$

*Referenced to chloroform at 7.24 ppm.

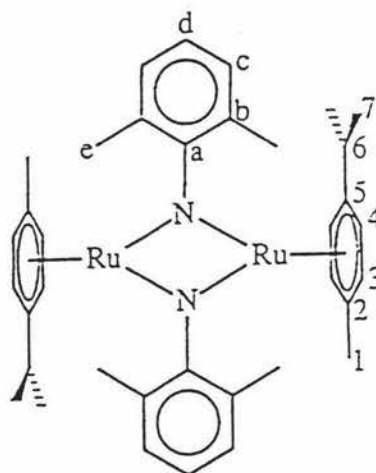

 ^1H NMR Data for $[(\eta^6\text{-cym})\text{Ru}(\mu\text{-NAr}'')]_2$

$\delta(\text{ppm})^*$	multi	J (Hz)	integral	hydrogen	assignment
7.33	d	7.3	2	a	$\text{Me}_2\text{C}_6\text{H}_3$
7.17	t	7.3	1	b	$\text{Me}_2\text{C}_6\text{H}_3$
4.37	d	6.0	2	c or d	$\text{MeC}_6\text{H}_4\text{CHMe}_2$
4.26	d	5.9	2	c or d	$\text{MeC}_6\text{H}_4\text{CHMe}_2$
2.35	s	-	6	e	$\text{Me}_2\text{C}_6\text{H}_3$
2.20	sept	6.9	1	f	$\text{MeC}_6\text{H}_4\text{CHMe}_2$
1.73	s	-	3	g	$\text{MeC}_6\text{H}_4\text{CHMe}_2$
0.97	d	7.0	6	h	$\text{MeC}_6\text{H}_4\text{CHMe}_2$

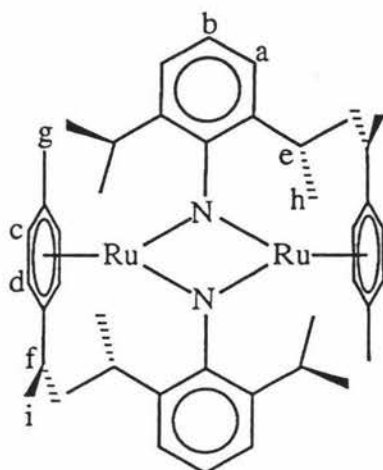
*Referenced to benzene at 7.15 ppm.

^{13}C NMR Data for $[(\eta^6\text{-cym})\text{Ru}(\mu\text{-NAr''})_2]_2$

$\delta(\text{ppm})^*$	assignment
169.7	a
127.7	b
126.0	c
121.6	d
100.6	5
89.2	2
81.8	3 or 4
79.2	3 or 4
31.7	6
23.7	7
19.6	e
19.1	1



*Referenced to benzene at 128 ppm.

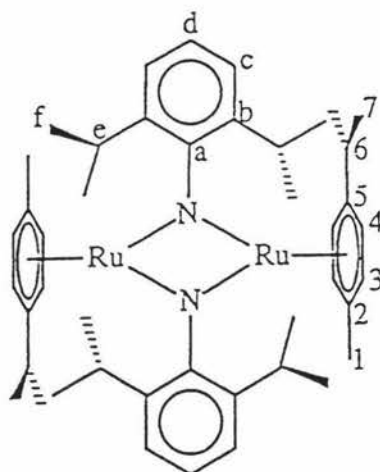

 ^1H NMR Data for $[(\eta^6\text{-cym})\text{Ru}(\mu\text{-NAr})]_2$

$\delta(\text{ppm})^*$	muti	J (Hz)	integral	hydrogen	assignment
7.33	d	1.8	2	a	$(\text{Me}_2\text{CH})_2\text{C}_6\text{H}_3$
7.20	t	small	1	b	$(\text{Me}_2\text{CH})_2\text{C}_6\text{H}_3$
4.74	d	5.9	2	c or d	$\text{MeC}_6\text{H}_4\text{CHMe}_2$
4.55	d	5.9	2	c or d	$\text{MeC}_6\text{H}_4\text{CHMe}_2$
3.61	br s	-	2	e	$(\text{Me}_2\text{CH})_2\text{C}_6\text{H}_3$
2.52	sept	6.8	1	f	$\text{MeC}_6\text{H}_4\text{CHMe}_2$
1.76	s	-	3	g	$\text{MeC}_6\text{H}_4\text{CHMe}_2$
1.43	d	6.6	12	h	$(\text{Me}_2\text{CH})_2\text{C}_6\text{H}_3$
1.03	d	6.6	6	i	$\text{MeC}_6\text{H}_4\text{CHMe}_2$

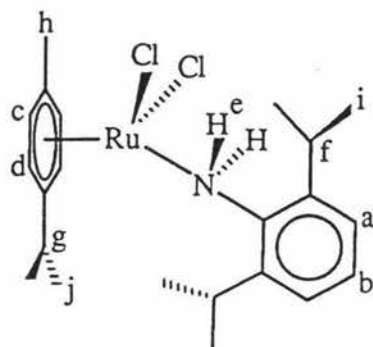
*Referenced to benzene at 7.15 ppm.

^{13}C NMR Data for $[(\eta^6\text{-cym})\text{Ru}(\mu\text{-NAr})_2]$

$\delta(\text{ppm})^*$	assignment
167.7	a
128.7	b
123.3	c
122.9	d
102.1	5
90.8	2
77.7	3 or 4
77.6	3 or 4
30.8	6
26.7	e
26.5	f
24.0	7
19.1	1



*Referenced to benzene at 128 ppm.

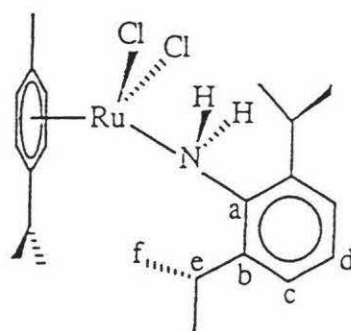

 ^1H NMR Data for $(\eta^6\text{-cym})\text{RuCl}_2\text{ArNH}_2$

$\delta(\text{ppm})^*$	multi	J (Hz)	integral	hydrogen	assignment
7.37	d	small	2	a	$(\text{Me}_2\text{CH})_2\text{C}_6\text{H}_3$
7.27	t	small	1	b	$(\text{Me}_2\text{CH})_2\text{C}_6\text{H}_3$
4.96	d	6.2	2	c or d	$\text{MeC}_6\text{H}_4\text{CHMe}_2$
4.82	d	6.2	2	c or d	$\text{MeC}_6\text{H}_4\text{CHMe}_2$
4.76	br s	4.8	2	e	NH_2
3.44	sept	6.7	2	f	$(\text{Me}_2\text{CH})_2\text{C}_6\text{H}_3$
2.91	sept	7.0	1	g	$\text{MeC}_6\text{H}_4\text{CHMe}_2$
2.09	s	-	3	h	$\text{MeC}_6\text{H}_4\text{CHMe}_2$
1.32	d	6.9	12	i	$(\text{Me}_2\text{CH})_2\text{C}_6\text{H}_3$
1.28	d	7.0	6	j	$\text{MeC}_6\text{H}_4\text{CHMe}_2$

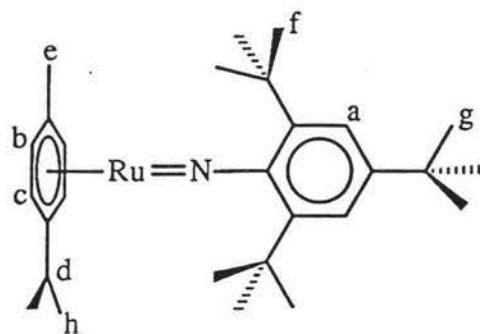
*Referenced to chloroform at 7.24 ppm.

^{13}C NMR Data for $(\eta^6\text{-cym})\text{RuCl}_2\text{ArNH}_2$

$\delta(\text{ppm})^*$	assignment
139.0	a
123.5	b
123.4	c
105.3	d
94.3	5
82.8	2
hidden by solvent	3 or 4
31.0	6
27.7	e
22.4	f
22.1	7
17.7	1



*Referenced to chloroform at 77.0 ppm.

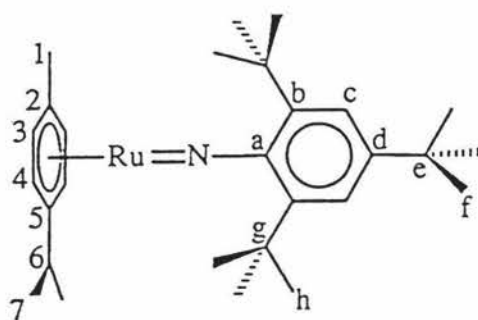

 ^1H NMR Data for $(\eta^6\text{-cym})\text{Ru}=\text{NAr}'$

$\delta(\text{ppm})^*$	multi	J (Hz)	integral	hydrogen	assignment
7.29	s	-	2	a	$(\text{CMe}_3)_3\text{C}_6\text{H}_2$
5.11	d	6.2	2	b or c	$\text{MeC}_6\text{H}_4\text{CHMe}_2$
5.03	d	6.2	2	b or c	$\text{MeC}_6\text{H}_4\text{CHMe}_2$
2.65	sept	6.8	1	d	$\text{MeC}_6\text{H}_4\text{CHMe}_2$
2.01	s	-	3	e	$\text{MeC}_6\text{H}_4\text{CHMe}_2$
1.87	s	-	18	f	$(\text{CMe}_3)_2\text{C}_6\text{H}_2\text{CMe}_3$
1.26	s	-	9	g	$(\text{CMe}_3)_2\text{C}_6\text{H}_2\text{CMe}_3$
1.19	d	6.9	6	h	$\text{MeC}_6\text{H}_4\text{CHMe}_2$

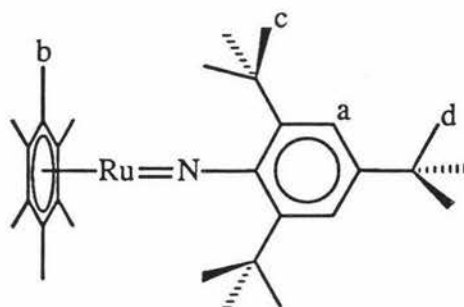
*Referenced to benzene at 7.15 ppm.

^{13}C NMR Data for $(\eta^6\text{-cym})\text{Ru}=\text{NAr}'$

$\delta(\text{ppm})^*$	assignment
157.9	a
148.1	b
145.6	d
121.7	c
102.4	5
90.3	2
79.4	3 or 4
77.4	3 or 4
38.0	h
35.5	g
32.9	6
31.5	e
31.2	f
23.9	7
20.8	1



*Referenced to benzene at 128 ppm.

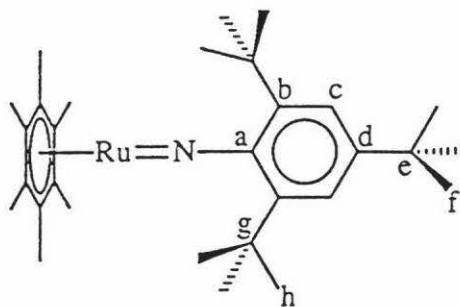

 $^1\text{H NMR Data for } (\eta^6\text{-C}_6\text{Me}_6)\text{Ru}=\text{NAr}'$

$\delta(\text{ppm})^*$	multi	J (Hz)	integral	hydrogen	assignment
7.20	s	-	2	a	$(\text{CMe}_3)_3\text{C}_6\text{H}_2$
2.11	s	-	18	b	Me_6C_6
1.81	s	-	18	c	$\text{CMe}_3\text{C}_6\text{H}_2(\text{CMe}_3)_2$
1.27	s	-	9	d	$\text{CMe}_3\text{C}_6\text{H}_2(\text{CMe}_3)_2$

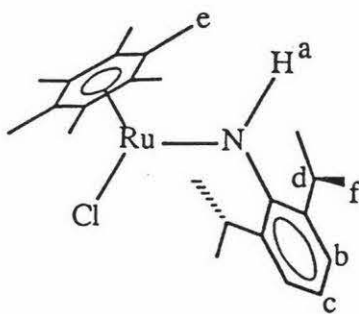
*Referenced to benzene at 7.15 ppm.

^{13}C NMR Data for $(\eta^6\text{-C}_6\text{Me}_6)\text{Ru}=\text{NAr}'$

$\delta(\text{ppm})^*$	assignment
146.9	a
128.7	b
128.4	d
121.6	c
89.2	C_6Me_6
38.2	h
31.3	e
30.9	g
30.6	f
18.2	C_6Me_6



*Referenced to benzene at 128 ppm.

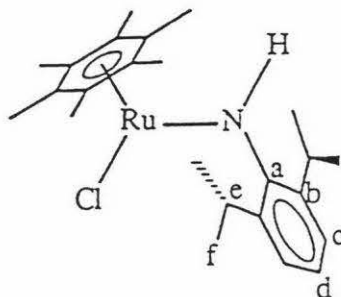

 ^1H NMR Data for $(\eta^6\text{-C}_6\text{Me}_6)\text{RuClINHAr}$

$\delta(\text{ppm})^*$	multi	J (Hz)	integral	hydrogen	assignment
10.18	s	-	1	a	NH
7.26	d	7.0	2	b	$(\text{Me}_2\text{CH})_2\text{C}_6\text{H}_3$
7.18	t	7.0	1	c	$(\text{Me}_2\text{CH})_2\text{C}_6\text{H}_3$
3.63	sept	6.6	2	d	$(\text{Me}_2\text{CH})_2\text{C}_6\text{H}_3$
1.69	s	-	18	e	C_6Me_6
1.16	d	7.0	12	f	$(\text{Me}_2\text{CH})_2\text{C}_6\text{H}_3$

*Referenced to benzene at 7.15 ppm.

^{13}C NMR Data for $(\eta^6\text{-C}_6\text{Me}_6)\text{RuClINHAr}$

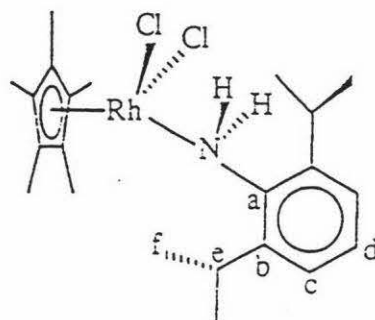
$\delta(\text{ppm})^*$	assignment
152.5	a
142.6	b
124.7	c
122.2	d
88.0	C_6Me_6
28.3	e
28.1	f
15.8	C_6Me_6



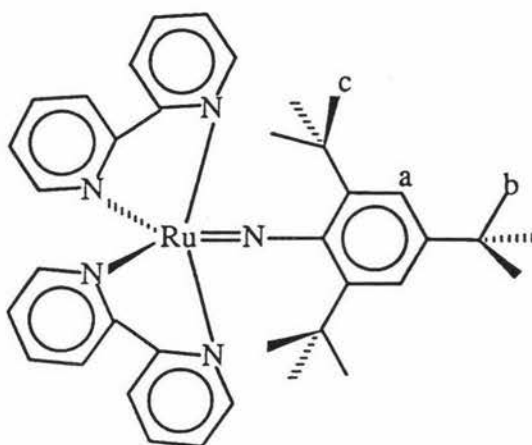
*Referenced to benzene at 128 ppm.

 ^{13}C NMR Data for $\text{Cp}^*\text{RhCl}_2\text{ArNH}_2$

$\delta(\text{ppm})^*$	assignment
138.8	a
128.3	b
123.0	c
94.1	d
93.9	C_5Me_5
27.6	e
22.8	f
9.4	C_5Me_5

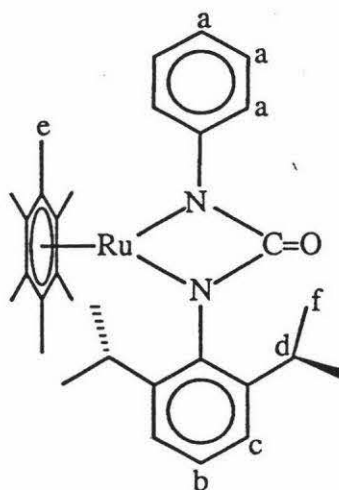


*Referenced to chloroform at 77.0 ppm.


 $^1\text{H NMR Data for } (\text{bpy})_2\text{Ru}=\text{NAr}^?$

$\delta(\text{ppm})^*$	multi	J (Hz)	integral	hydrogen	assignment
7.50-8.64	-	-	16	-	bipyridine aromatics
7.27	s	-	2	a	$(\text{CMe}_3)_3\text{C}_6\text{H}_2$
1.48	s	-	9	b	$(\text{CMe}_3)_2\text{C}_6\text{H}_2\text{CMe}_3$
1.31	s	-	18	c	$(\text{CMe}_3)_2\text{C}_6\text{H}_2\text{CMe}_3$

*Referenced to benzene at 7.15 ppm.



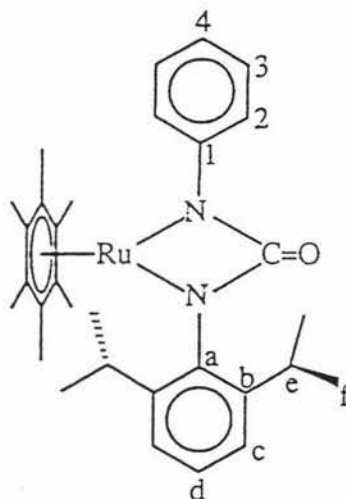
$${}^1\text{H NMR Data for } (\eta^6\text{-C}_6\text{Me}_6)\text{RuN(Ph)C(O)N(Ar)}$$

$\delta(\text{ppm})^*$	multi	J (Hz)	integral	hydrogen	assignment
7.30	m	-	5	a	Ph
7.18	t	7.7	1	b	$(\text{Me}_2\text{CH})_2\text{C}_6\text{H}_3$
7.07	d	8.1	2	c	$(\text{Me}_2\text{CH})_2\text{C}_6\text{H}_3$
3.13	br s	-	2	d	$(\text{Me}_2\text{CH})_2\text{C}_6\text{H}_3$
2.08	s	-	18	e	C_6Me_6
1.17	d	6.2	12	f	$(\text{Me}_2\text{CH})_2\text{C}_6\text{H}_3$

*Referenced to benzene at 7.15 ppm.

^{13}C NMR Data for $(\eta^6\text{-C}_6\text{Me}_6)\text{RuN}(\text{Ph})\text{C}(\text{O})\text{N}(\text{Ar})$

$\delta(\text{ppm})^*$	assignment
170.4	CO
152.4	a
140.2	3
129.0	4
127.4	b
127.2	c
125.6	5
123.9	6
120.8	d
89.4	C_6Me_6
25.9	e
25.1	f
18.0	C_6Me_6



*Referenced to benzene at 128 ppm.

Appendix

Crystal Structures

The results of 4 crystal structure determinations are presented in chapter two. The X-ray intensity data for the structure determination of $[(\text{cym})\text{Ru}(\mu\text{-NAr})]_2$ and $(\text{cym})\text{Ru}=\text{NAr}'$ were collected by Ward Robinson of Canterbury University. Dr. Anthony Burrell carried out the X-ray intensity data for the structure determination of $(\text{C}_6\text{Me}_6)\text{RuClNHAr}$ and $(\text{cym})\text{RuCl}_2\text{NH}_2\text{Ar}$ at Massey University. The structure determination and refinement of these complexes was carried out at Massey University by Dr. Anthony Burrell.

Details on data collection and structure refinement for the four complexes are given below.

[(cym)Ru(μ -NAr)]₂

Empirical Formula	C ₄₄ H ₆₂ N ₂ Ru ₂	
Formula Weight	821.10	
Temperature	183(2) K	
Wavelength	0.71073 Å	
Crystal System	monoclinic	
Space Group	P2(1)/c	
Unit Cell Dimensions	a=19.786(14) Å	alpha=90°
	b=10.238(9) Å	beta=99.47(6)°
	c=19.466(13) Å	gamma=90°
Volume	3889.5(14) Å ³	
Z	4	
Density (calculated)	1.402 mg/m ³	
Absorption Coefficient	0.809 mm ⁻¹	
F(000)	1712	
Crystal Size	0.76x0.5x0.26 mm	
Theta Range for Data Collection	2.09 to 24.02°	
Index Ranges	-22 ≤ h ≤ 22, -11 ≤ k ≤ 0, -22 ≤ l ≤ 8	
Reflections Collected	7408	
Independent Reflections	6088 [R(int) = 0.1436]	
Refinement Method	Full-matrix Least-squares on F ²	
Data/Restraints/Parameters	6081/0/433	
Goodness-of-fit on F ²	1.052	
Final R Indices [I > 2sigma(I)]	R ₁ = 0.0641, wR ₂ = 0.1177	
R Indices (all data)	R ₁ = 0.1400, wR ₂ = 0.1543	
Largest Diff. Peak and Hole	0.732 and -0.715 e.Å ⁻³	

$(\text{cym})\text{Ru}=\text{NAr}'$

Empirical Formula	C ₂₈ H ₄₃ N Ru	
Formula Weight	494.70	
Temperature	293(2) K	
Wavelength	0.71073 Å	
Crystal System	triclinic	
Space Group	P-1	
Unit Cell Dimensions	a=10.445(4) Å	alpha=90.51(3)°
	b=13.723(5) Å	beta=98.69(4)°
	c=20.101(6) Å	gamma=112.26(3)°
Volume	2629(2) Å ³	
Z	4	
Density (calculated)	1.250 mg/m ³	
Absorption Coefficient	0.610 mm ⁻¹	
F(000)	1048	
Crystal Size	0.84x0.4x0.3 mm	
Theta Range for Data Collection	2.06 to 22.51°	
Index Ranges	0 ≤ h ≤ 7, -14 ≤ k ≤ 13, -21 ≤ l ≤ 21	
Reflections Collected	5994	
Independent Reflections	5550 [R(int) = 0.1875]	
Refinement Method	Full-matrix Least-squares on F ²	
Data/Restraints/Parameters	5546/66/541	
Goodness-of-fit on F ²	1.087	
Final R Indices [I > 2sigma(I)]	R ₁ = 0.0810, wR ₂ = 0.1646	
R Indices (all data)	R ₁ = 0.1648, wR ₂ = 0.2115	
Largest Diff. Peak and Hole	1.504 and -1.053 e.Å ⁻³	

$(C_6Me_6)RuClNHAr$

Empirical Formula	C ₂₄ H ₃₆ Cl N Ru	
Formula Weight	475.06	
Temperature	187(2) K	
Wavelength	0.71073 Å	
Crystal System	monoclinic	
Space Group	P2(1)/c	
Unit Cell Dimensions	a=9.699(7) Å	alpha=90°
	b=14.095(14) Å	beta=100.82(8)°
	c=16.758(10) Å	gamma=90°
Volume	2250(3) Å ³	
Z	4	
Density (calculated)	1.402 mg/m ³	
Absorption Coefficient	0.824 mm ⁻¹	
F(000)	992	
Crystal Size	0.64x0.2x0.06 mm	
Theta Range for Data Collection	2.14 to 22.50°	
Index Ranges	-10 ≤ h ≤ 0, 0 ≤ k ≤ 15, -17 ≤ l ≤ 17	
Reflections Collected	3090	
Independent Reflections	2937 [R(int) = 0.1595]	
Refinement Method	Full-matrix Least-squares on F ²	
Data/Restraints/Parameters	2937/78/242	
Goodness-of-fit on F ²	1.046	
Final R Indices [I > 2sigma(I)]	R ₁ = 0.0997, wR ₂ = 0.1751	
R Indices (all data)	R ₁ = 0.2205, wR ₂ = 0.2281	
Largest Diff. Peak and Hole	1.022 and -0.717 e.Å ⁻³	

$(\text{cym})\text{RuCl}_2\text{ArNH}_2$

Empirical Formula	C ₂₂ H ₃₃ Cl ₂ N Ru
Formula Weight	483.46
Temperature	291(2) K
Wavelength	0.71073 Å
Crystal System	monoclinic
Space Group	Cc
Unit Cell Dimensions	a=19.865(4) Å alpha=90° b=6.930(4) Å beta=98.47(3)° c=33.57(2) Å gamma=90°
Volume	4571(4) Å ³
Z	8
Density (calculated)	1.405 mg/m ³
Absorption Coefficient	0.926 mm ⁻¹
F(000)	2000
Crystal Size	0.70x0.70x0.50 mm
Theta Range for Data Collection	1.23 to 24.99°
Index Ranges	0 ≤ h ≤ 23, 0 ≤ k ≤ 8, -39 ≤ l ≤ 39
Reflections Collected	4149
Independent Reflections	4149 [R(int) = 0.0000]
Refinement Method	Full-matrix Least-squares on F ²
Data/Restraints/Parameters	4144/2/481
Goodness-of-fit on F ²	1.072
Final R Indices [I > 2sigma(I)]	R ₁ = 0.0266, wR ₂ = 0.0850
R Indices (all data)	R ₁ = 0.0377, wR ₂ = 0.0986
Absolute Structure Parameter	0.04(8)
Largest Diff. Peak and Hole	0.494 and -0.413 e.Å ⁻³

References

1. (a) Pauling L. "The Nature of the Chemical Bond" 3rd edition, Cornell University Press, Ithaca, New York, 1960. (b) Palmer, K.J. *J. Am. Chem. Soc.* **1938**, *60*, 23-60. (c) Griffith, W.P. *Coord. Chem. Rev.* **1970**, *5*, 459.
2. (a) Haase, W.; Hoppe, H. *Acta. Cryst.* **1968**, *B24*, 282. (b) Dwyer, P.N.; Puppe, L.; Buchler, J.W.; Scheidt, W.R. *Inorg. Chem.* **1975**, *14*, 1782. (c) Hiller, W.; Strähle, J.; Kobel, W.; Hanack, M. *Z. Kristallogr.* **1982**, *159*, 173.
3. Sharpless, K.B.; Flood, T.C. *J. Am. Chem. Soc.* **1971**, *93*, 2316.
4. Nugent, W.A.; Mayer, J.M. "Metal-Ligand Multiple Bonds" References 1 to 4, page 45, Wiley, New York, 1988.
5. Nugent, W.A.; Mayer, J.M. "Metal-Ligand Multiple Bonds" Wiley, New York, 1988.
6. Nugent, W.A.; Mayer, J.M. "Metal-Ligand Multiple Bonds" References 5 to 12, page 45, Wiley, New York, 1988.
7. (a) Pipes, D.W.; Meyer, T.J. *Inorg. Chem.* **1986**, *25*, 3256. (b) Valencia, E.; Santarsiero, B.D.; Geib, S.J.; Rheingold, A.L.; Mayer, J.M. *J. Am. Chem. Soc.* **1987**, *109*, 6896.
8. Nugent, W.A.; Mayer, J.M. "Metal-Ligand Multiple Bonds" References 7 to 12, page 45, Wiley, New York, 1988.
9. (a) Mayer, J.M.; Thorn, D.L.; Tulip, T.H.; *J. Am. Chem. Soc.* **1985**, *107*, 7454. (b) Mayer, J.M.; Tulip, T.H.; Calabrese, J.C.; Valencia, E. *J. Am. Chem. Soc.* **1987**, *109*, 157.
10. Fatiadi, A.J. *Synthesis* **1987**, 85.
11. Lee, D.G.; Van den Engh, M. in "Oxidation in Organic Chemistry, Part B" Trahanovsky, W.S., ed. Academic, New York, 1973.
12. Schröder, M. *Chem. Rev.* **1980**, *80*, 187.
13. (a) Corey, E.J.; Suggs, J.W. *Tetrahedron Lett.* **1975**, 2647. (b) Dirand, J.; Ricard, L.; Weiss, R. *J. Chem. Soc., Dalton Trans.* **1976**, 278.

14. Ortiz de Montellano, P.R., ed. "Cytochrome P-450: Structure, Mechanism, and Biochemistry" Plenum, New York, 1986.
15. Holm, R.H.; Berg, J.M. *Acc. Chem. Res.* **1986**, *19*, 363.
16. (a) Keulks, G.W.; Krenzke, L.D.; Notermann, T.M. *Adv. Catal.* **1978**, *27*, 183.
(b) van den Elzen, A.F.; Rieck, G.D. *Acta Cryst.* **1973**, *B29*, 2433. (c) van den Elzen, A.F.; Rieck, G.D. *Acta Cryst.* **1973**, *B29*, 2436.
17. Grzybowska, B.; Haber, J.; Janas, J. *J. Catal.* **1977**, *49*, 150.
18. (a) Machiels, C.J.; Sleight, A.W. *J. Catal.* **1982**, *76*, 238. (b) Ohuchi, F.; Firmment, L.E.; Chowdhry, U.; Ferretti, A. *J. Vac. Sci. Technol. A* **1982**, *2*, 1022.
(c) Farneth, W.E.; Ohuchi, F.; Staley, R.H.; Chowdhry, U.; Sleight, A.W. *J. Phys. Chem.* **1985**, *89*, 2493. (d) Compare: Tatibouet, J.M.; Germain, J.E. *J. Catal.* **1981**, *72*, 375.
19. Chabardes, P.; Querou, Y.; Brit. patent 1 204 754, 1970; *Chem. Abstr.* **1970**, *72*, 43923g.
20. (a) Herrman, W.A. *J. Organomet. Chem.* **1986**, *300*, 111. (b) Schrauzer, G.N.; Schlemper, E.O.; Liu, N.H.; Wang, Q.; Rubin, K.; Zhang, X.; Long, X.; Chin, C.S. *Organometallics* **1986**, *5*, 2452. (c) Bokiy, N.G.; Gatilov, Yu.V.; Ustynyuk, N.A. *J. Organomet. Chem.* **1973**, *54*, 213.
21. Fritzsche, J.; Struve, H. *J. Prakt. Chem.* **1847**, *41*, 97.
22. Werner, A.; Dinklage, K. *Chem. Ber.* **1901**, *34*, 2698.
23. Chatt, J.; Garforth, J.D.; Rowe, G.A. *Chem. Ind.* **1963**, 332.
24. (a) Dehnicke, K.; Strähle, J. *J. Angew. Chem., Int. Ed. Engl.* **1981**, *20*, 413.
(b) Miskowski, V.; Gray, H.B.; Poon, C.K.; Ballhausen, C.J. *Mol. Phys.* **1974**, *28*, 747.
25. Chatt, J.; Garforth, J.D.; Rowe, G.A. *J. Chem. Soc. A* **1966**, 1834.
26. Toth, L.E. "Transition Metal Carbides and Nitrides" Academic, New York, 1971.
27. Wheeler, R.A.; Hoffmann, R.; Strähle, J. *J. Am. Chem. Soc.* **1986**, *108*, 5381.
28. DuBois, D.L.; Hoffmann, R. *Nouv. J. Chim.* **1977**, *1*, 479.

29. Hidai, M.; Mizobe, Y.; Sato, M.; Kodama, T.; Uchida, Y. *J. Am. Chem. Soc.* **1978**, *100*, 5740.
30. (a) Chatt, J.; Dilworth, J.R.; Richards, R.L. *Chem. Rev.* **1978**, *78*, 589. (b) Hidai, M. in "Molybdenum Enzymes"; Spiro, T.G., ed. Wiley, New York, 1985.
31. (a) Chatt, J.; Heath, G.A.; Richards, R.L. *J. Chem. Soc., Chem. Comm.* **1972**, 1010. (b) Cotton, F.A.; Wilkinson, G. "Advances in Inorganic Chemistry" 5th ed., page 1139, Wiley-Interscience, New York, 1988. (c) Schrock, R.R. *Acc. Chem. Res.* **1979**, *12*, 98. (d) Seyferth, D. "Transition Metal Carbene Complexes" Verlag Chemie, Weinheim, 1983. (e) Goddard, R.J.; Hoffmann, R.; Jemmis, E.D. *J. Am. Chem. Soc.* **1980**, *102*, 7667. (f) Taylor, T.E.; Hall, M.B.; *J. Am. Chem. Soc.* **1984**, *106*, 1576.
32. Fischer, E.O.; Maasböl, A. *Angew. Chem., Int. Ed. Engl.* **1964**, *3*, 580.
33. Brookhart, M.; Studabaker, W.B. *Chem. Rev.* **1987**, *87*, 411.
34. Hegedus, L.S.; McGuire, M.A.; Schultze, L.M.; Yijun, C.; Anderson, O.P. *J. Am. Chem. Soc.* **1984**, *106*, 2680.
35. Dötz, K.H. *Pure Appl. Chem.* **1983**, *55*, 1689.
36. Schrock, R.R.; *J. Organomet. Chem.* **1986**, *300*, 249.
37. Tebbe, F.N.; Parshall, G.W.; Reddy, G.S. *J. Am. Chem. Soc.* **1978**, *100*, 36-11.
38. Brown-Wensley, K.A.; Buchwald, S.L.; Cannizzo, L.; Clawson, L.; Ho, S.; Meinhardt, D.; Stille, J.R.; Straus, D.; Grubbs, R.H. *Pure Appl. Chem.* **1983**, *55*, 1733.
39. Schrock, R.R. *J. Am. Chem. Soc.* **1976**, *98*, 5399.
40. Wittig, G. *J. Organomet. Chem.* **1975**, *100*, 279.
41. Ivin, K.J. "Olefin Metathesis" Academic Press, London, 1983.
42. Dragutan, V.; Balaban, A.T.; Dimonie, M. "Olefin Metathesis and Ring Opening Polymerization of Cyclo-Olefins" Wiley-Interscience, Chichester, 1985.
43. Ivin, K.J.; Rooney, J.J.; Stewart, C.D.; Green, M.L.H.; Mahtab, R. *J. Chem. Soc., Chem. Comm.* **1978**, 604.

44. Kostic, N.M.; Fenske, R.F. *J. Am. Chem. Soc.* **1981**, *103*, 4677.
45. Fischer, E.O.; Kreis, G.; Kreiter, C.G.; Müller, J.; Huttner, G.; Lorenz, H. *Angew. Chem., Int. Ed. Engl.* **1973**, *12*, 564.
46. McLain, S.J.; Wood, C.D.; Messerle, L.W.; Schrock, R.R.; Hollander, F.J.; Youngs, W.J.; Churchill, M.R. *J. Am. Chem. Soc.* **1978**, *100*, 5962.
47. (a) Sancho, J.; Schrock, R.R. *J. Mol. Catal.* **1982**, *15*, 75. (b) Freudenberger, J.H.; Schrock, R.R.; Churchill, M.R.; Rhinegold, A.L.; Ziller, J.W. *Organometallics* **1984**, *3*, 1563.
48. Clifford, A.F.; Kobayashi, C.S. Abstracts, 130th National Meeting of the American Chemical Society, Atlantic City, NJ, Sept. 1956, p.50R.
49. Chatt, J.; Rowe, G.A. *J. Chem. Soc.* **1962**, 4019.
50. Wigley, D. *Prog. Inorg. Chem.* **1994**, *42*, 239.
51. (a) McGlinchey, M.J.; Stone, F.G.A. *J. Chem. Soc., Chem. Comm.* **1970**, 1265. (b) Ashley-Smith, J.; Green, M.; Mayne, N.; Stone, F.G.A. *J. Chem. Soc. Dalton Trans.* **1972**, 1805.
52. (a) Patrick, D.W.; Truesdale, L.K.; Biller, S.A.; Sharpless, K.B. *J. Org. Chem.* **1978**, *43*, 2628. (b) Herranz, E.; Sharpless, K.B. *J. Org. Chem.* **1978**, *43*, 2544.
53. Chong, A.O.; Oshima, K.; Sharpless, K.B. *J. Am. Chem. Soc.* **1977**, *99*, 3420.
54. (a) Burrington, J.D.; Kartisek, C.T.; Grasselli, R.K. *J. Catal.* **1984**, *87*, 363. (b) Chan, D.M.-T.; Fultz, W.C.; Nugent, W.A.; Roe, D.C.; Tulip, T.H. *J. Am. Chem. Soc.* **1985**, *107*, 251. (c) Chan, D.M.-T.; Nugent, W.A. *Inorg. Chem.* **1985**, *24*, 1422.
55. Meisel, I.; Hertel, G.; Weiss, K. *J. Mol. Catal.* **1986**, *36*, 159.
56. Schaverien, C.J.; Dewan, J.C.; Schrock, R.R. *J. Am. Chem. Soc.* **1986**, *108*, 2771.
57. (a) Chao, Y.-W.; Rodgers, P.M.; Wigley, D.E.; Alexander, S.J.; Rheingold, A.L. *J. Am. Chem. Soc.* **1991**, *113*, 6326. (b) Mayer, J.M.; Curtis, C.J.; Bercaw, J.E. *J. Am. Chem. Soc.* **1983**, *105*, 2651.

58. Nugent, W.A.; Harlow, R.L. *Inorg. Chem.* **1980**, *19*, 777.
59. Clifford, A.F.; Kobayashi, C.S. *Inorg. Synth.* **1960**, *6*, 207.
60. Antonelli, D.M.; Schaefer, W.P.; Parkin, G.; Bercaw, J.E. *J. Organomet. Chem.* **1993**, *462*, 213.
61. Rocklage, S.M.; Schrock, R.R.; Churchill, M.R.; Wasserman, H.J. *Organometallics* **1982**, *1*, 1332.
62. (a) Chambers, O.R.; Harman, M.E.; Rycroft, D.S.; Sharp, D.W.A.; Winfield, J.M. *J. Chem. Res. (M)* **1977**, 1849. (b) Harmon, M.; Sharp, D.W.A.; Winfield, J.M.; *Inorg. Nucl. Chem. Lett.* **1974**, *10*, 183.
63. Preuss, F.; Towae, W. *Z. Naturforsch. B: Anorg. Chem. Org. Chem.* **1981**, *36B*, 1130.
64. (a) Williams, D.N.; Mitchell, J.P.; Poole, A.D.; Siemeling, U.; Clegg, W.; Hockless, D.C.R.; O'Neil, P.A.; Gibson, V.C. *J. Chem. Soc. Dalton Trans.* **1992**, 739. (b) Gibson, V.C.; Williams, D.N.; Clegg, W.; Hockless, D.C.R. *Polyhedron*, **1989**, *8*, 1819. (c) Jolly, M.; Mitchell, J.P.; Gibson, V.C. *J. Chem. Soc. Dalton Trans.* **1992**, 1331.
65. (a) Kolomnikov, I.S.; Koreshkov, Yu.D.; Lobeeva, T.S.; Volpin, M.E. *Akad. Nauk SSSR, Ser. Khim.* **1971**, 2065. (b) Kolomnikov, I.S.; Koreshkov, Yu.D.; Lobeeva, T.S.; Volpin, M.E. *J. Chem. Soc., Chem. Comm.* **1970**, 1432.
66. (a) Pedersen, S.F.; Schrock, R.R.; *J. Am. Chem. Soc.* **1982**, *104*, 7483. (b) Bradley, D.C.; Hursthouse, M.B.; Malik, K.M.A.; Nielson, A.J.; Short, R.L. *J. Chem. Soc., Dalton Trans.* **1983**, 2651. (c) Nielson, A.J. *Inorg. Synth.* **1986**, *24*, 194. (d) Maatta, E.A.; *Inorg. Chem.* **1984**, *23*, 2560. (e) Ashcroft, B.R.; Clark, G.R.; Nielson, A.J.; Rickard, C.E.F. *Polyhedron* **1986**, *5*, 2081.
67. (a) Rocklage, S.M.; Schrock, R.R. *J. Am. Chem. Soc.* **1982**, *104*, 3077. (b) Rocklage, S.M.; Schrock, R.R. *J. Am. Chem. Soc.* **1980**, *102*, 7808.
68. (a) Hubert-Pfalzgraf, L.G.; Aharonian, G. *Inorg. Chim. Acta* **1985**, *100*, L21. (b) Nugent, W.A.; Mayer, J.M. "Metal-Ligand Multiple Bonds" References 203 to 215 page 106, Wiley, New York, 1988.

69. (a) Cotton, F.A.; Duraj, S.A.; Roth, W.J. *J. Am. Chem. Soc.* **1984**, *106*, 4749.
(b) Canich, J.A.M.; Cotton, F.A.; Duraj, S.A.; Roth, W.J. *Polyhedron* **1986**, *5*, 895.
70. Joslin, F.L.; Johnson, M.P.; Mague, J.T.; Roundhill, D.M. *Organometallics* **1991**, *10*, 2781.
71. Schrock, R.R.; Fellmann, J.D. *J. Am. Chem. Soc.* **1978**, *100*, 3359.
72. Doxsee, K.M.; Farahi, J.B. *J. Chem. Soc., Chem. Comm.* **1990**, 1452.
73. Bishop, M.W.; Chatt, J.; Dilworth, J.R.; Neaves, B.D.; Dahlstrom, P.; Hyde, J.; Zubieta, J. *J. Organomet. Chem.* **1981**, *213*, 109.
74. Shapley, P.A.; Kin, H.S.; Wilson, S.R. *Organometallics* **1988**, *7*, 928.
75. Takahashi, Y.; Onoyama, N.; Ishikawa, Y.; Motojima, S.; Sugiyama, K. *Chem. Lett.* **1978**, 525.
76. Gray, S.D.; Smith, D.P.; Bruck, M.A.; Wigley, D.E. *J. Am. Chem. Soc.* **1992**, *114*, 5462.
77. Bishop, M.W.; Chatt, J.; Dilworth, J.R.; Hursthouse, M.B.; Jayaweera, S.A.A.; Quick, A. *J. Chem. Soc., Dalton Trans.* **1979**, 914.
78. Chatt, J.; Dilworth, J.R.; Leigh, G.L. *J. Chem. Soc. A* **1970**, 2239.
79. Cotton, F.A.; Shamsoum, E.S. *J. Am. Chem. Soc.* **1984**, *106*, 3222.
80. La Monica, G.; Cenini, S. *J. Chem. Soc., Dalton Trans.* **1980**, 1145.
81. (a) Glueck, D.S.; Wu, J.; Hollander, F.J.; Bergman, R.G. *J. Am. Chem. Soc.* **1991**, *113*, 2041. (b) Glueck, D.S.; Hollander, F.J.; Bergman, R.G. *J. Am. Chem. Soc.* **1989**, *111*, 2719.
82. (a) Michelman, R.I.; Bergman, R.G.; Andersen, R.A. *Organometallics* **1993**, *12*, 2741. (b) Michelman, R.I.; Bergman, R.G.; Andersen, R.A. *J. Am. Chem. Soc.* **1991**, *113*, 5100.
83. Tooze, R.P.; Wilkinson, G.; Motevalli, M.; Hursthouse, M.B. *J. Chem. Soc., Dalton Trans.* **1986**, 2711.
84. Osborne, J.H.; Trogler, W.C. *Inorg. Chem.* **1985**, *24*, 3098.
85. Thompson, M.S.; Meyer, T.J. *J. Am. Chem. Soc.* **1981**, *103*, 5577.

86. Leung, W.-H.; Wilkinson, G.; Hussain-Bates, B.; Hursthouse, M.B. *J. Chem. Soc. Dalton Trans.* **1991**, 2791.
87. Danopoulos, A.A.; Wilkinson, G.; Hussain-Bates, B.; Hursthouse, M.B. *Polyhedron* **1992**, *11*, 2961.
88. Kee, T.P.; Park, L.Y.; Robbins, J.; Schrock, R.R. *J. Chem. Soc., Chem. Comm* **1991**, 121.
89. Burrell, A.K.; Steedman, A.J. *J. Chem. Soc., Chem. Comm.* **1995**, 2109.
90. (a) Patrick, D.W.; Truesdale, L.K.; Biller, S.A.; Sharpless, K.B. *J. Org. Chem.* **1978**, *43*, 2628. (b) Chi, Y.; Liu, L.-K.; Huttner, G.; Zsolnai, L. *J. Organomet. Chem.* **1990**, *390*, C50. (c) Ge, Y.-W.; Sharp, P.R. *J. Am. Chem. Soc.* **1990**, *112*, 3667. (d) Glueck, D.S.; Hollander, F.J.; Bergman, R.G. *J. Am. Chem. Soc.* **1989**, *111*, 2719.
91. Michelman, R.I. Ph.D. Dissertation, University of California, Berkeley, CA, 1993.
92. Burrell, A.K.; Bryan, J.C. *Angew. Chem., Int. Ed. Engl.* **1993**, *32*, 94.
93. Burrell, A.K.; Bryan, J.C. *Organometallics* **1993**, *12*, 2426.
94. Danopoulos, A.A.; Longley, C.J.; Wilkinson, G, Hussain-Bates, B.; Hursthouse, M.B. *Polyhedron* **1989**, *8*, 2657.
95. Toreki, R.; Schrock, R.R.; Davis, W.M. *J. Am. Chem. Soc.* **1992**, *114*, 3367.
96. Anhaus, J.T.; Kee, T.P.; Schofield, M.H.; Schrock, R.R. *J. Am. Chem. Soc.* **1990**, *112*, 1642.
97. Danopoulos, A.A.; Wilkinson, G, Hussain-Bates, B.; Hursthouse, M.B. *J. Chem. Soc., Dalton Trans.* **1991**, 269.
98. (a) Bennett, M.A.; Robertson, G.B.; Smith, A.K. *J. Organomet. Chem.* **1972**, *43*, C41. (b) Bennett, M.A.; Smith, A. *J. Chem. Soc., Dalton Trans.* **1974**, 233. (c) Bennett, M.A.; Huang, T.N.; Matheson, T.W.; Smith, A.K. *Inorg. Synth.* **1982**, *21*, 74.
99. (a) Zelonka, R.A.; Baird, M.C. *J. Organomet. Chem.* **1972**, *35*, C43. (b) Zelonka, R.A.; Baird, M.C. *Can. J. Chem.* **1972**, *50*, 3063.
100. Iwata, R.; Ogata, I. *Tetrahedron* **1973**, *29*, 2753.

101. Winkhaus, G.; Singer, H. *J. Organometal. Chem.* 1967, 7, 487.
102. Bennett, M.A.; Matheson, T.W.; Robertson, G.B.; Smith, A.K.; Tucker, P.A. *Inorg. Chem.* 1980, 19, 1014.
103. Kang, J.W.; Moseley, K.; Maitlis, P.M. *J. Am. Chem. Soc.* 1969, 91, 5970.
104. (a) Manriquez J.M.; Fagan, P.J.; Schertz, L.D.; Marks, T.J. *Inorg. Synth.* 1982, 21, 181. (b) Threlkel, R.S.; Bercaw, J.E.; Seidler, P.F.; Stryker, J.M.; Bergman, R.G. *Org. Synth.* 1987, 65, 42.
105. Cullinane, N.M.; Leyshon, D.M. *J. Chem. Soc.* 1954, 2942.
106. Bartlett, D.B.; Roha, M.; Martin Stiles, R. *J. Am. Chem. Soc.* 1954, 76, 2349.
107. Thermal Ellipsoids at 30% Probability Level.
108. Begley, M.J.; Harrison, S.; Wright, A.H. *Acta Cryst.* 1991, C47, 318.
109. Campion, B.K.; Heyn, R.H.; Tilley, T.D. *J. Chem. Soc., Chem. Comm.* 1988, 278.
110. Blake, R.E.; Heyn, R.H.; Tilley, T.D. *Polyhedron* 1992, 11, 709.
111. Redshaw, C.; Clegg, W.; Wilkinson, G. *J. Chem. Soc., Dalton Trans.* 1992, 2059.
112. Fatiadi, A.J. *Synthesis* 1987, 85.
113. Lay, P.A.; Sargeson, A.M.; Taube, H. *Inorg. Synth.* 1986, 24, 291.
114. Bennett, M.A.; Huang, T.-N.; Matheson, T.W.; Smith, A.K. *Inorg. Synth.* 1982, 21, 74.
115. Wolf, J.R.; Bazan, G.C.; Schrock, R.R. *Inorg. Chem.* 1993, 32, 4155.
116. Robbins, J.; Bazan, G.C.; Murdzek, J.S.; O'Regan, M.B.; Schrock, R.R. *Organometallics* 1991, 10, 2902.
117. Weinstock, I.A.; Schrock, R.R.; Davis, W.M. *J. Am. Chem. Soc.* 1991, 113, 135.
118. Walsh, P.J.; Baranger, A.M.; Bergman, R.G. *J. Am. Chem. Soc.* 1992, 114, 1708.
119. Chao, Y.-W.; Wexler, P.A.; Wigley, D.E. *Inorg. Chem.* 1989, 28, 3860.

